UNITED KINGDOM · CHINA · MALAYSIA

Preparation, characterisation and optimisation of cellulose nanoparticles from kenaf fibre and its application in polylactic acid reinforcement

A PhD thesis, submitted to:

Chemical & Environmental Engineering Department

Faculty of Engineering

The University of Nottingham

By:

Mohammad Reza Ketabchi

Supervised by:

Dr Mohammad Khalid

Dr Chantara Thevy Ratnam,

Dr Ing Kong

Dr Md Enamul Hoque

September 2016

ABSTRACT

In this work, cellulose nanoparticles (CNP) were extracted from kenaf fibre and were used to reinforce natural rubber/polylactic acid biocomposites. The kenaf fibre was subjected for pretreatment by three different techniques namely, alkali treatment, bleaching, and sonication. A full factorial design of experiment was conducted in order to optimise the extraction process. The optimisation levels were adjusted according to single and full factorial studies of micro cellulose fibres. The extracted CNP was then structurally and morphologically characterised. The optimum nanoparticles were next employed to prepare the biocomposite. Prior to blending, processing parameters of polylactic acid **(**PLA) were optimised by a full factorial design of experiment including the main three compounding parameters i.e. speed, temperature, and duration. It was found that the alkali pre-treatment of the kenaf fibre had the most influencing effect to delignify kenaf fibre. An average cellulose particle diameter of ~100 nm was achieved when 0.2 g of NaOH/4 g of kenaf was used during alkali treatment, 5 ml of $NaClO_2$/4 g of kenaf was employed during bleaching stage, and sonicated for 20 min. The compounding temperature was found to play a significant role; PLA samples prepared at higher temperatures than 180 °C displayed lower mechanical properties. Later, two single factorial compounding optimisations were carried for CNP/PLA and natural rubber/PLA nanocomposites preparations. Incorporation of 3 wt. % of CNP, and 10 wt. % of natural rubber was found adequate to enhance the elongation and impact resistance of PLA respectively. Therefore, the biocomposite was based on composition of 3 wt. % of CNP, and 10 wt. % of natural rubber hosted by PLA. The composition resulted in 1 %, 92 %, and 96 % improvements in tensile strength, young's modulus, and impact resistance of PLA respectively. It was observed that the biocomposite last for nearly 3072 h in soil and had a moderate biodegradation rate at ~0.15 % h^{-1}. Moderate biodegradation of the biocomposite was found suitable to stabilise and control the fertiliser nutrients release in the soil. This finding has potential to be beneficial in view of environmental preservation and cost reduction for the production of kenaf fibre based biocomposites.

LIST OF PEER-REVIEWED JOURNAL PUBLICATIONS AND CONTRIBUTIONS

(During the Course of My PhD Program)

1) M.R. Ketabchi, M. Khalid, C. Ratnam, S. Manickam, W. Rashmi, M. E. Hoque (2016) "*Sonosynthesis of cellulose nanoparticles from Kenaf fibre: Effect of processing parameters*", Fibers and Polymers journal, 17: p. 1352-1358.

2) M.R. Ketabchi, M. Khalid, M. E. Hoque, C. Ratnam, W. Rashmi (2015) "*Eco-friendly and Cost-effective Isolation of Cellulose Microfibres and Nanocrystals from Kenaf Fibres*", Recent Advances in Environment, Ecosystems and Development, p. 146-152.

3) M.R. Ketabchi, M.E. Hoque, M. Khalid (2015) "*Critical concerns on manufacturing processes of natural fibre reinforced polymer composites*" Manufacturing of Natural Fibre Reinforced Polymer Composites. Springer International Publishing, p. 125-138.

4) M.R. Ketabchi, M. Khalid, S. Manickam "*Optimization of ultrasonic-assisted extraction of microcellulose from kenaf fibre*", Natural Fibers journal (accepted for publication).

5) M.R. Ketabchi, M. Khalid, F.M. Michael, C.T. Ratnam "*Effect of high processing temperature on mechanical properties of neat polylactic acid*", Plastics Rubber and Composites journal (Submitted).

6) M.R. Ketabchi, M. Khalid, C. T. Ratnam "*Natural fibre pretreatment methods and their influence on mechanical properties of polymer composites*", Journal of Wood Science (Submitted).

7) M.R. Ketabchi, M. Khalid, C. T. Ratnam "*Manufacturing process of eco-friendly cellulose nanoparticles/ polylactic acid bionanocomposites*", Polymer Composites journal (Submitted).

8) M.R. Ketabchi, M. Khalid, C. T. Ratnam "*Polylactic acid/natural rubber/cellulose nanoparticles bionanocomposites processing and mechanical properties*", Polymers and the Environment journal (Submitted).

9) M.R. Ketabchi, M. Khalid, C. T. Ratnam "*Kinetic modelling of polylactic acid biocomposites biodegradation and water absorption process; potential fertiliser coating material*", Composites Part A: Applied Science and Manufacturing journal (Submitted).

PEER-REVIEWED CONFERENCES

1) M.R. Ketabchi, I. Kong, M. Khalid, R. Walvekar (2016) "*Efficient isolation of cellulose nanoparticle from kenaf fibre using response surface methodology*", 24th International Conference on Composites/Nano Engineering (ICCE-24), Hainan island, China.

2) M.R. Ketabchi, M. Khalid, M.E. Hoque (2015) "*Eco-friendly and cost effective isolation of cellulose microfibres and nano-crystals from kenaf fibres*", 13th International Conference on Environment, Ecosystems and Development, World Scientific and Engineering Academy and Society (WSEAS), Kuala Lumpur, Malaysia.

LIST OF ACADEMIC AWARDS

(During the Course of My PhD Program)

1) **Research Away Day** 12/2015

(University of Nottingham, Malaysia Campus)

Awarded the "Best PhD Research Output and Contribution" certificate and had the privilege to collect my award from Professor Sivakumar Manickam, Head of the Manufacturing and industrial processes division.

2) **Intra-Campus Postgraduate Research Showcase** 05/2015

(University of Nottingham, UK campus)

Awarded the best poster award and had the privilege to collect my award from Mr Ed Parsons, a Geospatial Technologist at Google.

3) **Intra-Campus Three-Minute Thesis Competition** 10/2014

(University of Nottingham)

Awarded first place for a three-minute presentation of my PhD thesis and accordingly became University of Nottingham's representative at the prestigious Universitas 21 3MT Competition. My research was covered by the Times Higher Education (THE) supplement as one of four UK university representatives at this international competition.

4) **Faculty of Engineering Postgraduate Research Showcase** 09/2014

(University of Nottingham, Malaysia Campus)

Awarded first place, above 42 other candidates, for my poster representing my PhD thesis. As a result, I was sponsored to travel to the UK campus to present my work, which was judged alongside representatives from the university's China and UK campuses.

5) **Three Minute Thesis Competition** 09/2014

(University of Nottingham, Malaysia Campus)

Awarded first place for a three-minute presentation of my PhD thesis.

Awarded the 'People's Choice' prize for a three-minute presentation of my PhD thesis.

6) **Ph.D. Scholarship** 10/2013 – 10/2016

(Faculty of Engineering, University of Nottingham, Malaysia Campus)

Awarded a scholarship to complete a PhD at University of Nottingham *Malaysia Campus*.

ACKNOWLEDGEMENTS

The presented research has been conducted under the supervision of Dr. Mohammad Khalid to whom I sincerely express my utmost gratitude and respect for his continuing assistance, guidance and inspiration. I would like to thank you for encouraging my research and for allowing me to grow as a research practitioner. Your advice on both research as well as on my career have been of invaluable importance.

I would also like to specially thank Dr. Chantara Thevy Ratnam, Dr. Md Enamul Hoque, Dr. Ing Kong, and Dr. Salman Masoudi Soltani for their assistance in my research that enlightened me to take appropriate steps during the course of my PhD.

Finally, special thanks to my family, words cannot express how grateful I am to my parents and brother for all of the sacrifices that they made for me. Thank you for supporting me for everything, and especially I cannot thank you enough for cheering me throughout this experience.

DECLARATION

The investigation presented in this thesis was conducted at the University of Nottingham, Malaysia Campus, Department of Chemical & Environmental Engineering between October 2013 and October 2016. Hereby, I declare that this work is based purely on my own research findings and has not been submitted for any degree to any other institution.

TABLE OF CONTENTS

LIST OF TABLES

LIST OF FIGURES

ABBREVIATIONS

ASTM	American society for testing and materials
CNP	Cellulose nanoparticles
CrI	Crystallinity index
DMA	Dynamic mechanical analysis
DSC	Differential scanning calorimetry
DTG	Differential thermogravimetry
FTIR	Fourier transform infrared spectroscopy
LDPE	Low density polyethylene
LLDPE	Linear low density polyethylene
MA	Maleic anhydride
MCF	Micro cellulose fibres
PE	Polyethylene
PLA	Polylactic acid
PN	Cellulose nanoparticles/Polylactic acid biocomposite
PNR	Cellulose nanoparticles/Natural rubber/Polylactic acid biocomposite
PP	Polypropylene
PR	Natural rubber/Polylactic acid biocomposite
rpm	Rotation per minute
SEM	Scanning electron microscope
SNR	Polystyrene-modified natural rubber (SNR)
TEM	Transmission electron microscopy
Tg	Glass transition temperature
TGA	Thermogravimetric analysis
Tm	Melting temperature
UV	Ultra-violet
wt	Weight

CHAPTER 1

INTRODUCTION

1.1. Research background

Reports from the United Nations' Environment Program (UNEP) as well as the Toxic Release Inventory (TRI) program have indicated that every year an approximate amount of 10 million tons (310 kg sec^{-1}) of toxic chemicals are released into the air, land, and aqueous environments by industrial facilities around the world [1]. These toxic chemicals can result in long term destructive effects to both humans and other habitual environments. Moreover, the growing needs of humans, due to increasing rates of world population growth and adoption of modern lifestyles, have meant a substantial increment in the per capita consumption of synthetic materials.

Environmental awareness rose among our community, has commenced new rules and regulation forcing industries to seek more ecological friendly material for their product. As a result, to reach this standard, there has been a notable increase in interest in using biodegradable and renewable materials. Such materials have found their application in many basic industries such as packaging, biomedical, pharmaceutical, agricultural and horticultural, textile, household goods, and automotive [2]. This is mainly due to the challenging degradation of fossil-based materials which require complex studies on the mechanisms to dispose them. According to USA Biodegradable Products Institute (BPI) standards, biomaterials are required to disintegrate within 3-month [3].

Natural fibres have lately become a promising feedstock material in the production of biodegradable materials. This is particularly due to their low cost, low density, comparable specific tensile properties, non-abrasiveness to the equipment, non-irritation to the skin, optimised energy consumption, less health risk, renewability, recyclability as well as biodegradability [4, 5]. Large quantities of natural fibres are available from agriculture and forest that consist of mainly lignin, hemicellulose, and cellulose [6]. Lignin and hemicellulose are hydrophilic and employment of such components can result in an unwanted moisture adsorption.

Therefore, to maintain the application of lignocellulosic fibres in different industries, researchers have been focusing on lignin and hemicellulose removal methods [7, 8]. These treatments further enhance the fibre homogenisation, crystallisation degrees, adhesion between fibre and matrix, and flame retardant properties. Moreover, thermal degradation and dimensional stability of the end product also improved significantly with biomass pretreatment. Following this growing trend, bioplastics have attracted a great interest to host natural fibres. This is for a diverse range of applications such as their renewability, biodegradability, and commercial viability [9, 10].

1.2. Problem statement

Development in the use of bioplastics and biocomposites is proceeding rapidly, yet, there are number of cases in which such materials lack the properties needed to replace petroleum based products. A large unsolved problem of bioplastics is lack of biocompatibility, strength, heat resistance, performance and ease of processing as compared to petroleum based products. Such concerns become vital when they are used not temporarily but permanently. Meanwhile, natural fibre has found recent use as reinforcing material for bioplastics. However, the drawbacks of using natural fibre as reinforcing agent are its poor compatibility with polymer matrix, low degree of fibre dispersion, and its poor moisture resistance that limits its applications. Other factors, which notably affect the reinforced composite properties, are concerned with aspect ratio, geometry and dispersion of filler particles in the matrix.

1.3. Scope of study

The main focus of this research is to enhance the properties of polylactic acid by blending with the extracted cellulose nanoparticles from kenaf fibre. To further improve their compatibility, the applicability of polystyrene-modified natural rubber as a compatibiliser has been studied. Incorporation of CNP in PLA is expected to enhance thermal and mechanical properties of PLA to a satisfactory degree. PLA has poor thermal and mechanical resistant at high temperatures and stress. On the other hand, CNP tends to aggregate in order to decrease the total surface energy. This incident can result in poor dispersion and therefore inferior properties. Hence, optimisations and improvement on treatments, and processing techniques together with the application of a compatibiliser have been considered to address these issues.

1.4. Research objectives

This research work may be broken down into four specific objectives:

1. To optimise and model extraction of micro cellulose fibres and cellulose nanoparticles from kenaf fibre using response surface methodology.

2. To optimise and model processing parameters of polylactic acid and investigate the effects of cellulose nanoparticles reinforcement.

3. To investigate the blending effects of natural rubber on cellulose nanoparticles/polylactic acid biocomposite properties.

4. To investigate the biodegradation and water absorption behaviour of cellulose nanoparticles/ synthetic rubber/polylactic acid biocomposites.

1.5. Thesis structure

This PhD research is divided into five chapters; introduction, literature review, methodology, results and discussions, and finally conclusions and future research. The chapters are based on experimental objectives.

The introduction chapter highlights research background in this field, problem statement, scope of study, research objectives, and thesis structure. A comprehensive literature review on natural fibres is presented in chapter two. It reviews the earlier works on extraction of cellulose from natural fibres using different treatment techniques. The application of response surface methodology in such extractions is also reviewed and discussed. The chapter also discusses reinforcement of polymer materials with natural fibre and their processing techniques to understand their benefits and drawbacks.

Chapter three outlines the methodology, materials, preparation methods and characterisation techniques employed in this research. The results and discussion in chapter four, are based on the experimental objectives. This includes characterisation of extracted cellulose fibres as well as

mechanical, dynamical, morphological, thermal, and structural properties of polylactic acid biocomposites. Also, the results from soil burial, water absorption and thermal stability tests based on the optimised products are discussed. At the end of every section, the optimum procedure is concluded and finally a suitable application for the prepared biocomposite is recommended.

CHAPTER 2

LITERATURE REVIEW

2.1. Introduction

This chapter presents a review of the literature on treatment of natural fibre and its applications in reinforcement of biocomposite materials. An overview on treatment of natural fibre and extraction of micro cellulose fibres and cellulose nanoparticles is discussed in section 2.2.1 and 2.2.2 respectively. Different processing technique of composite materials reinforced with natural fibres is detailed in section 2.3. Mechanical properties of reinforced biocomposites is discussed in section 2.3.2. Finally, applications of reinforced biocomposite materials were given in section 2.2.4.

2.2. Natural fibres

Natural fibres have been described in literature as coverage for body and construction of housing since early 4000 BC in Europe, 3000 BC in Egypt and 6000 BC in China. Flax was the first vegetable fibre to be used for clothing by humans. In general, natural fibres fall into three main categories depending on their origin (plant, animal, and mineral). Plant fibres include bamboo, hemp, flax, jute, sisal, bagasse, ramie and kapok [11, 12]. Such plants are hydrophilic as they are derived from lignocellulose materials. Lignocellulosic biomass contains three main natural polymers; cellulose $[C_6H_{10}O_5]x$ (35–83% dry weight basis), hemicelluloses $[C_5H_8O_4]m$ (0–30% dry weight basis) and lignin $[C_9H_{10}O_3{\cdot}(OCH_3)0.9–1.7]n$ (1–43 % dry weight basis) [6]. Cellulose is one of the leading biopolymers in nature, which is a linear homopolymer of β-(1→4)-glycosidic bond linked D-anhydroglucopyranose [13]. Due to vast availability of cellulosic fibres, cellulose containing composites have generated much interest amongst various industries, especially the automotive industry [14, 15].

Unlike cellulose, hemicellulose is not chemically homogeneous and different hydrolytic technologies and various biological and non-biological treatment options are available both for fractionation or solubilisation of hemicellulose from biomass resources [16]. Lignin keeps the water in fibres, acts as a protection against biological attack, and as a stiffener to give stem its

resistance against gravity forces and wind. Lignin is a mononuclear phenolic amorphous polymer consisting of phenylpropane units found in the cell wall of certain biomass, especially wood species, based on three monolignols; p-coumaryl alcohol, coniferyl alcohol, and sinapyl alcohol [17]. A wide range of chemicals can be obtained by chemical and thermal decomposition of lignin. Such chemicals include polyesters, polyethers, and polystyrene derivatives that can be used as starting materials for synthetic polymers [18, 19]. Lignin acts as a matrix together with hemicelluloses for the cellulose microfibres, formed by ordered polymer chains that contain tightly packed crystalline regions [20]. Hemicellulose found in natural fibres was believed to be a compatibiliser between cellulose and lignin [21].

Manufacturers have always been searching for higher strength, lower weight, inexpensive and ecofriendly materials to build novel products by taking advantage of these characteristics. Through this competitive engineering challenge, a number of forward thinking scientist in the chemical industry raised ideas aimed at driving a successful transition to renewable alternatives. Nowadays, many novel renewable materials are in production or development, and there are significant business opportunities in the sector. For instance, researchers recycled old newspaper by achieving the wood fibres and recommended the achieved fibres to manufacture semi-structural products such as doors, windows, furniture, and automotive interior parts [22]. Renewable materials have a number of advantages over their nonrenewable counterparts. They often have added valuable properties and are less toxic and also the greenhouse gas emissions could be reduced if renewable materials are used [23]. Besides, they can be produced without exhausting our natural resources. In the meantime, the development of polymer composites based on renewable resources such as natural fibres and biodegradable polymers have attracted an increasing amount of attention in the composite science [24, 25].

Natural fibres have been classified according to their origin, and grouped into leaf: abaca, cantala, curaua, date palm, henequen, pineapple, sisal, banana; seed: cotton; bast: flax, hemp, jute, ramie; fruit: coir, kapok, oil palm; grass: alfa, bagasse, bamboo and stalk: straw (cereal). The bast and leaf (hard fibres) types are the most commonly used in composite applications [21, 26]. These natural microscale reinforcement material provide toughness and strength to the composites [27]. Natural fibres that are reported in literature to reinforce different polymer

matrices include wood [28-30], bagasse [31-34], rice straw [34-36], rice husk [37-40], kenaf [41, 42], wheat straw [43-45] ,flax [46], hemp[47, 48], pineapple leaf [37, 49, 50], oil palm[51], rapeseed waste [52], date palm [53], doum fruit [54], ramie [55], curaua [56], jowar [57], sisal[58], bamboo[59], and jute[60]. Therefore, based on the reported studies, natural fibre reinforced composites offer specific eminent properties; however, as mentioned earlier, natural fibres have disadvantages including moisture absorption, quality variations, low thermal stability and poor compatibility with the hydrophobic polymer matrix [61, 62]. Hence, to improve interfacial adhesion between hydrophilic fibres and hydrophobic polymers, organic reagents such as maleic anhydride were introduced as a compatibiliser [63]. As for kenaf/polypropylene composites, maleated polypropylenes (MAPP) was reported to be essential to improve the compatibility between fibre and polymer matrix [64, 65]. Interfacial adhesion between fibre and polymer matrix was recently improved by employing silicon dioxide (SiO_2) nano powder [66]. Addition of synthetised compatibilisers was considered costly and as a result, researchers suggested treatment of natural fibres.

2.2.1. Natural fibre treatment techniques

The interest in using biomass as reinforcing material increased in recent years due to the many advantages that they promote. Meanwhile lack of good interfacial adhesion, and poor resistance to moisture absorption are the main concerns in this field [61]. Hence, researchers suggested chemical, physical, and thermal treatment of fibres to overcome these issue. Such treatments can chemically modify the fibre surface, increase the resistance to moisture adsorption as well as the surface roughness.

Chemical or physical surface modifications of lignocellulose particles have been explored with the aim of changing the surface properties or creating reactive sites to improve the fibre/matrix interfacial bonding. Studies reported various mechanical and chemical treatment processes such as grinding, oven drying, alkali treatment, steam explosion, silane treatment, and acetylation treatment. Descriptions of a number of important fibre mechanical and chemical modifications were summarised in the following subsections.

2.2.1.1. Grinding of fibres

The reinforcing ability of fillers is influenced by three primary characteristics of the filler; particle aspect ratio and its distribution, filler/polymer bonding, and particle shape complexity [67]. Although not decisive but, these factors play an important role in the development of an enhanced polymer composite material. The filler aspect ratio, shape and range of active sites present on the filler surfaces requires appropriate analysis [68]. Figure 1 shows the single fibre dimensions and its active sites for better understanding. The particle diameter of the filler has the most significant influence on reinforcement. It has a direct impact on the specific surface area of the filler. Furthermore, the large amount of reinforcement surface area means that a relatively small amount of filler reinforcement can have an observable effect on the macro scale properties of the composite. On the other hand, particle complexity has a more notable effect on processing behaviour such as during extrusion, than on reinforcement and provides important benefits in this area. Fibres are ground and sieved to reach an ideal aspect ratio and shape. The optimum length, diameter, and shape of the fibre can be defined based on the scopes of a project. For instance, wood flour was ground to 250 µm and improvements in mechanical properties including impact resistance of polypropylene were obtained [69]. Through a similar work, parallel results were achieved with particle size of 143.4 µm [29].

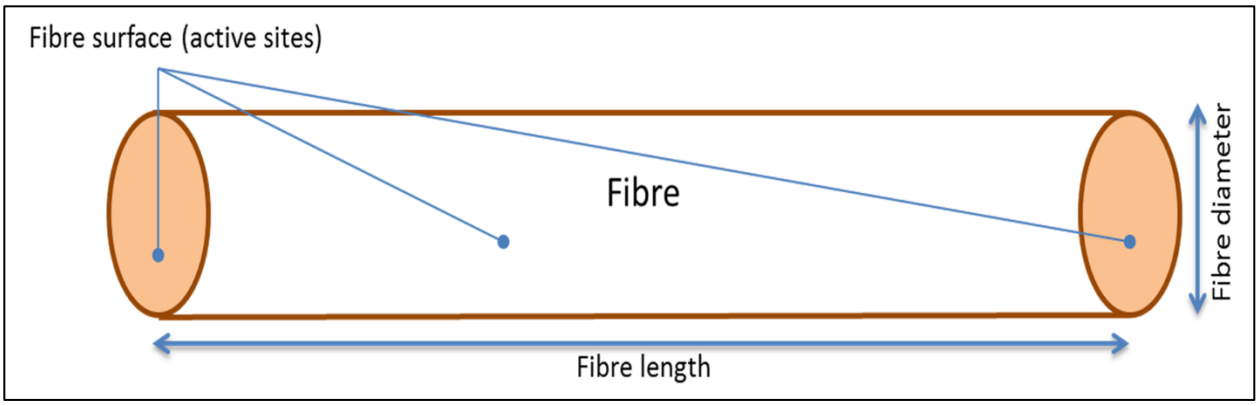

Figure 1: Schematic diagram of a single fibre

Table 1 shows the optimum particle aspect ratio of the fibres used as a reinforcing agent. From Table 1 and other similar studies, it was implied that the fibres with a diameter below 500 µm

have better performance as a reinforcing material. This highlights the importance of particle dimensions in the field of polymer composites. Additionally, as a result of recent improvements in terms of technology, studies have shifted from using micron sized particle to nano sized particle to enhance the performance of the polymer composites while using a smaller amount of material at the same time [70, 71].

Table 2: Optimum micron size (length/diameter) of the fibres as reinforcing materials in polymer composites

Fibre source	Reinforced polymer	Fibre length/diameter (µm)
Wood	Polypropylene [28, 69]	250
	Polypropylene [29]	143.4
Almond Shells	Polypropylene [72]	100
Bagasse	Polyvinyl chloride [33]	~325
Rice straw	Low density polyethylene [34]	500
Doum Fruit	Low density polyethylene [54]	200
Kenaf	Low density polyethylene [41]	400
	High density polyethylene [42]	500
Bamboo	Natural rubber (NR) [73]	~225
Rapeseed waste	Linear low density polyethylene [52]	400

2.2.1.2. Drying of fibres

Due to the hydrophilic nature of natural fibres, they contain a notable amount of moisture. This moisture content is suitable for moulds to grow which affect the performance of natural fibre reinforced products both in short and long term. As a result, drying of biomass could be important in different aspects and this matter becomes more important when they are used in humid regions where the moisture content of fibre increases by nature. In addition, since water acts as a plasticiser and lowers the glass transition temperature, moisture content needs to be addressed before fibre/polymer compounding. Oven drying and open air drying are the two common methods used to decrease moisture content. Treatment duration, temperature, and

heating rate require appropriate consideration as natural fibres have a low thermal stability at high temperatures. Table 2, shows the optimum temperature used in different studies during oven drying.

Table 3: Optimum temperature and duration of fibre drying process through different studies

Fibre type	Oven temperature (ºC)	Duration (h)
Wood	100 [30]	24
	105 [74]	24
	100 [75]	24
	103 [76]	16
Rice straw	80 [36]	12
Rice husk	105 [38]	24
	105 [39]	18
	100 [40]	24
	100 [77]	5
	100 [78]	24
Wheat straw	80 [45]	4
	80 [79]	4
Date palm fibres	80 [80]	2
Ramie	80 [55]	24
	105 [81]	1
Sisal	70 [82]	12
	80 [58]	16
	40 [83]	24
Abaca	105 [84]	24
Corn straw	80 [79]	4
Soy stalk	80 [79]	4
Cork powder	70 [85]	12
Henequen	60 [86]	24
Kenaf	80 [87]	6

The maximum temperature used for drying was found to be about 100 ºC which agrees that the purpose of this treatment is to drive out all the moisture content, without damaging the fibre itself. At higher temperatures, the drying process has been carried out in a shorter periods of time to maintain finer physical and chemical properties. A complete drying process was observed after 24 h; the temperature during this period could vary based on the fibre characteristics.

2.2.1.3. Mercerisation of fibres

Developments towards environmentally friendly polymer composite systems is based on incorporation of natural fibres with polymer matrices [88]. Nevertheless, both advantages and disadvantages of this reinforcement require consideration. Alkali treatment of fibres has been introduced to reduce several reinforcement effects such as linear density, shrinkage in dimension and also to make the fibrillar structure visible as well as to enhance the mechanical properties. Alkali treatment of natural fibres, also known as mercerisation, is the common method to produce surface modified fibres. Notable improvements in mechanical properties such as tensile strength of fibres were detected after mercerisation process [89, 90]. Hence, this treatment can be also known as a mechanical treatment for fibres. However, it should be noted that the improvements in mechanical properties greatly depend on a treatment time and a concentration of alkali solution.

During treatment, natural fibres are subjected to concentrated aqueous solution of a strong base, to produce a sufficient swelling. The alkaline solution used in this type of treatment has significant effect on lignin and hemicellulose parts than the inner cellulose structure. This treatment is capable of decreasing fibre diameter and removing outer layers (the outcome may vary depending on the process condition).

In addition to the alkali solution strength, treatment duration plays an important role as well. Table 3 shows type of chemical and durations used in alkali treatment. It was observed that NaOH is the most common reliable chemical used during mercerisation. This could be due to the ease of availability as well as the price of this chemical compared to other bases. Therefore, it

can be seen that there is a lack of studies on comparing the effect of different bases on mercerisation process.

Table 4: Type and percentage of chemical used during different alkali treatments

Fibre	Employed chemical	Alkali concentration (wt. %)	Duration (h)
Baggase	NaOH [32]	1.5	1
Rice husk	NaOH [37]	5	1
	NaOH [77]	10	3
	NaOH [79]	-	-
Hemp	NaOH [47]	5	1
	NaOH [91]	4, 6, 8, and 10	3
	NaOH [92]	6	48
Pineapple leaf	NaOH [93]	5	5
	NaOH [50]	2	1
Soy stalk	NaOH [79]	-	-
Palm Oil	NaOH [94]	5	48
	NaOH [95]	17.5	2
	NaOH [96]	25	3
	NaOH [97]	1	24
Date palm	NaOH [53]	3, 6, and 9	24
Curaua	NaOH [98]	5, 10, and 15	1, and 2
Sisal	NaOH [82]	2	2
	NaOH [99]	2	1
	NaOH [100]	2, 5, 10 and 12	0.50
	NaOH [58]	5	2
Jute	NaOH [101]	5	2
	NaOH [102]	2	1
	NaOH [103]	5	0.75
Abaca	NaOH [84]	5	0.16
Kenaf	NaOH [104]	6	48 and 144

Banana	NaOH [34]	10	2
Doum	NaOH [54]	-	48
Corn straw	NaOH [79]	-	-
Basalt	NaOH [105]	-	24
Henequen	NaOH [86]	2	1

2.2.1.4. Graft copolymerisation of a monomer/polymer onto fibres

Among the above mentioned methods, graft copolymerisation has been reported to be an effective technique for surface modification of natural fibres and has been broadly used by many researchers since 1980 [106]. Many studies reported notable improvements in elasticity, absorbency, ion exchange capabilities, thermal resistance and hydrophilicity of the hosting polymer with monomer-grafted fibres [107]. More recently, the activation energy of the degradation of grafted Oil Palm Empty Fruit Bunch (OPEFB) was found lower than the pure OPEFB [108]. Additionally, morphological studies showed clearer and smoother surface of the grafted fibre compared to the untreated fibre as the grafted monomers/polymers cover the grooves and holes on the surface of the original fibre [109].

Percentage of grafting depends on reaction conditions such as reaction temperature, reaction period, and concentration of the monomer/polymer, solvents, and initiators. This method can be introduced to the applications where degradability of the hosting polymer composite is in priority.

One of the well-known grafting treatments is silane treatment. Silanes are known as effective coupling agents widely applied in composites and adhesive formulations [110]. Silane coupling agents are intermediary compounds with functional groups that bond with both organic and inorganic materials. Silanes were successfully applied in inorganic filler reinforced polymer composites [111]. The interaction of silane and polymer matrix is based on the organo functionality of silane and the matrix characteristics. Main advantage of these chemicals is that they are commercially available in a large scale [112]. Silanes are hydrolysed forming reactive

silanols and are adsorbed and condensed on the fibre surface (sol–gel process) at a specific pH and temperature. The bifunctional structures of silanes attracted much attention as a coupling agent in natural fibre/polymer composites, since natural fibres bear reactive hydroxyl groups similar to glass fibre. In regards to a silane treatment, studies reported notable improvements in specific tensile and flexural strength of fibres [112, 113].

Silane is a multifunctional molecule which is used as a coupling agent to modify fibre surfaces. It usually involves soaking fibres in a weak solution of a silane diluted in a water/alcohol or water/ketone mixture. Following a complete review on silane coupling agents, it was reported that the most common silanes applied in natural fibre/polymer composites are trialkoxysilanes bearing a nonreactive alkyl or reactive organo functionality [114].

For characterisation purposes, researchers carried out Fourier transform infrared (FTIR) spectroscopy analysis on an untreated and silane treated hemp fibres (Table 4) [91]. The treatment was observed to be less damaging to the fibre content, as the fibre layers were clearly visible in FTIR analysis, before and after the treatment.

Table 5: Infrared transmittance peaks (cm^{-1}) of (a) untreated and (b) treated hemp fibres

	–OH stretching (cellulose)	**C=O stretching (hemicelluloses)**	**C=O stretching (hemicelluloses)**	**C=O stretching (lignin)**
a	3407	1737	1643	1249
b	3386	1737	1652	1251

During silanisation, silane experiences several stages of hydrolysis, condensation and bond formation. The bonding formation in between silane and the fibre layers (mainly hemicellulose, lignin, and cellulose) has several advantages in addition to its surface modification properties. The layers carrying hydroxyl groups are capable of absorbing atmospheric moisture. Silane treatment reduces the fibre moisture absorption capacity as silane molecules cover the hydroxyl groups on the fibre surface. At the same time the compatibility of silane functional groups with the hosting polymer matrix need to be considered. Table 5 lists the suitable silane functionalities

for different types of polymer compositions [115]. Suitable treatment and functional groups significantly improved interfacial adhesion and also mechanical and outdoor performance of the resulting fibre/polymer composites.

Table 6: List of suitable silane functionalities for different types of polymers

Aimed Polymer	Suitable Silane functionality
Butyl rubber	Amino, and Glycidoxy
NR	Alkyl, and Mercapto
Polyacrylate	Amino, and Vinyl
Polyethylene	Amino, Alkyl , Chlorine, Methacryl, and Vinyl
Polypropylene	Azide, Vinyl
Polysulfide	Glycidoxy
Polyvinyl chloride	Amino, Chlorine, and Mercapto

2.2.1.5. Acetylation treatment

Chemicals such as alkaline, silane and acetylation react with hydrophilic hydroxyl groups of fibre and thus improve hydrophobic characteristics and provide enhanced bonding properties with polymer matrix. Meanwhile, acetylation is one of the most popular reactions of lignocellulosic materials. It involves replacement of hydrogen atom of a hydroxyl group with an acetyl group (CH_3CO). It is acknowledged to enhance the dimensional stability, strength and biological properties of fibre and fibre reinforced composites [116, 117]. According to cost and performance ratio analysis, it is found to be the most efficient treatment respectively.

Acetylation in vapour phase was found to decrease the fibres hydrophilic properties more efficiently and improve its thermal stability [118]. Remarkable improvement in interfacial shear strength of fibre was observed as acetylation changes fibre surface morphology and results in the surfaces to become much smoother [119]. Untreated fibres are rich in hydrocarbon nature compounds, such as waxes and wax like substances. This type of treatment alters the fibre surface characteristics, by removing the outer surface layer and producing a smoother fibre

surface. However, it should be noted that this change in morphological aspect after acetylation influences both the fibre and the hosting polymer mechanical performances. For instance, acetylation showed a negative effect on tensile strength of date palm tree fibres [120]. This decrease in tensile strength was referred to influence of acid on the fibre structure. Addition of acetylated sugarcane bagasse decreased the mechanical properties of polypropylene composite as well [32]. Contrarily, in another research on the influence of fibre chemical modifications reported, notable increase in tensile properties of acetylated sisal reinforced polyethylene [100].

In any treatment process, type of chemicals used plays the most important role. For instance, application of acetyl chloride was reported to be harmless to the crystalline structure of micro cellulose fibres, while acetic anhydride reduced the crystallinity of cellulose chains [121-123]. Hence, based on the aims of a project various treatments and chemicals could be considered and applied.

2.2.1.6. Steam explosion of fibres

As the global financial crisis continues to unfold, the number of studies on more commercial and less costly preparation methods has been increased. Among the list of treatment methods, steam explosion is known as an economical and environment friendly processing method, which is widely used for the treatment of lignocellulosic materials [124, 125]. The simplicity of this treatment made it popular. Additionally, this treatment is only based on water/steam at high temperatures. It is suitable to conduct an efficient delignification and extract celluloses [125].

Steam explosion is considered as hydrothermal treatment method. The physico chemical treatment crushes the samples through a sudden reduction of pressure from high to atmospheric level after steaming the samples for a certain amount of time in a reactor. The rapid decompression that takes place during this treatment is the stage that makes it different from the already known steam treatment (sometimes called auto hydrolysis treatment) method. This decompression results in isolation of fibre compounds and generates a solid fraction with a more open structure [126, 127]. Based on the application, this change in fibre structure could be considered beneficial.

Nevertheless, steam explosion is found to be more efficient compared to the other hydrothermal treatment methods. More recently, researchers reported improvements in performance of treated fibres by applying acidic catalysts such as SO_2 or H_2SO_4 during the treatment [128, 129]. As observed through different studies, steam explosion of fibres takes place in less than 5 minutes (Table 6). This short retention time is due to the both high temperature and pressure, and more importantly to protect the fibre from any damages during high temperatures. The minimum temperature to run this treatment was observed at 180 ºC. Meanwhile, softwood biomass treated at 281 ºC, is claimed to be the highest value in the world. As a result, based on the fibre capabilities as well as the equipment availability, the treatment temperature range could be carried out from 180–281 ºC.

Table 7: Optimum temperature and pressure and retention time duration followed for steam explosion treatment during different studies

Fibre type	Treatment temperature (ºC)	Treatment pressure (bar)	Retention time (min)
Sasa palmate	180–260 [130]	10-49	0.5–20
Spruce bark	205 [128]	16.3	5
Softwood biomass	281 [131]	67	1–10
Globulus	183 [124]	10	5 and 10
Sumac fruit	190 and 200 [132]	15	3 and 5
Maize stalk	198 [133]	15	1.5
Wheat harvest	200 [127]	15.5	10
Corn stover	200 [134]	-	5
Banana	220 [135]	-	4

2.2.1.7. Sonication of fibres

To extract or access the fibre's components, process efficiency is a compromise of process stability and process speed. To improve the efficiency of treatment, application of ultrasound has been suggested [136] . Ultrasound can result in turbulent flow and produce physical and

chemical effects which both are found significant to delignification and surface treatment of natural fibres. After the application of ultrasound, each component can be isolated via chemical conversion, hydrolysis, and/or centrifugation. The magnitudes can be altered during the optimisation process based on different parameters such as type of fibre, chemicals, treatment duration, ultrasonic frequency, and reactor geometry. Therefore, the employment of ultrasound for such treatments must consider the variation of ultrasonic influences to exploit the main features of ultrasound.

For instance, starch yields from ultrasonic treatments of corn were found comparable to conventional wet milling (~68 %) [137]. Furthermore, the application of ultrasonic was found beneficial as it efficiently separated the starch particles. One of the main drawbacks of natural micro/nano fibres is the aggregation, which could result in an inhomogeneous dispersion in different solutions and applications. Natural fibres tend to aggregate in order to decrease the total surface energy [138]. This incident can result in poor dispersion and therefore inferior properties. This becomes more important in reinforcement of composite materials where a homogeneous dispersion is required to maintain the stress transfer from the matrix to the fibres [139]. Furthermore, to prevent any damage to the components structure, studies suggested low frequency ultrasonic treatment, coupled with alkaline solutions [140]. However, to conduct an energy and time efficient process, high frequency ultrasound, oxidising solutions, and use of combined alternative treatment techniques were found beneficial [141]. Hence, optimisation of parameters is important in terms of achieving high performance and low cost treated fibres.

Plastic materials, lower density compared to metals makes them ideal for lightweight structures. They have replaced many routine materials due to their great benefits such as ease of processing, high productivity, low cost, and their versatility. However, the supply of oil is depleting faster than expected; hence clear effects can be observed on shortage of petrochemical based products [142]. As a consequence, since 1980s, natural fibres are experiencing increased demand as fillers in polymer matrices. This is due to their advantages over conventional glass and carbon fibres. Meanwhile deforestation concerns have led to the growth of the application of biomass resources to fulfil the market [143]. Lignocellulosic biomass is not only cheap but also renewable resource and most abundant source of organic components on the earth. As mentioned earlier they consist

of three main structural polymers: the polysaccharides cellulose, and hemicelluloses and the aromatic polymer lignin (Figure 2) [6]. The hemicellulose and lignin part of a natural fibre affect the final properties of the plastics as they carry hydrophilic nature resulting moisture adsorption. Therefore, researchers have focused on removal of these content and application of cellulose microfibres and nano particles in plastic materials [14, 144]. Studies in this field have shown that the extraction of Cellulose Nano Particles (CNP) from natural fibres requires a combination of several treatment processes [8, 145, 146].

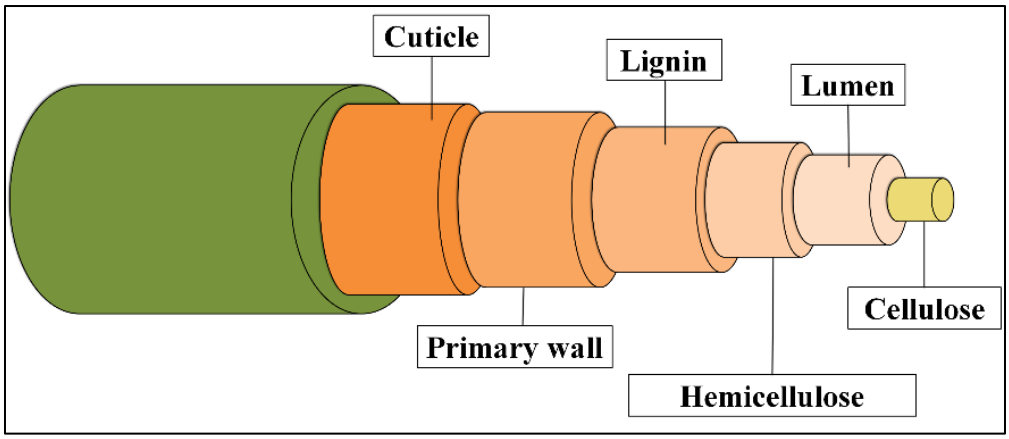

Figure 2: Simplified schematic diagram of lignocellulosic fibre layered structure

In this research, kenaf fibre as a source for extraction of cellulose was selected. This selection was mainly due to the worldwide availability of kenaf and its crystalline cellulose content (~55 %). Kenaf (also known as Hibiscus cannabinus L) is one of the most well-known natural fibres to be used as reinforcement in thermoplastic materials. It is an herbaceous annual plant that can be grown under a wide range of weather conditions and produces more than 3 m within 3 months even in moderate ambient conditions [147]. The highest growing rate may be up to 10 cm per day. However, different environments will still yield various heights of kenaf plant, such as the cultivar, planting date, photosensitivity, length of growing season, plant populations, and plant maturity [148]. The core of kenaf is a wood-like structure that makes up to 60–70 % of the weight. The core has an amorphous pattern, while the bark has an oriented high crystalline fibre pattern [149].

Kenaf has the ability to absorb the nitrogen and phosphorus in the soil. These minerals are able to help increase the crop height, cumulative weed weight, stem diameter, and fibre yield [150]. Also it transforms carbon dioxide to oxygen at a significantly higher rate as compared to other lignocellulosic fibres [151]. Efficient transformation of carbon dioxide can enhance the photosynthesis rate of fibre. Therefore, kenaf is not only environmentally friendly in terms of its biodegradability, but in the fact it produces a lot of oxygen as well as reducing carbon dioxide.

For chemical treatment purposes, to use a minimum amount of chemicals, a vapour line autoclave has been used. The high vacuum pressure of autoclave has made this investigation more unique by allowing the treatment process to take place using lesser amount of chemicals and also to happen within shorter period of time compared to the other studies. The high pressure has shown to be able to expand the fibres and to present the chemicals an easier access to the fibre layers.

Different treatments including alkali treatment, steam explosion, silane treatment, and acetylation treatment were found suitable to extract microcellulose fibre (MCF). They are mainly acknowledged to enhance dimensional stability, strength and biological properties of fibre and fibre reinforced composites [152]. Such changes in structure are expected to result in higher interfacial shear strength of fibre. Therefore, in this research, a combination of alkali and acetylation treatment was selected and statistically optimised. The acetylation treatment was accomplished through a bleaching process. Following the MCF extraction optimisation, extraction of CNP was optimised.

The decomposition of lignocellulosic fibre has been categorised into four leading stages for characterisation purposes [153]. The three main natural polymers are devolatilised in a temperature range of 180–400 °C. Hemicellulose, cellulose, and lignin content are found to decompose in a temperature range of 220–315 °C, 315–400 °C, and >400 °C, respectively (Figure 3). In this research, these temperature ranges were applied during thermal analysis.

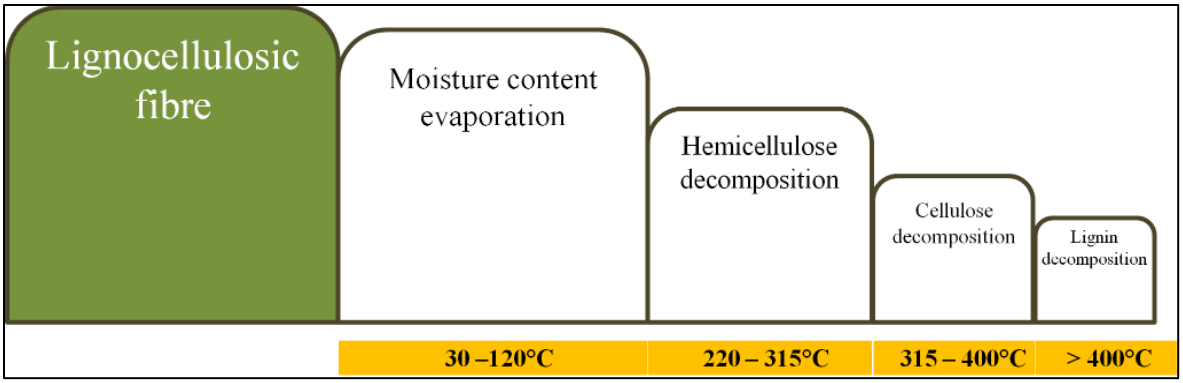

Figure 3: Thermal degradation schematic diagram of a lignocellulosic fibre

2.3. Biocomposites

Polylactic acid (PLA) was selected as biodegradable matrix to host the prepared CNP. PLA, an aliphatic polyester, is made up of lactic acid (2-hydroxy propionic acid) building blocks. This hydrophobic material is derived from natural feedstock such as corn, barley, sugar beets, wheat and rice [154, 155]. Researchers have improved the mechanical properties of PLA by introducing suitable plasticisers [156, 157]. However, addition of a synthesised additive could be considered costly which requires further processing optimisation. Therefore, researchers have focused on modification of PLA itself to enhance the temperature stability of the polymer and reduce the residual monomer content [158]. The resulting modified PLA can be processed similarly as polyolefin and other thermoplastics although the thermal stability could be better.

The processing methods and parameters exhibit significant effects on the final product [159]. In addition to solvent casting, melt compounding/extrusion is commonly carried out to introduce PLA granules to different compositions [160-162]. Through melt compounding, the processing parameters are mainly temperature, mixing speed and time. The production lines based on PLA matrices are strictly limited during the processing procedure due to the nature of PLA. As a result of this limitation, studies mainly employed the granules at ~170 °C [163-165]. This was to reduce the thermal impact on PLA as a natural feedstock derivative. The processing temperature can become more important in cases where higher temperatures are required to melt other components.

One of the aims in this research emphasises the importance of the processing temperature on mechanical properties of PLA. To investigate the maximum processing temperature for neat PLA, via the least possible number of experiments, response surface methodology (RSM) was employed. Studies showed beneficial outcomes using this method as it involves selecting the optimal experimental design [157, 166]. The most important advantage of RSM over classical one variable at a time optimisation, is its applicability to investigate several observations at once. As compared to the multivariate techniques such as two level factorial design, it has the ability to explore, experimentally, the main effects, interaction effects and the relationship between several independent variables and dependent variables [167]. This can save a huge amount of time and money by reducing number of experimental runs needed to provide sufficient information for statistically acceptable results. Another advantage of RSM over other mathematical modelling techniques used is that, after initial 'training', a model response can be rapidly and efficiently obtained [168]. It has the ability to optimise objective functions with unknown variance along with high levels of uncertainty [169]. Earlier to this optimisation, four processing techniques were reviewed to finalise a suitable processing technique to prepare a neat PLA matrix to host CNP.

2.3.1. Processing techniques of biocomposites

The use of natural materials, biodegradable and recyclable polymers and their composites for a wide range of engineering applications has resulted in reducing carbon footprints and the usage of petrochemical materials. Meanwhile, due to the complexity of fibre structures, different mechanical performances of the composites are achieved even with the use of the same fibre types with different matrices. Some critical issues like poor wettability, poor bonding and degradation at the fibre/matrix interface (a hydrophilic and hydrophobic effect) and damage of the fibre during the manufacturing process are the main causes of the reduction of the composite strength. This drop is generally attributed to the pretreatment process of fibre and enhanced manufacturing process of the composites. Following the introduction to lignocellulosic materials, the suitability of known manufacturing processes, based on the fibres and matrices materials, mechanical and thermal properties were discussed in detail.

Appropriate manufacturing processes are essential to be employed to convert the raw materials to the desired product. Manufacturing engineers mainly focus on numbers of principles including preferred application, properties, size and shape of resultant composites, processing characteristics of raw materials, the production speed and the manufacturing cost. For the initial assessment on a suitable type of manufacturing processes to be applied, the size of the composites is a leading factor. Injection moulding and compression moulding are endorsed for small to medium sized components due to their simplicity and fast processing. For a simple form of composites product, compression moulding is recommended. Similarly, open moulding and autoclave processes usually manufacture large structures. Furthermore, the product shape complexity influences the type of manufacturing processes to be used likewise. Recently a comprehensive review on the effect of different processing conditions and different surface modification techniques on the cellulose fibres as well their composites has been carried out [170].

For short fibre and nanomaterial based processing injection moulding and compression moulding are employed while for producing long and uniform cross-section parts pultrusion is mainly used [171]. Pultrusion is a continuous composite processing method that combines reinforcement impregnation with composite consolidation. In this method, individual prepreg layers are flattened out and a bond is formed between them. The shape of the product is highly dependent on the shape of the die. Several continuous stages of heat control are required to cure the composite product. Depending on the performance of composites products, suitable raw materials (thermosets/thermoplastics, high/low viscosity, and processing temperature) should be chosen with a suitable composite fabrication technique. The elementary principle of pultrusion process is the continuous melt impregnation of fibre ropes (roving) in a pultrusion tool (shown in Figure 4). In terms of reducing the energy consumption, the location of the implanted heaters can be more influential than the number or the power of the heaters [172]. In addition to long and uniform cross-section parts, studies have employed pultrusion process to manufacture phenolic foam composites [173].

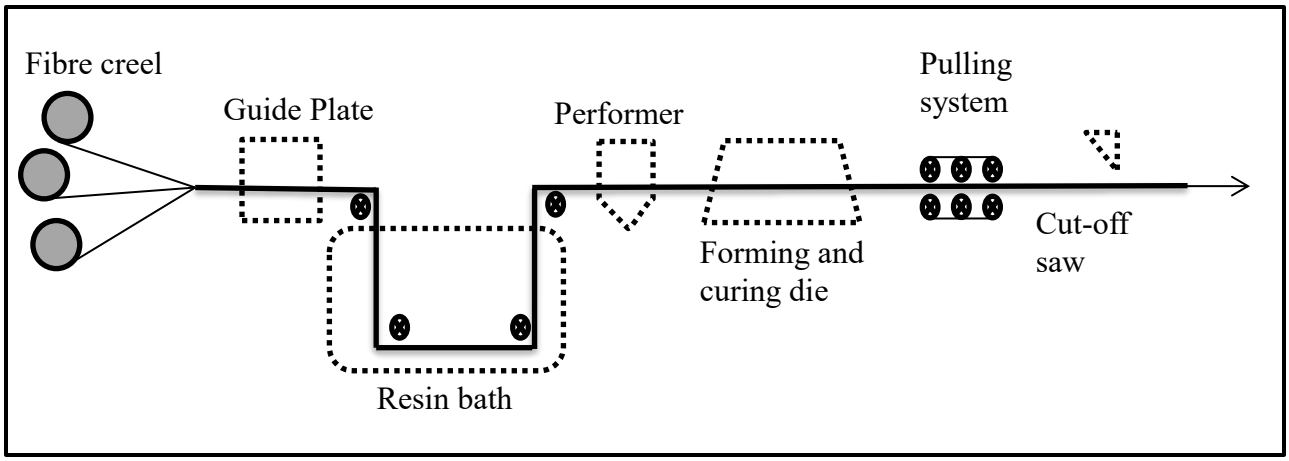

Figure 4: Schematic diagram of pultrusion process

The principles of selecting the right manufacturing processes for natural fibre composites are different with that to be used for traditional polymers. The properties of reinforced composites are significantly reliant on the content, orientation, length and diameter of fibre. The surface condition of the fibre also plays a key role, as it would affect the fibre-matrix interface. To enhance this interface, mercerisation is an eminent treatment process suitable for surface treatment of fibres. Removal of a surface coating or pretreatment of fibre by using chemical treatment is required to ensure good bonding properties. Fibre treatment enhances the matrix-fibre interface; thus it allows the stress to transfer from the matrix to the fibre which holds the higher flexural modulus of the composites. The incorporation of hydrophilic fibres in polymers leads to heterogeneous systems whose properties are inferior due to poor adhesion at the fibre-matrix interface [174, 175].

Therefore, the treatment of natural fibres for adhesion improvement is a critical step in the development of the composites. Such treatments can chemically modify the fibre surface, increase the resistance to moisture adsorption as well as the surface roughness. Chemical or physical modifications on the surface of lignocellulose particles have been explored with the aim of changing the surface properties or creating reactive sites to improve the fibre–matrix interfacial bonding. Meanwhile, in addition to the surface treatment, processing techniques have been reported to play an important role as well. Four major processing techniques were reviewed in detail; injection moulding, compression moulding, hot press, and resin transfer moulding.

For thermoplastic based processing, injection moulding and compression moulding processes are recommended. Developments have been directed toward performing rheological measurements in conjunction with injection moulding machines [176, 177] and extruders [178]. In addition to in-line shear viscosity measurements, extensional viscosity has also been evaluated through contraction flow analysis. Use of an injection moulding machine delivers an advantage in that the volumetric flow rate can be directly determined from the axial screw speed during the injection, provided that the leakage flow through the sealing ring of the non-return valve is negligibly small, and that the screw speed maintains the set value exactly. The servomotor driven all-electric injection moulding machines enable accurate control of the screw speed; hence they are more suitable to be used as a rheometer than hydraulic machines.

Injection moulding of composites is a process that forces a measured amount of mixture which contains molten polymer and fibre into mould voids. Various studies have been conducted on the potential of reinforcing polymer composites through injection moulding [179-182]. Mainly the original thermoplastic polymer used by this process has been considered for plastic pellets. For fibre reinforced composites, the pellets with chopped fibres are fed individually through a funnel-shaped feed hopper into a heated compression barrel with a rotating screw (‘‘screws’’ for twin-screw extruder) shown in Figure 5. The purpose of heating the barrel is to transform the solid pellets into viscous liquid which can be drove through the sprue nozzle and lastly forced into the matched-metal closed mould cavities. The mould is tightly clamped against injection pressure where the polymer solidifies, freezing the orientation and supply of fibres. The composite is then removed from the closed mould after it is appropriately cooled to be ejected to form a part of desired shape. As the mixture is required to move toward to the sprue nozzle, polymer is pressurised because of the screw mechanism.

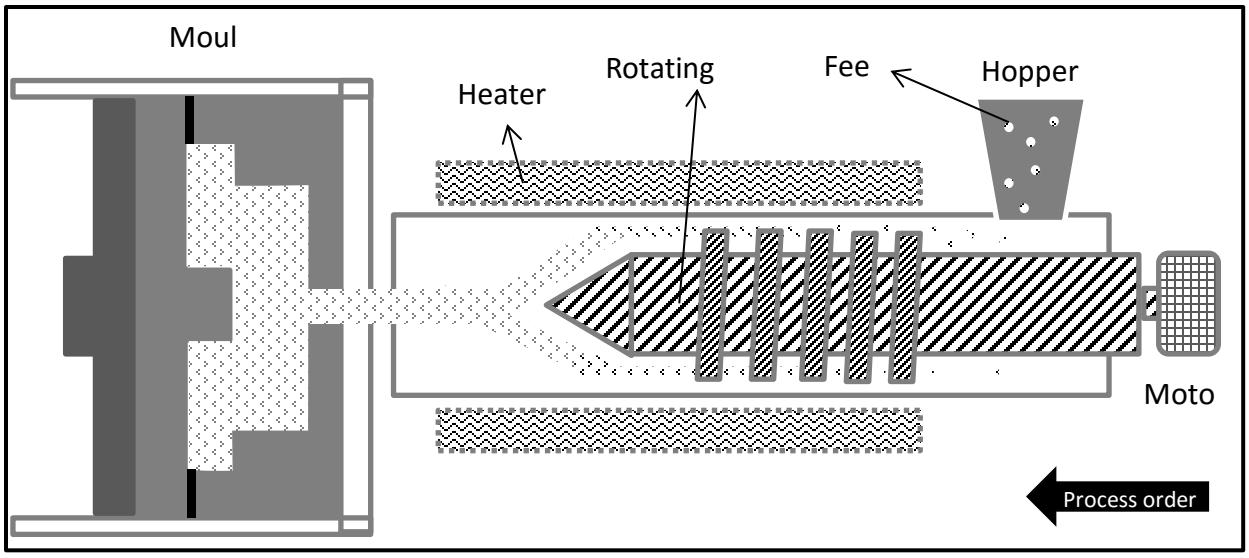

Figure 5: Schematic diagram of an injection moulding machine

The purposes of using screws are as follows:

- To produce heat by viscous shearing to melt the polymer. The heat is used for melting pellets evolved from the friction in between pellets, barrel and screw.
- To apply the shear force to mix the polymer and fibre.
- To act as a piston to drive the mixture of fibres and molten polymer through sprue nozzle into a matched-metal closed mould.

As the temperature increases, the shear viscosity of biodegradable polymers such as PLA would decrease which makes the flow easier. Besides, as the shear rate increases, the viscosity of the polymer melts would also be decreased significantly. Mainly the breaking of PLA molecule chains due to the strong shear forces and temperature causes this change of viscosity.

The fibre used in the injection moulding is commonly chopped into short fibre according to the critical fibre length principle; the stress should be completely transferred from the matrix to the fibre and the fibre can be loaded to its full capacity assuming a good interfacial bonding is resulted. However, the traditional injection moulding process limits the fibre length that solidifies in the final part since the high shear rates in the barrel and the passage of fibres through

narrow gates and openings in the mould which cause major fibre attrition. Therefore, the fibre length in practice is normally shorter than the predicted fibre length because of the fibre attrition. This fibre attrition causes the fibre length below the critical length as expected, the fibres shorter than the critical length would not be able to carry their maximum load effectively.

In an extreme case, the fibre rather acts as a defect in the material not only because of its length effect, but also on the poor bonding properties. Nevertheless, if the fibre length is beyond the pre-determined critical length, it will carry an increasing fraction of the applied load and may fracture prior to the failure of the matrix. Therefore, it is necessary to carefully determine the critical length of the fibre before injection moulding is performed. On the other hand, increasing fibre content would ideally improve the stiffness and the strength of resultant composites. However, in practice, the traditional injection modelling process would limit the amount of fibres to be injected because of the fibre cluttering, narrow gate and sprue and, viscosity of the fibre/polymer mixture. There are several critical issues that affect the modulus distribution of the injection moulded composites; the volume expansion of the fibre after mixing with the liquid form of matrix, residual stress, and fibre orientation with respect to the depth.

Residual stress is an internal stress which happens as a result of the fast cooling of molten polymer in the absence of external forces. Generally, the residual stress distribution shows tensile stresses at the surface and core regions and compressive stress at the intermediate region, which is well known as the characteristic residual stress distribution in injection-moulded parts [183]. Since 1990s, thee levels of stress in laminated structure has been recognised; the ‘micro-stresses’ present among fibres within each ply, the ‘macro-stresses’ developing in multi-axial laminates at the ply-to-ply scale, and a third more dominant level of stress resulting from different thermal histories of different parts of a laminate during the cooling sage [184].

In a neat thermoplastic polymer and in its fibre composites, residual stress causes a former fracture of the composites which directly affects the quality of products. The pressure history of the molten mixture at the beginning of the injection moulding process to the end of filling up the mould cavity influences the stress distribution along the flow path [185]. The residual stress

results in shrinkage of the final product; the dimensional accuracy and properties of the final products are highly related to the residual stress distribution in the moulded part consequently.

Furthermore, following the high process temperature, change in moisture absorption characteristics, in addition to impurities and voids formation inside injection moulded composite could take place. Therefore, studies on residual stress can play a critical role in parameters selection. Process, material and geometric parameters need to be optimised to avoid any progress of residual stress causing warpage, stress cracking, or long term deformation. This prevention involves controlling the melt temperature, injection and screw speeds, injection pressure and the mould temperature during the process. Increasing mould temperature results in a decreasing overall stress level, while the compressive stress region is shifted onto the surface [186, 187]. Molten polymer rheology, and fibre type and content are the material parameters which have a direct influence on the manufacturing process and the properties of resultant composites [188, 189]. Moreover, the geometric parameters such as the mould cavity shape and size, the locations of injection gates and the vents that allow the air to escape also play a key role on the residual stress formation [190] .

Natural fibres are only subjected to a low thermal stress [191]. Fibres have rarely appeared to have a direct effect on the matrix orientation and direct effects has been observed following an increase in fibre concentration [192]. Following the heat generated during the injection moulding, fibres are therefore oriented. During the solidification of the matrix, the orientation of the fibres is fixed. At low flow rates, the rotating screws make a decrease in alignment parallel to the flow direction. The fibres alignment follows the shearing as well as the stretching direction of the injection flow; this takes place near the mould walls called the skin shown in Figure 6. Beneath the skin layer, the molten mixture remains undergoing the shear and fibres orient along the shear lines accordingly. After the skin formation, the core layer is formed as the fibres are swayed by the bulk deformation of the flow in the mould. The skin-core structure shown in Figure 6, presents a common ‘micro-structural’ observation.

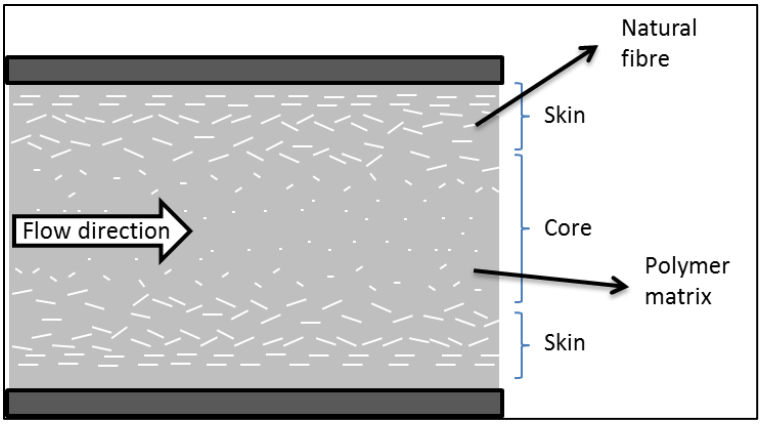

Figure 6: Influence of flow on fibre orientation during injection moulding

The technique to observe the skin-core arrangement in lab scale preparations with low fibre content is challenging. During 2001, dumbbell shaped composites have been suggested to enhance the observation [193]. Recently, studies have suggested the application of Computational Tomography (CT-scan) to identify the amount, dispersion and orientation of components in the hosting matrix [194].

2.3.2. Mechanical properties of biocomposites

Fibres as reinforcing materials are classified based on their impact on polymer composites. During the last one decade, addition of fibres into polymer matrix, regarding their shapes, particle sizes and the source that they are brought from, found to result in different microstructures. Meanwhile, the mechanical and thermal properties, which are the main concerns among both manufacturers and consumers, noticeably improved since fibres had a much higher strength and stiffness values than those of the polymer matrices (Table 7). Brief descriptions of common mechanical properties of reinforced biocomposites are summarised in the following subsections.

Table 8: Mechanical properties of common (a) polymers [42, 195, 196] and (b) fibres [197-199] used in biocomposite fabrications

	Tensile strength (MPa)	Elastic modulus (GPa)	Elongation (%)
(a)			
PP	26–41.4	0.95–1.77	15–700
LDPE	40–78	0.055–0.38	90–800
HDPE	14.5–38	0.4–1.5	2.0–130
PS	25–69	4–5	1–2.5
(b)			
Cotton	350–450	5.5–12.6	7.0–8.0
Coir	500–600	4.0–6.0	30–40
Flax	500–1500	27.6–28.5	2.7–3.2
Hemp	600–700	70–80	2–4
Jute	390–770	26.5–28.5	1.5–1.8
Kenaf	900–950	53–57	1.6–1.8
Ramie	400–938	61.4–128	3.6–3.8
Sisal	500–630	9.4–22	2.0–2.5
Softwood	900–1000	40–50	4.4–5.1

2.3.2.1. Tensile properties

Tensile strength is important for a material that under goes stress or tension during strain. During the tensile test, the force required to break a sample specimen is measured and the extent to which the specimen stretches or elongates to breaking point is recorded. The outcome of this test is a stress strain diagrams used to determine tensile properties. Additionally, data collected through this test can help specify optimal materials, design parts to bear application forces, and deliver key quality control checks for materials.

Fibres are much stiffer than polymer matrix and as a result the added stiffness to the biocomposite is expected accordingly. For instance, remarkable improvements in tensile strength at the presence of only 8 wt. % of cellulosic material was reported [28]. In a similar work, an

increase in tensile properties was referred to the reinforcing fibre stiffness correspondingly [75]. Identically, it was found that coupling of fibre with functionalised polymer, increases tensile yield stress, tensile strength and more importantly deformability considerably [29]. Meanwhile, stabilisers are found to be beneficial to enhance the tensile strength properties. Irgastab and Tinuvin were concluded to be efficient stabilisers for cellulose reinforced composites [200]. Also, on the other hand, studies provided a noble indication of tensile properties reduction due to any moisture content.

One of the world's most widely used petrochemical products is polypropylene. It is used in a wide range of commercial and household applications such as automotive components and films. polypropylene is a linear polyolefin hydrocarbon polymer, expressed as C_nH_{2n}. It is one of those most available versatile polymers with applications, both as a structural plastic and also as a fibre. Table 8, listed the final tensile strength values achieved through reinforcement of polypropylene based composites with natural fibre materials.

Table 9: Polypropylene based biocomposites tensile strength values

Fibre type	Tensile strength (MPa)	Fibre content (wt. %)
Hemp [201]	51	30
Oil palm shell concrete [202]	50	-
Flax [201]	50	30
Recycled newspaper [22]	49	50
Sisal [201]	48	30
Grape seeds [203]	25	30
Eucalyptus globulus sawdust [203]	23	30
Energy grass [203]	21	30
Brassica rapa [203]	20	30
Norway spruce [203]	19	30
Pine cones [203]	19	30
Alfa [204]	31.9	5

Hemp [205]	29	10
Hemp [206]	28	20
Doum [207]	26	15
Baggase [204]	32.9	15
Flax [208]	40	30
Date palm wood flour [209]	21	5
Kenaf [210]	32	25
Abaca strands [211]	48.8	40
Wood [28]	38	32
Oil palm empty fruit bunch [95]	33	30
Luffa [212]	35	2
Flax [213]	48	30

Following Table 8, the range for tensile strength of neat polypropylene was reported to be 26–41.4 MPa; hence, to attract the attention of both manufacturers and consumers, a value higher than 40 MPa for tensile strength is required. Based on the values in Table 8, as well as the findings through a research on natural fibres reinforced biocomposites during the year 2000–2010 [214], the reinforcement of recycled newspaper seems to be one of the most novel material amongst the commonly cited fibres. Until today, towards enhancing the tensile properties of polypropylene, reinforcements based on oil palm biomass, hemp, flax, abaca and sisal fibres appear to be more suitable compared to the other fibres [215].

Decreases in tensile values by increasing the fibre loading amount were observed [216-218]. This reduction in tensile properties was referred to the fibre length and fragile characteristic, as well as the decohesion between the matrix and fibres under stress [54]. It was explained that this decohesion provides a stress concentration which increases the sample breakability. Meanwhile, it can be seen that compared to polypropylene, there are few studies focusing on the influence of natural fibres on the tensile properties of LDPE and HDPE.

Tensile properties similar to LDPE and HDPE reinforced with fibres were observed during the studies on reinforcements of polystyrene with hemp fibre. It was found that the tensile and flexural strength of hemp reinforced polystyrene composites are 8% lower than fibre glass composites [219]. In order to preserve this composition (hemp/polystyrene) competitive fibre glass, a chemical treatment with alkyl ketene dimmer (AKD) was introduced to maintain the composite properties and also to improve the tensile and flexural properties as well. The treatment of hemp fibre with AKD decreases the fibre polarity and also enhances the interfacial adhesion and compatibility between the matrix and fibre. Hence, following this type of treatment, the tensile and flexural strength of hemp/polystyrene composites becomes close to the strength of fibre glass composites. Moreover, bamboo fibres were found to be one of the suitable reinforcing fibres for polystyrene based matrices [220, 221]. Furthermore, alkali and silane treatment of fibre was recommended to increase the tensile and flexural properties; they increase the fibre durability and decrease the fibre hydrophilic activities [222, 223].

Natural fibre reinforcement results deformability of the rigid interface between the fibre and matrix which could be another reason for this decrease in tensile properties of such polymers (LDPE and HDPE) [224]. Mercerisation of fibres was suggested to enhance fibre–matrix interfacial bonding and tensile properties of biocomposites [90, 225]. Hence, following the available gap in studies and more importantly the huge demand of consumers, further studies are required to investigate the optimum methods to enhance the tensile properties of LDPE and HDPE based biocomposites reinforced with natural fibres.

2.3.2.2. Impact properties

Impact strength describes the ability of a material to absorb shock and impact energy without breaking. Based on ASTM D256, a pendulum swing on its track and strikes a notched, cantilevered plastic sample. The energy lost (required to break the sample) as the pendulum continues on its path is measured from the distance of its follow through. Methods such as Izod, Charpy, Gardner, tensile impact, and others different methods are followed to measure the impact resistance of the materials.

Basically, poor performances are reported during notched Izod test, for polymers that are sensitive to the stress concentrations. To overcome this issue, the researchers suggested reinforcement of fibres, while it should be noted that not all reinforcements resulted enhancement. Hence, to assure the enhancement of matrix impact strength by fibre reinforcement, studies strongly advised fibre treatments prior to any reinforcement. Nevertheless, it should be mentioned that the amount of reinforcement is the other fact that requires consideration.

During the reinforcement of polypropylene with abaca, microspaces at the interface of fibre/matrix were observed due to the poor interfacial bonding [84]. It was found that these microspaces caused microcracks and due to the crack propagation a decrease in the impact strength was detected. On the other hand, the treated abaca/polypropylene composites showed higher impact strengths (up to about 50 %) than those of the untreated ones, indicating that enhanced interfacial bonding between the matrix and the filler occurred upon chemical treatment. Meanwhile, sisal fibres were found to be more suitable to polypropylene based composite due to the porous nature of the sisal fibre, its microfibrillar angle and lumen size, which are able to increase the impact strength [60]. Many researchers using oil palm empty fruit bunches (EFB) as reinforcing materials reported an improvement in the impact properties.

The incorporation of cellulose fibres isolated from EFB showed significant enhancement in the impact properties of polypropylene [226]. This was due to the better adhesion and compatibility of cellulose fibre with the polymer matrix resulting in higher impact strength compared to the EFB fibre reinforced composites. Table 9, showed the highest value of impact strength achieved by a natural fibre reinforced polymer composite.

Table 10: Impact strength of a natural fibre reinforced polymer composite

Reinforced polymer	Fibre source	Impact strength (J m^{-1})	Fibre content (wt. %)
Polypropylene	Wood [28]	29 (Notched Izod)	32
	Oil palm empty fruit bunch [95]	38 (Izod)	50

	Soy stalk [79]	24.40 (Notched Izod)	30
	Sisal [82]	2.00 (Unnotched Izod)	10
	Sisal [227]	81.57 (Izod)	15
	Abaca [84]	50 (Notched Izod)	25
	Wheat Straw/polypropylene Polyethylene (6%) copolymer [45]	4.20 (Unnotched Izod)	1
High-density polyethylene	Rice Straw [36]	0.53 (Izod)	40
	Rice husk [35]	0.75 (Notched Izod)	30
	Straw stem [35]	0.75 (Notched Izod)	30
Polycarbonate	Pineapple [93]	0.70 (Izod)	5
Polypropylene	Flax [228]	1.9 (Unnotched Charpy)	40

Based on the demand as well as the future plan of a manufacturer, the amount of fibre content could play an important role. For instance reinforcement of polypropylene with 50 wt. % of oil palm empty fruit bunch presented about 97 % improvement in impact strength value [95]. Meanwhile, in cases where reinforcement of natural fibres disadvantages plays a critical role, lower fibre content could be recommended; nevertheless, in many cases lower content of natural fibre resulted in notable mechanical enhancements. Researchers were able to improve the impact properties by up to 97%, reinforcing polypropylene with 15 wt. % of sisal fibre [227]. Also, it should be noted that the treatment of fibres could play a significant role in the fibres performance during reinforcement; this may result in selecting an ideal amount of fibre content during reinforcement.

At present, there are knowledge gaps requiring further studies; for instance, the impact properties of fibre reinforced polymers composite based on several known polymers such as LDPE, ABS, HIPS, PE, or PET. Additionally, based on several studies, the addition of a small amount of glass fibre as a reinforcing agent, in addition to the natural fibre reinforcement, could be recommended for future studies [229].

2.3.2.3. Flexural properties

This mechanical testing method measures the behaviour of specimen subjected under three-point bending conditions. Similar to elastic modulus in tensile testing, flexural modulus is the slope as determined by stress over strain in the elastic region of the force versus deflection curve. Based on different standards specific procedures and structures are followed; Based on ASTM D790, the test is stopped when the specimen reaches 5% deflection or the specimen breaks before 5 % while following ISO 178, the test is stopped when the specimen breaks. A variety of specimen shapes can be used for this test, but the most commonly used specimen size for ASTM is 3.2 mm x 12.7 mm x 125 mm and for ISO is 10 mm x 4 mm x 80 mm.

Table 10 presented the highest values achieved for flexural strength properties during several different studies. It was observed that fibres, based on their natural properties, have different effect on the flexural properties of the composite. In comparison, it can be seen that Sisal fibres seem to be more suitable to improve the flexural strength of polypropylene. Polyester composites reinforced with jute fibres presented a better flexural property accordingly. Furthermore, using jute fibres [102], the flexural properties of LDPE improved up to 29 MPa. Another research [54], reported an increase up to about 380 MPa with the addition of 20 wt. % of doum fibre. It is interesting to know that the jute fibre used by Sever et al. [102], was treated with an alkali solution as well as an oligomeric siloxane solution, while the doum fibre used by Arrakhiz et al. [54] was only treated with an alkali solution. This shows that not only the treatment process, but also the nature of the fibre itself can play an important role during reinforcement. Furthermore, this shows the progress that is continuously taking place to enhance the methods used during the last decade.

Table 11: Highest flexural strength value achieved during polymer composite reinforcement

Reinforced Polymer	Fibre source	Flexural strength (MPa)
Polypropylene	Wood [28]	51
	Wood [74]	57.7
	Bagasse [32]	35.5

	Wheat straw [79]	53.8
	Ramie [55]	80
	Sisal [82]	68.84
	Sisal [227]	67.49
	Wheat straw [79]	53.8
	Corn straw [79]	49.3
	soy stalk [79]	50.8
	Abaca [84]	54
High-density polyethylene	Rice straw [36]	41.3
	Sisal [58]	32.5
	Continuous henequen [86]	130
LDPE	Doum [54]	380
	Jute [102]	28.8
LLDPE	Rapeseed waste [52]	15
polyvinyl chloride	Bagasse [33]	33
Polyethylene	Rice husk [77]	23.5
Polypropylene	Hemp [47]	140

Treatment of fibre has a key role in the finishing product performance. For instance, the flexural modulus of PE based composite prepared with 10 wt. % of acetylated rice husk fibre was found to be higher (about 1.04 times bigger) than the one reinforced with untreated rice husk [77]. Fibre treatment enhances the matrix/fibre interface; therefore, allowing stress to transfer effectively from matrix to fibre. Use of jute fibres to enhance the flexural properties of the composites was reported by many researchers [230, 231]. Similarly, several treatment processes were used for sisal fibres, which efficiently enhanced the flexural properties of polymer composites [58].

2.3.2.4. Dynamic mechanical analysis (DMA)

Dynamic Mechanical Analysis (DMA) is a testing technique that measures the viscoelastic and physical properties of solids and polymer melts, reports modulus and damping, and is programmable to measure force, stress, strain, frequency and temperature. DMA is also described as rheology of solids and also Dynamic Mechanical Thermal Analysis (DMTA) when combining the information with temperature response. Normally, as the fibre content increases, mechanical damping linearly increases.

In rheology, the linear range is determined by observing the variation in complex modulus (E*) with increasing deformation. A decrease in the parameter indicates the boundary region of linear strain. Furthermore, following the graphical results of this test, the changes in tan δ curve indicates a relaxation process and it is associated with the movement of small groups and chains of molecules within the polymer structure. Besides, quantity of fibre content has been always one of the main concerns for both manufacturers and researchers.

Studies have observed that the complex modulus (E*) is much more sensitive to changes related the particles content, than the loss factor. During a very recent investigation on reinforcement of polypropylene with Almond shells (AS) particles, to increase the stiffness, modulus and polymer chain displacement, the maximum volume of AS particles has been found to be 20 wt. % [72]. Additionally, through this research, maleic anhydride as a coupling agent has been suggested to yield the dynamical properties as they improve the chemical bonding and tensile properties correspondingly. Such coupling agents have been known to be able to amortise and decrease the stress transfer from the matrix to the particles as they reduce the rigidity of composite. Similarly in another study, a strong influence on glass transition temperature, an increase in the level of the storage modulus as well as a decrease in damping properties has been observed due to the addition of maleic anhydride [227]. Hence, the compatibility of fibre/matrix is another point requiring further attention.

For a Phenol formaldehyde based hybrid-composite, maximum loading amount of oil palm fibres to increase the modulus and damping characteristics is reported to be 30 wt. % [232]. It is

observed that the reinforcement of oil palm has increased the damping value and at the same time decreased the glass transition temperature. Furthermore, it has been found that hybridisation increases the damping value and decreases both the glass transition temperature and the activation energy.

Addition of 31 v. % ramie fibre was found to be sufficient to improve the mechanical properties of polyester resin while at the same time negligible changes have been observed on glass transition temperature [81]. Similarly, during a research on the reinforcement of polypropylene with biomass materials (Wheat straw, Corn straw and Soy stalk), minor changes in the glass transition temperature and decrease in damping properties have been observed in comparison with the neat PLA [79]. The glass transition temperature is one of the main concerns of manufacturers because the change in the glass transition temperature directly affects the product quality and performance.

Producing a lower weight composite with intermediate water absorption characteristic has been found to be the outcomes of hybridisation. The highest value of storage and loss module for kenaf reinforced HDPE composite has been found with a maximum loading amount of 17.5 wt. % of fibre [42]. Control on fibre loading brought better reinforcement effect to the system due to the optimised dispersion of fibre within the matrix. Moreover, improvement in fibre dispersion notably increased the stiffness of the matrix which resulted in a higher storage modulus value. The high E′ values with higher filler loading over the range of temperatures have been associated with better fibre dispersion within the matrix. Furthermore, it has been found that the increase in kenaf loading reduces the magnitude of tan δ max values except for the low loading fibre of 3.4 wt. %.

Based on the dynamic mechanical studies, the properties of polypropylene reinforced with flax fibre has improved compared with the neat polypropylene [228]. Moreover, the incorporation increased the softening temperature from about 50 °C for pure polypropylene to 60 °C with flax fibres [206]. However, these results changed with the addition of triacetin plasticiser due to the plasticising effect. It is believed that triacetin is capable to act as a compatibiliser for the flax/polypropylene system. Therefore, the addition of triacetin has resulted in increasing tan δ

temperature from 55 °C to 70 °C for the composites. It was also reported that the triacetin plasticiser had negative effect on mechanical properties of the composite. The results of mechanical testing indicate that triacetin changes the fibre structure by making the fibres more brittle as all mechanical properties have strongly decreased by the use of triacetin. Hence, further studies are required to select the appropriate additive, compatibiliser or plasticiser for polypropylene based natural fibre reinforced composites. Therefore, in this research, in order to introduce a more ecofriendly material, PLA was used instead of polypropylene.

2.3.3. Reinforcement of polylactic acid biocomposites

The increasing environmental pollution has forced both industries and researchers to focus on environmental friendly techniques and biodegradable materials. As a result, biocomposite materials have been introduced. They are generally product of bioplastic materials reinforced with natural bioresources. Natural bioresources have recently found their position in our daily life mainly due to their worldwide availability and also economic benefits. The application of such materials includes food packaging, automotive and biomedical sectors.

The reinforcements have shown to enhance thermal, mechanical, and structural properties of the hosting composites [144, 233]. Different biocomposites have been prepared using various bioplastic matrices such as PLA, polyhydroxyalkanoates (PHA), polyhydroxy butyrate (PHB), polycaprolactones (PCL), and poly(butylene succinate) (PBS) [234]. Following the current environmental concerns, the main advantage of biocomposites is their biodegradability. Moreover, even at very low reinforcement content (~3 wt. %), the application of bioresources results in superior properties as compared to conventional composites; lighter product, and generally enhanced recyclability [235, 236]. Density of natural fibre is nearly half of that of glass fibre which eventually assures lighter composition.

Recently researchers have reported notable improvements using cellulose nanoparticles (CNP) as reinforcing agents [237]. By using CNP, they achieved superior mechanical and thermal properties as compared to clay-based composites while maintaining the product optical transparency. Hydrophobic behaviour of cellulose content has the ability to enhance the

composite water resistant properties [238]. Cellulose as a fibril component is regularly found in naturally occurring composites, such as wood based fibres. It has a general crystalline formula of $C_6H_{10}O_5$. The cellulose content varies in each natural fibres considering the cultivation condition; Cotton: ~90 %, Flax: ~71 %, Hemp: ~70 %, Sisal: ~70 %, bamboo ~70 %, Oil palm EFB: ~65 %, Kenaf: ~50 % [221, 239].

Preparation of biocomposites based on cellulose was first through solvent casting method where aqueous solutions were developed based on bioplastic matrices [240, 241]. In addition to solvent casting, melt compounding/extrusion technique has been employed to introduce CNP to different compositions [242, 243]. Meanwhile, researchers faced aggregation and agglomeration issues using micro cellulose powders while recently following the lower reinforcement content of CNP, more efficient dispersion were observed through both techniques [244]. In general, both cellulose micro and nano particles have a polar surface and require further attention during their application in non-polar matrices. Therefore, polar matrices have been more compatible with cellulose particles. Researchers have overcome this issue by coating the cellulose surface with Beycostat NA (BNA) which is a phosphoric ester of polyoxyethylene(9) nonylphenyl ether [245, 246].

Biocomposites are mainly based on two parts; a bioplastic material (hosting matrix) and a biofiller (reinforcing agent). Among bioplastics, PLA is one the most favourable thermoplastic aliphatic polyesters. Following its acceptable mechanical and thermal properties, it has found its position in various fields, especially food packaging industries [247]. On one hand, permeability and adequate crystallinity of PLA has resulted into achieving superior mechanical properties [10]. On the other hand, the drawbacks have forced researchers to come up with solutions to overcome its poor toughness, poor impact strength, and poor processability [248, 249]. In addition to the processing parameters optimisation, addition of natural elastomers showed to enhance PLA matrix performance [248]. Researchers observed improvements in physical and mechanical properties of PLA by adding 10 wt. % of NR through melt compounding at 180 °C, 15 min and 100 rpm [250]. Addition of 10 wt. % of NR toughened PLA composites and in this way higher impact strength values were achieved [251]. In addition to impact strength, higher elongation at break values were reported by blending PLA composites with 10 wt. % of NR

[252].

NR as a toughing agent, is an eco-friendly elastomer mainly extracted from latex of Hevea brasiliensis tree found in South America [253]. Rapid crystallisation has given tear growth resistance and high tensile strength properties to NR [254, 255]. Interfacial adhesion quality between NR and the hosting matrix as well as the elastic stress transfer from the matrix to NR were found to be the two main factors that promote toughness [256]. Moreover, researchers recommended similar melt viscosity values of both NR and the hosting matrix. Polarity of NR (due to the presence of carboxyl group) needs to be considered while blended with non-polar matrices [257]. NR and PLA were acceptably compatible while it was thought that a third component could improve this compatibility. Composition of PLA with biofillers was previously found to be economically and environmentally beneficial [258, 259]. The biofillers showed to be an effective compatibilser.

Meanwhile aggregation is one of the main concerns through reinforcement of bioplastics with biofillers including CNP [244]. Studies have used various swelling agents such as Phosphoric acid (H_3PO_4), Sodium hydroxide (NaOH), dimethylsulfoxide (DMSO) to reduce nano particles aggregation in the matrix [260, 261]. Until now, through melt compounding, no studies are available on preparation of a biocomposite based on both optimised resource preparation and processing technique. PLA has an acceptable stiffness and strength while its toughness, thermal stability and impact resistance properties requires improvements.

Therefore, in this research, an optimisation was carried for CNP extraction from kenaf fibre to reinforce commercially available PLA. Standard tests were performed to achieve the optimum amount of reinforcement content as well as the best processing condition. The tests include mechanical testing, morphological analysis, thermal gravimetric analysis (TGA) and dynamic mechanical analysis (DMA). Minor drawbacks were observed which were recovered by introducing a nature plasticiser. The prepared biocomposite (CNP/PLA) was toughened using an optimum amount of polystyrene-modified natural rubber (SNR). SNR, a rubbery cis l,4 polyisoprene, is a versatile and adaptable material which has been used successfully in engineering applications [262, 263]. SNR has excellent dynamic properties, excellent resistance

to fatigue, cut growth and tearing, high resilience, low heat build-up, efficient bonding to reinforcing materials, low cost and ease of manufacture. SNR is mainly used as a modifier to improve the bonding between matrix and natural fillers by improving the surface of natural filler [264]. The main advantage of SNR over other conventional rubber is its wider range of operating temperature. It has the ability to carry a high load under compression, yet function at high strains and low stiffness compared to metals. One of the advantages of SNR over natural rubber is the more satisfactory hue of SNR. In applications where transparency or light colours are required, the application of SNR becomes more essential and beneficial as natural rubber has a yellowish-brown hue [265]. This advantage has shifted the attentions of industries and scientists towards the production and use of SNR instead of natural rubber.

2.3.4. Applications of reinforced biocomposites

The interest in natural fibre reinforced polymer composite materials is rapidly growing both in terms of industrial applications and fundamental research [170]. Industries are now increasingly looking directly at natural inputs in a more positive and proactive manner: Natural inputs are considered not only as technically valid components, but also as elements that can contribute to the premium pricing of final products because of their superior environmental attributes and their compatibility with socially responsible production and disposal requisites. In general, the most important technologies that incorporates natural fibre composite materials are natural fibres for injection moulding, bioplastics, and press moulding and also modified fibres for advanced applications. The percentage of natural fibre in the composite may vary from 10–40 %, according to the product strength and flexibility modification.

2.3.4.1. Automotive industry

The main end users that are most interested in new developments in this field are automotive, aerospace and marine industries. For instance, many interior and exterior automotive parts like, centre console and trim, various damping and insulation parts, C-pillar trim, rear parcel shelf, seat cushion parts and door trim panels are being made from natural fibres reinforced polymer composites [266]. The body of East German Trabant car in the 1950’s was the first production vehicle to be built from cotton embedded within a polyester matrix [267]. In the 1980s the first

use of natural fibre and bioresin was used in combination to create the first all biocomposite automotive door panel. In the 90's, Daimler Benz pioneered the use of coconut fibres with latex in trucks for about nine years with backrests, head restraints, bunk cushions and sun visors being produced, demonstrating the potential of indigenous fibres. Moreover, Daimler Chrysler's innovative application of abaca fibre in exterior under floor protection for passenger cars was recently recognised [268]. These panels are used on the cover for the spare wheel compartment in the three door version of the Mercedes Benz A-Class model. Owing to the extremely high mechanical strength of the fibre as well as its length, application of abaca even in highly stressed components offers great potential for different automotive and industrial applications [269].

A rich application of natural fibres was reported in Lamborghini Aventador LP 700-4 Roadster and Mercedes Benz E class. The automotive company Ford (Germany) used kenaf fibres imported from Bangladesh in the Ford Mondeo and the door panels of the Ford were manufactured by kenaf reinforced PP composites.

FlexForm is another product based on natural fibre composite. It is formulated using a carding system to vary natural and synthetic fibre formulation [270]. FlexForm's natural fibre composites were used in vehicle areas such as rear package trays, pillar covers, centre consoles, door panel, inserts and headliners for heavy duty trucks. In addition, to automotive interior trim, it is suitable for heavy duty trucks, trailers, recreational vehicle, office furniture, ceiling tile and packaging applications. Natural fibre composites used by major car manufacturers were listed in Table 11 [271].

Table 12: Applications of natural fibres in automotive industry

Automotive manufacturer	Model	Applications
Audi	A2, A3, A4, A6, A8, Roadster, Coupe	Seat backs, side and back door panels, boot lining, hat rack, spare tyre lining
BMW	3, 5, 7 series	Door panels, headliner panel, boot lining, seat backs, noise insulation panels

Citroen	C5	Interior door panelling
Ford	Mondeo CD 162, Focus	Door panels, B-pillar, boot liner
Lotus	Eco Elise	Body panels, Spoiler, Seats, Interior carpets
Mercedes Benz	Trucks	Internal engine cover, engine insulation, sun visor, interior insulation, bumper, wheel box, roof cover
Peugeot	406	Seat backs, parcel shelf
Renault	Clio, Twingo	Rear parcel shelf
Rover	2000 and others	Insulation, rear storage shelf/panel
Toyota	Brevis, Harrier, Celsior, Raum	Door panels, seat backs, spare tyre cover
Volkswagen	Golf, Passat, Bora	Door panel, seat back, boot lid finish panel, boot liner
Volvo	C70, V70	Seat padding, natural foams, cargo floor tray
Vauxhall	Corsa, Astra, Vectra, Zafira	Headliner panel, interior door panels, pillar cover panel, instrument panel

The use of natural fibre in automotive industry offers significant potential advantages in terms of mass saving, especially if the fibre volume fraction is appreciable. This has real potential for lower CO_2 emissions and lower fuel consumption when composites reinforced with natural fibres replace those reinforced with glass fibre in transportation applications. In addition, composites reinforced with natural fibres were recognised as having advantages in the end-of-life phase.

2.3.4.2. Aerospace industry

In aerospace, composites, particularly natural fibre composites, were used as early as 1920s in making airscrews [272]. Much of this early work on natural fibre reinforcement for synthetic resins was spurred on by the search for lighter materials for use in aircraft primary structures [272]. One particular example was that of "Gordon-Aerolite" developed in 1930s, a composite of

unidirectional, unbleached flax yarn impregnated with phenolic resin and hot pressed. This was used to produce a full scale main wing spar and also in aircraft fuselages during World War II, when materials supplies were restricted [273].

Cotton/polymer composites were reported to be the first fibre reinforced plastic used by the military for aircraft radar [274, 275]. After the World War II, the application of natural fibre in aerospace materials came to a near halt. However, at the end of 1990s, a surge for a lightweight and sustainable aircraft material has put the natural fibre into the spotlight again. The Advanced Manufacturing Technology Strategy (AMTS) is one such initiative to address the research problems aiming to fulfil the technical need for structural and exterior components [276]. Researchers at the State University of New York developed wood based cellulose using nanotechnology that was strong enough to strengthen plastics for aerospace application. A wood and sisal reinforced honeycomb core was also developed with high mechanical performance and other functional properties for aerospace application.

2.3.4.3. Construction industry

Another important area where natural fibre composites are finding wide applications are construction industries. Highly engineered blends of recycled paper products and colour additives can combine to provide a strong, durable composite that is functionally similar to wood. It can be used where the appearance of stone and workability of wood is desired. The grain pattern is present throughout the material, which allows the three dimensional shaping. The high stiffness and the ecofriendly composition make natural fibre composite also an ideal choice for moulded housewares and cosmetic packaging, besides decking and railing systems.

2.3.5. Biodegradation and water absorption of biocomposites

Environmental concerns have forced the manufacturers to consider the degradability of their product. According to USA Biodegradable Products Institute (BPI) standards, biomaterials are required to disintegrate within 3-month (2160 h) [3]. Degradation involves fragmentation and changes in molecular arrangement of the materials. There are different types of degradation including thermal degradation, thermos-oxidative degradation, direct and indirect photo-

degradation, irradiation degradation, mechanochemical degradation, chemical degradation, and biodegradation [277, 278]. The degradation of a biodegradable material is rarely found to be hasardous as they are a blend of several organic resources and their disposal to the soil could be actually beneficial. In the soil (disposal condition), the microorganisms employ the biomaterial to isolate chemical energy for their survival. During the natural degradation process (biodegradation), the organic resources in presence of oxygen are oxidised and convert in to ecologically accepted molecules including minerals, water, and carbon dioxide [279]. According to the European standard EN 13432, in absence of oxygen they transform in to minerals, carbon dioxide, and methane [280]. Their compatibility with soil has gained much attention amongst agricultural sectors as they have been focusing on utilising disposed biocomposites while achieving considerable increases in yield [2]. In this sector, biocomposites have directly or indirectly (as a carrier) shown their applicability to enhance the soil properties in many ways.

Farmers have been using fertilisers for many decades to improve the soil efficiency and performance. Fertilisers contain hydrophilic minerals and salts. Fast dissolution of these salts cause irrecoverable damages to both soil and plant nutrient uptake. To control the dissolution process various methods have been introduced. One method is introduction of compounds with low water solubility to slow down the dissolution process [281]. Through this method, the synthesised compounds release the nutrients over longer period of time. Depending on the soil condition (temperature, oxygen level, and pH) and plant requirements, the synthesis could be considered costly. Another method is to coat the actual fertiliser with organic compound which will progressively release the nutrients following its biodegradation in the soil. In this way, the nutrients release is followed by the biodegradation speed. This speed can be optimised by adjusting the coating thickness or employing more/less rigid compositions depending on the application. Therefore, application of bioplastics becomes more reasonable as their production is considered economic and eco-friendly, and are completely biodegradable [282].

Bioplastics are extracted from natural resources such as corn, potato, and sugarcane [283]. They became an alternative to petroleum based plastics following their global availability and facile cultivation of natural resources. Through different agriculture atmospheres, the plants are cultivated, harvested and then chemically and physically treated to collect their starch content.

The isolated starch is then refined using special enzymes to produce a specific biopolymer [284]. This product is completely biodegradable resulting mainly water and carbon dioxide. Biodegradable polymers are either plants bacterial based or synthesised using a biobased monomer. PLA is a synthesised bioplastic based on lactic acid monomers [285]. Poor thermal and mechanical performance and also high production cost are the key drawbacks of PLA [286]. Its performance is directly linked to its content and processing parameters. It is hoped that improvements in processing parameters (such as temperature and time) help the biopolymer market realisation. At the same time, as mentioned earlier, their biodegradation process needs to be considered.

An acceptable biodegradation of PLA was confirmed by researchers, despite its low degradation rate as compared to other aliphatic bioplastics [287, 288]. Through early stages of PLA degradation, the PLA chains with high molecular weight (ester bonds) are hydrolysed to form lower molecular weight chains [289, 290]. Amorphous regions provide higher hydrolysis rate as compared to crystalline regions [291]. Increase in biodegradation rate was observed following reinforcement of PLA with starch; as starch is amorphous in nature [292]. Increase in PLA crystallinity was reported to decrease its biodegradation rate [288, 293]. Introduction of a basic or acidic solution to the soil, and elevation in both temperature and humidity were found beneficial to accelerate this reaction [294]. Complete degradation and mineralisation of PLA is reported to take about 6480 h (9 month) at 30 °C whilst this value becomes 84 h at 70 °C [295]. Biodegradation rate of PLA plastic films in soil was reported at 28 mg per 24 h at 28 °C with 27 % conversation to CO_2 [296]. Higher degradation rates were observed at the core of the sample due to the high concentration of carboxylic acid groups which enhance the ester hydrolysis [297]. Meanwhile bacterial and fungal microbes can act as a catalyser [298]. Such microorganisms (polysaccharide utilisers) break ester bonds to an acid or an alcohol, which form low molecular weight chains and convert in to CO_2, water, and humus [299]. Development of fungal mycelia on PLA surface was reported after 8 weeks in soil [288].

As having thoughts of a fertiliser coating material, the biocomposites were prepared. Following ASTM standards, their biodegradation and water absorption behaviour were determined and

fitted to a polynomial model respectively. Natural conditions and parameters were selected to promote convenient and economic biodegradation process.

2.4. Summary of the literature review

Fibres with a diameter less than 500 μm had better performance as a reinforcing material. A treatment temperature of about 80–100 ºC was found to be suitable to dry the fibres. Additionally, sodium hydroxide was concluded to be the most compatible and efficient chemical for an alkali treatment, while further studies could be done to find alternatives. Moreover, alkali treatment was found to be suitable for surface treatment of fibres which could result in enhancement of fibre/matrix interface. In addition to alkali treatment, silanisation of fibres was found to be a suitable treatment for interface modification and at the same time notable improvements in specific tensile and flexural strength properties of fibres were reported following this type of treatment. Also, acetylation application was found beneficial to achieve smother fibre surface. Acetylation in vapour phase was reported to decrease the hydrophilic properties of the fibres and enhance the thermal stability. In addition, steam explosion was also presented as one of the well-known treatments during the last two decades, while based on the latest technologies, this treatment can take place in less than 5 minutes while having much higher outcomes compared to the processes used during 1990s. Moreover, alkali and silane treatment of fibres were known to enhance the tensile and flexural properties, respectively. Following the critical effect of chemical treatments, application of optimisation was found necessary. Kenaf fibre, with high content of cellulose, notably presented a higher tensile strength property as compared to other natural fibres.

There were numerous sources of biomass introduced that can be recommended for reinforcement of polymers such as the peel of mango and banana, date seed and recycled newspaper. Also, based on the mechanical properties of polymers, there are several types of polymers such as PLA, HDPE, LDPE, LLDPE, ABS, HIPS, and PET that yet require further attention. Also, in addition to plant based natural fibres, animal fibres like cocoon silkworm, chicken feather and spider silk could be suggested for future studies to provide useful solutions for the new materials developer. Furthermore, since 2012, it was observed that studies shifted from using micron sized particle to nano sized particle to enhance the performance of the polymer composites, while

using a smaller amount of material at the same time. It is clear that the tide rushing towards environmentally friendly manufacturing and product output is surging and will continue to rise for many years to come. The ongoing effort is to develop biocomposite materials with improved performance for global applications with several noble abilities.

RTM process was found to be suitable for thermoset based processes while injection moulding and compression moulding process were found to be more suitable for simple thermoplastic based processing. Compression moulding was found to be a very productive and economical technique for producing reinforced composites. During the production of such composites, increase in yield ratio as well as decrease in cycle time were recommended to be cost effective. Following the limited natural fibre length, processes such as pultrusion were not applicable as high tensile strength fibres are necessary during pultrusion process. Conventional dosing in an extruder was challenging in case of poor flow ability of natural fibres. A homogeneous dispersion of fibres in to the polymer matrix was found to have a high impact on the product mechanical performance. Furthermore, the wettability of fibres was found to play an essential role during the process. Pre-treatment of fibres was suggested to enhance the performance natural fibres through all processing stages. To fill some of the mentioned knowledge gaps, the objectives of this research were based on reinforcement of PLA.

CHAPTER 3

METHODOLOGY

3.1. Introduction

This chapter details the materials and methods used in this study. The details of methodologies and techniques adopted have been clearly documented here.

3.2. Materials

Polylactic acid (Ingeo biopolymer) (grade 2003 D, melt index 6 g/10 min, density 1.22 g cm^{-3}) was supplied by Nature Works LLC product, USA. Biopolymer granules were oven dried at 60 °C for 12 h prior to the compounding process. Polystyrene-modified natural rubber (SNR) (grade LIR-30 Molecular weight: 28000, Tg: -63 °C by Kuraray Co. Ltd., Japan) was used as the plasticiser. 10 Kg of kenaf fibre was provided by Lembaga Kenaf dan Tembakau Negara (LKTN) Company, Kelantan, Malaysia. The fibre length was < 3 cm, with 90 % cleanliness.

Five major chemicals were employed; Sodium Chlorite ($NaClO_2$, 25% solution in water, Merck Sdn Bhd); Acetic acid (CH_3COOH, 100% anhydrous, Merck Sdn Bhd); Sulfuric acid (H_2SO_4, 95–97%, Merck Sdn Bhd); Nitric acid (HNO_3, 65%, Merck Sdn Bhd); Sodium hydroxide (NaOH, pure, Merck Sdn Bhd). All the chemicals were analytical grade and used as received.

3.3. Experimental

3.3.1. Extraction of cellulose micro fibres and nanoparticles from kenaf fibre

3.3.1.1. Single factorial method

Pilot experimental designs were performed to establish a suitable ratio of distilled water to kenaf fibre through different stages of treatment. The value was finalised using the sonication equipment. It was based on the fibres circulation efficiency in distilled water during 1 hour of sonication. This finalised ratio was maintained through all treatment processes. Further to this determination, various sets of treatment with different arrangements and orders were designed to investigate the productivity of each treatment process. First set of experimental design linking

cavitation treatment to steam explosion, acid hydrolysis and mercerisation process was presented in Table 12. Where "✓" and "-" shows the presence and absence of that particular stage or chemical respectively.

Table 13: First batch of experiments; delignification efficiency

Sample	**Treatment stage**		
	Stage 1	Stage 2	
	Cavitation (400W/ 30 min)	Steam explosion (120 ºC/ 60 min)	Chemical content during stage 2
A1	✓	✓	-
A2	✓	✓	✓ (4 wt. % of KOH)
A4	✓	✓	✓ (3 v. % of acetic acid)
A5	-	-	-
A6	-	✓	-

The second experimental condition was designed to investigate the bleaching efficiency of sodium chlorite ($NaClO_2$). The experimental condition of the bleached batch was presented in Table 13.

Table 14: Second batch of experiments; bleaching efficiency

Sample	**Treatment process** (steam explosion (120 ºC / 90 min))	**Chemical content during treatment** (v. % of $NaClO_2$)
W1	✓	1
W2	✓	4
W3	✓	6
W4	✓	2

Based on the results of the first and the second batch of experiments, Table 14 was designed. This set involved 3 continues stages; sonication, mercerisation and bleaching process. The mercerisation process was carried out using 6 wt. % of KOH.

Table 15: Third batch of experiments; combination of mercerisation and sonication process

	Treatment stages			
	Stage 1		Stage 2	Stage 3
Sample	Steam explosion (120 ºC/ 90 min)	Chemical content during stage 1 (v. % of $NaClO_2$)	Sonication (500 W/ 30 min)	Mercerisation (20 ºC/ 120 min)
WSK1	✓	2	✓	✓
WSK2	✓	3	✓	✓
WSK3	✓	4	✓	✓
WSK4	✓	6	✓	✓

Further to the design presented in Table 13, the application of sodium hydroxide (NaOH) has been studied as shown in Table 14. The essential role of the cavitation power and frequency was observed following the outcomes of the third and fourth experimental design. Hence, a further experimental condition was designed using the 1000W sonication probe as shown in Table 15.

Table 16: Fourth batch of experiments; influence of mercerisation prior to cavitation process

	Treatment stage				
	Stage 1		Stage 2		Stage 3
Sample	Steam explosion (120 ºC/ 90 min)	Chemical content (v. % of $NaClO_2$)	Steam explosion (120 ºC/ 90 min)	Chemical content (wt. % of NaOH)	Sonication (600 W/ 30 min)

R1	✓	3	✓	250	✓
R2	✓	3	✓	250	✓
R3	✓	3	✓	250	✓
R4	✓	3.50	✓	370	✓
R5	✓	3.50	✓	370	✓
R6	✓	3.50	✓	370	✓
R7	✓	4	✓	370	✓
R8	✓	4	✓	370	✓
R9	✓	4	✓	370	✓
R10	✓	4	✓	500	✓
R11	✓	4	✓	500	✓
R12	✓	4	✓	500	✓
R13	✓	5	✓	500	✓
R14	✓	5	✓	625	✓

The effect of two strong acids was studied. Fifth batch of experiments was designed based on the thermal and morphological results achieved through the first five designs (Table 16). Where “S” and “N” denote sulfuric acid and nitric acid respectively. Table 17 was designed to investigate the possibilities of reducing the treatment duration, energy, and chemical consumption.

Table 17: Fifth batch of experiments; influence of acidic, basic, and bleaching treatment prior to sonication process

	Treatment stage						
	Stage 1		Stage 2		Stage 3		Stage 4
Sample	Steam explosion (120 ºC/	Chemical content (6 v. %	Steam explosion (80 ºC/	Chemical content (15 wt.	Steam explosion (80 ºC/60	Chemical Content (v. %)	Sonication (700 W/ 18 ºC

	90 min)	of $NaClO_2$)	60 min)	% of NaOH)	min)		bath) (min)
P1	✓	✓	✓	✓	✓	0.05S+0.15N	15
P2	✓	✓	✓	✓	✓	0.05S+0.15N	30
P3	✓	✓	✓	✓	✓	0.05S+0.15N	45
P4	✓	✓	✓	✓	✓	0.3S	15
P5	✓	✓	✓	✓	✓	0.3S	30
P6	✓	✓	✓	✓	✓	0.3S	45
P7	✓	✓	✓	✓	✓	0.1S+0.2N	15
P8	✓	✓	✓	✓	✓	0.1S+0.2N	30
P9	✓	✓	✓	✓	✓	0.1S+0.2N	45
P10	✓	✓	✓	-	✓	-	15
P11	✓	✓	✓	-	✓	-	30
P12	✓	✓	✓	-	✓	-	45

Table 18: Sixth batch of experiments; influence of treatment orders

	Treatment stage				
	Stage 1	Stage 2			Stage 3
Sample	Steam explosion (120 ºC/ 15 min)	Chemical content; (N1-N14: wt. % of NaOH); (N15-N16: v. % of $NaClO_2$)	Steam explosion (120 ºC/ 15 min)	Chemical content; (N7-N12: v. % of $NaClO_2$); (N13-N14: v. % of sulfuric acid); (N15-N16: wt. % of NaOH)	Cavitation (700 W/ 18 ºC bath) (min)

N1	✓	5	✓	-	15
N2	✓	5	✓	-	30
N3	✓	10	✓	-	15
N4	✓	10	✓	-	30
N5	✓	15	✓	-	15
N6	✓	15	✓	-	30
N7	✓	5	✓	2	15
N8	✓	5	✓	2	30
N9	✓	10	✓	2	15
N10	✓	10	✓	2	30
N11	✓	15	✓	2	15
N12	✓	15	✓	2	30
N13	✓	5	✓	65	15
N14	✓	5	✓	65	30
N15	✓	2	✓	5	15
N16	✓	2	✓	5	30

3.3.1.2. Extraction of micro cellulose fibre using response surface methodology (RSM)

Response surface methodology (RSM) was employed to extract MCF from kenaf fibre efficiently. Beneficial outcomes were observed using this method [300]. To have a more specific range of investigation, central composite design (CCD) was selected. Following the earlier preparations and characterisations (single factorial designs), factors levels were arranged based on three main stages; mercerisation, bleaching, and sonication. Responses of this design were based on morphological (scanning electron microscopy (SEM)) and thermal (derivative thermogravimetric analysis (DTG)) analysis. Further to confirm the removal of non-cellulosic contents results, Fourier transform infrared (FTIR) analysis was carried out.

The vapour autoclave was employed to reduce the treatment time and minimise the use of chemicals. Vapour-autoclave performs treatment process under high vacuum (~1.7 atm) that expands fibres and eases the job of chemicals for treatment purposes.

Design Expert software (V8) was used to define the response of each set of experimental design. A three-factor (A, B, and C) and three levels CCD, was designed to achieve maximal data about the process from a least number of possible experiments (Table 18). Independent variables were dosage of NaOH at first stage (A, g), amount of $NaClO_2$ during second stage (B, ml) and sonication time during stage 3 (C, min) while dependent variables (response variables) were size quality based on fibre diameter (µm), and degradation point based on DTG results (ºC). Each variable was coded at three levels, -1, 0 and +1. All levels were based on 4g of raw untreated kenaf fibre soaked in 200 ml of distilled water at any stage of treatment. Each experiment was performed in replicate and average values were taken as the response, Y. Experimental data were fitted to quadratic polynomial as well as 2-factor interaction model (2FI) model. Fitness of the models was inspected by regression coefficient R^2. Furthermore, F-value and P-value were used to check the regression coefficient significances.

Table 19: Levels of independent variables

Independent variables	**Codes**	**Type**	**Levels**					
			Minimum	Maximum	-1 Actual	+1 Actual	Mean	Std. Dev.
NaOH (g)	A	Numerical	0.08	0.24	0.08	0.24	0.16	0.06
$NaClO_2$ (ml)	B	Numerical	2.00	6.00	2.00	6.00	4.00	1.41
Sonication (min)	C	Numerical	10.00	30.00	10.00	30.00	20.00	7.07

A base mixture of 200 ml of water with 4 g of ground kenaf fibre was prepared in each run. Each chemical treatment was done in an autoclave at 120 °C, and 1.7 atm for a contact time of 15 min. During the sonication stage, a bench-top industrial ultrasonic processor (UIP 1000 hd, 20 kHz,

1000 W, Hielscher, Teltow, Germany) was used. It was equipped with an electrical generator, an IP65 grade transducer and a cylindrical titanium sonotrode (horn). Mercerised bleached fibres were subjected to ultrasound and were cooled using an external cooling jacket, where the temperature was maintained at 20 °C. During the sonication, power amplitude was set at 80 % in all runs. This resulted in a power output of 800 W.

3.3.1.3. Extraction of cellulose nanoparticles using response surface methodology (RSM)

After MCF extraction validation, CNP extraction was carried using RSM. A Similar approach using three-factor (A, B, and C) and three levels CCD, was used to achieve maximal information about the process from a least number of possible experiments (Table 19). The independent variables were dosage of NaOH at first stage (A, g), amount of $NaClO_2$ during second stage (B, ml) and sonication time during stage 3 (C, min) while the dependent variables (response variables) were size quality based on morphological studies (Given code: 1, 2, and 3; 3 is desired nano size), and degradation point based DTG results (ºC). Each variable was coded at three levels, -1, 0 and +1 (Table 19). All the levels are based on 4 g of raw untreated kenaf fibre soaked in 200ml of distilled water at any stage of treatment. Each experiment was performed in replicate and the average values were taken as the response, Y. Experimental data were fitted to a quadratic polynomial model.

Table 20: Levels of the independent variables

Independent variables	**Codes**	**Type**	**Levels**					
			Minimum	Maximum	-1 Actual	+1 Actual	Mean	Std. Dev.
NaOH (g)	A	Numerical	0.10	0.20	0.10	0.20	0.15	0.04
$NaClO_2$ (ml)	B	Numerical	4.00	5.00	4	6	4.5	0.35
Sonication (min)	C	Numerical	20.00	30.00	20	30	25	3.54

Design Expert software V8 was employed to determine the response of each set of experimental design and optimised conditions. The robustness of the quadratic polynomial model was inspected by the regression coefficient R^2. Furthermore, F-value and P-value were used to check the significances of the regression coefficient.

A constant mixture of 200 ml of water with 4 g of ground kenaf fibre was prepared in Scott bottle and chemicals were added according to the experimental design. The extraction was carried in an autoclave at 120 °C, and 1.7 atm for 15 min. The bleaching process was carried out at pH 4.0. Later, the extracted cellulose fibres were sonicated using a bench-top industrial ultrasonic processor (UIP 1000 hd, 20 kHz, 1000W, Hielscher, Teltow, Germany). It consists of an electrical generator, an IP65 grade transducer and a cylindrical titanium sonotrode (horn). The ultrasound was equipped with external cooling jacket for maintaining the temperature at 20 °C. Sonication parameters (intensity, time, and temperature) play the main role during this type of treatment and alterations result in totally different product properties. Following our earlier single factor optimisation, in this research, the power amplitude in all runs was set at 80 %. This resulted in power output of 800 W.

3.3.2. Optimisation of polylactic acid processing parameters

In order to optimise the PLA processing, the interaction of blending factors (mixing speed (rpm) (A), mixing temperature (°C) (B) and mixing duration (min) (C)) was analysed using RSM. The selected factors (blending parameters) and their levels were presented in Table 20. The factors (independent variables) were analysed based on their mechanical performance; maximum stress, young modulus, and impact strength. The mechanical responses were the dependent variables. Design Expert software (V8) generated a set of experimental trials to reach maximum results with minimal number of possible experiments (Table 20). The experimental trials were based on 3 factors and 5 levels of CCD method. The responses were then fitted to polynomial models. Quadratic polynomial model suitability was then determined by regression coefficient R^2. Moreover, F-value and P-value were employed to confirm the regression coefficient significances value.

Table 21: Levels of independent variables

Independent variables	Codes	Type	Levels					
			Min	Max	-1 Actual	+1 Actual	Mean	Std. Dev.
Mixing speed (rpm)	A	Numeric	50.00	100.00	50.00	100.00	75.00	17.68
Mixing temperature (°C)	B	Numeric	180.00	210.00	180.00	210.00	195.00	10.61
Mixing duration (min)	C	Numeric	5.00	10.00	5.00	10.00	7.50	1.77

Melt compounding of PLA granules was carried out in a Brabender PL2000-6 twin-screw compounder according to the experimental design conditions (Table 20). The compounded PLA granules were then moulded into BS6746 and ASTM D256 standards using a bench top injection moulding machine (RR3400, RAY-RAN Injection Moulding Machine, United Kingdom), at 180 °C and 90 °C for barrel and mould temperatures, respectively. Holding time for the BS6746 and ASTM D256 samples were 4 and 8 seconds, respectively. All specimens were conditioned at ambient condition for 7 days before conducting any tests.

3.3.3. Preparation of cellulose nanoparticles/polylactic acid biocomposites

The optimum processing condition of PLA was employed to prepare CNP/PLA (PN) biocomposites. The melt compounding of dry-mixed CNP with PLA granules composition was carried out using the Brabender PL2000-6 twin-screw compounder at 180 °C, 10 min and 100 rpm. The compositions detail was listed in Table 21. The compounded biocomposites were then moulded into BS6746 and ASTM D256 standard moulds using a bench top injection moulding machine (RR3400, RAY-RAN Injection Moulding Machine, United Kingdom), at 180 °C and 90 °C for barrel and mould temperatures, respectively. Holding time for the sample based on

BS6746 mould was 4 seconds and for D256 was 8 seconds. All prepared samples were placed at ambient condition for 7 days.

Table 22: Composition of the biocomposite samples

Sample name	PLA content (wt. %)	CNP content (wt. %)
PLA	100	-
PN1	99	1
PN2	97	3
PN3	95	5

3.3.4. Preparation of cellulose nanoparticles/natural rubber/polylactic acid biocomposites

SNR/PLA (PR) and CNP/SNR/PLA (PNR) biocomposites were prepared using Brabender PL2000-6 twin-screw compounder at 180 °C, 10 min and 100 rpm. PLA granules were mixed with SNR loadings of 5 wt. % (PR1), 10 wt. % (PR2), 15 wt. % (PR3) and 20 wt. % (PR4) respectively. The optimum composition (with highest mechanical and thermal performance) was selected for the final product preparation. To prepare the final product (PNR), 3 wt. % of CNP was gradually added to the stabilised and homogeneous PR blend. Similar compounding parameters were employed. CNP and PLA granules were dried at 60 °C for 12 h prior to the compounding process. All compounds were moulded into BS6746 and ASTM D256 standard moulds using a bench top injection moulding machine (RR3400, RAY-RAN Injection Moulding Machine, United Kingdom), at 180 °C and 90 °C for barrel and mould temperatures, respectively. Holding time for the BS6746 and ASTM D256 samples were 4 and 8 seconds, respectively. All specimens were conditioned at ambient condition for 168 h before conducting any tests. At this stage, PLA specimens were also employed for comparison purpose.

3.3.5. Biodegradation characteristics

Nine different type of compositions based on ASTM D256 standard dimensions were selected (Table 22). Biodegradation process of PLA based biocomposites was carried out based on a natural soil environment using accessible tools and materials. The test was done according to the

criteria defined by Harmaen et al. [297, 301]. As kenaf was collected from Malaysia, it was thought to choose the soil source from Malaysia as well to obtain more compatibility between the biocomposites and the soil. The soil for this investigation was earlier collected from the central Malaysian palm oil jungles at the University of Nottingham Malaysia campus. The soil had a pH of 6.5 (1:2 soil and water suspension) and did not contain any composting materials or enzyme activity. Same amount of natural soil was put in to 9 identical plastic containers and they were labelled as in Table 22. The nine biocomposites were buried in their respective containers. The containers containing biocomposites were placed in a room at a temperature ~28–30 °C, with a relative humidity of about 80 %. This test was carried out for continues period of 2160 h (90 days) and biocomposites were analysed subsequently using a lab-scale balance. The change in biocomposites weight was determined after 6, 12, 24, 48, 72, 96, 120, 1440, 1680, 1920, 2160 h burial in soil. During every analysis, each biocomposite was first rinsed under tab water to wash out the soil residues and then dried at 80 °C to fully remove the moisture until a constant dry weight was achieved. The initial weight of sample (before test) was recorded and named as S_0 and the secondary weight (after test) was documented and coded as S_1 respectively. The weight loss percentage was calculated using Equation 1.

Table 23: Compositions name and content

Sample	PLA content (wt. %)	CNP content (wt. %)	SNR content (wt. %)
PLA	100	-	-
PN1	99	1	-
PN2	97	3	-
PN3	95	5	-
PR1	95	-	5
PR2	90	-	10
PR3	85	-	15
PR4	80	-	20
PNR	87	3	10

Weight loss %= $((S_0 - S_1) / S_0) \times 100$ **Eq. (1)**

3.3.6. Water absorption test

Water absorption test was performed in accordance with the ASTM D 570 standard [302]. Plastic containers were used and they were filled with distilled water. The containers were kept at room condition in Malaysia (at ~28–30 °C and 80 % humidity) and the water level was maintained the same throughout the test period. This test was done for a period of 2160 h and biocomposites were weighed using a lab-scale balance. The water absorption of the biocomposites was determined after 6, 12, 24, 48, 72, 96, 120, 1440, 1680, 1920, 2160 h of soaking in distilled water. Throughout every analysis, biocomposites were moderately dried using a towel to remove the excess water on the surface until a constant weight was achieved. The water absorption percentage was calculated using Equation 2.

Water absorption % = $((W_0 - W_1) / W_{0)} \times 100$ **Eq. (2)**

Where W_0 and W_1 are the weight of sample before and after water absorption test.

3.4. Characterisation

3.4.1. Morphological analysis

Morphological studies of treated fibres and biocomposites were carried out using a field emission scanning electron microscope (FESEM) (FEI QUANTA 400F, Netherlands). Fibre samples were characterised based on their average diameter (an average value of the highest and the lowest fibre diameter in each image) and biocomposite samples were analysed and compared based on their fractured surface structure. Furthermore, transmission electron micrographs (TEM) of cellulose fibres were taken with an ultra-high resolution TEM (JEOL JEM–2100, Japan). The CNP samples were deposited from an aqueous dilute dispersion on a copper grid coated with a thin carbon film (~200 nm). The samples were observed at an accelerating voltage of 200 kV.

3.4.2. Thermal analysis

Thermal gravimetric analysis and differential thermal gravimetric analysis (TGA and DTG) measurements were carried out using ~7 mg of the samples at a heating rate of 10 °C min^{-1} from room temperature to 500 °C min^{-1} in a nitrogen atmosphere, using a thermogravimetric analyser (PerkinElmer STA 6000, USA). The tests were conducted with the samples placed in high quality nitrogen (99.5 % nitrogen, 0.5 % oxygen content) atmosphere with a flow rate of 20 mL min^{-1}, in order to avoid unwanted oxidation. For each analysis the main peak from differential thermogravimetric (DTG) analysis data was chosen as the representative of each run for comparison purpose.

3.4.3. Fourier Transform Infra-red (FTIR) spectroscopy

Changes in component content from raw kenaf fibre to MCF and CNP were analysed in an FTIR spectroscopy using a Nexus Thermo FTIR (ThermoNicolet, USA) spectrophotometer. Samples were oven dried at 70 °C for 12 h. The dried samples were mixed with KBr in a ratio of 1:200 (w/w) and pressed under vacuum to form pellets. FTIR spectrum of samples was recorded in transmittance mode in a range of 4000–400 cm^{-1}.

3.4.4. Structure and phase analysis (XRD)

X-ray powder diffraction (XRD) patterns were achieved using a high resolution X-ray diffractometer (PANalytical X'Pert PRO PW3040, Netherlands) diffractometer with Cu-K_α radiation (l = 0.154184 nm), which was operated at 45 kV and 40 mA. Scans were acquired in continuous mode over a range of 20–40 (2θ) with a step size of 0.02. Also the crystallinity index (CrI) of both samples was calculated using an empirical method shown in Equation 3 [303, 304]; $I_{002:}$ maximum intensity of the (0 0 2) lattice diffraction peak; I_{am}: intensity scattered by the amorphous part of the sample.

$$CrI\% = ((I_{0\,0\,2} - I_{am})/ (I_{0\,0\,2})) \times 100 \qquad \textbf{Eq. (3)}$$

3.4.5. Mechanical properties

3.4.5.1. Tensile strength

The samples moulded with BS6746 standard were employed for evaluation and to compare the tensile properties of PLA with the biocomposites. The test was carried out using tensile tester (TOYOSEIKI Strograph R-1, Japan). The crosshead speed utilised was 5 mm min^{-1}. Total of 7 samples were tested and an average of 5 samples was taken.

3.4.5.2. Impact resistance

The impact properties of the notched biocomposite samples prepared in ASTM D256 standard were tested using CEAST Impact Pendulum Tester (CE UM-636, USA), with a 4 J hammer. Total of 7 samples were tested and an average of 5 samples was taken.

3.4.5.3. Dynamic mechanical analysis

Dynamic storage modulus (E′), and tan δ were measured by a dynamic mechanical analyser (Perkin-Elmer Diamond DMA 8000, USA) at temperatures ranging from 30 °C to 120 °C with heating rate of 3 °C min^{-1} and a frequency of 1 Hz using single cantilever. Samples having dimensions of 10 mm length, and 2.5 mm thickness were used for DMA.

CHAPTER 4

RESULTS AND DISCUSSIONS

4.1. Introduction

This chapter addresses the aims of this study which is mainly to improve thermal and mechanical properties of PLA using CNP. Extraction of CNP and processing parameters of pure PLA were optimised using RSM and discussed in sections 4.2 and 4.3 respectively. Compatibility of CNP with PLA was determined through morphological, thermal, and mechanical analysis (section 4.4). Compatibility of CNP with PLA was improved using SNR as plasticiser and discussed in section 4.5. Finally, biodegradation, thermal degradation and water absorption behaviour of biocomposites were studied and discussed in section 4.6.

4.2. Extraction of cellulose micro fibres and nanoparticles from kenaf fibre

4.2.1. Single factorial method

4.2.1.1. Kenaf fibre characterisation

Thermal stability of raw kenaf fibre (A5) was determined using the TGA techniques (Figure 9). Kenaf starts to degrade at about 220 ºC. This point presented the degradation of lignin. Hence, this region was used as reference point to check for the lignin removal from the fibre at different stages of treatment. Through thermal analysis, the main weight loss (main drop) was expected to take place at a temperature in a range from 300–400 ºC. In this region, fibres are observed with high cellulose purity and minimum lignin and hemicellulose content.

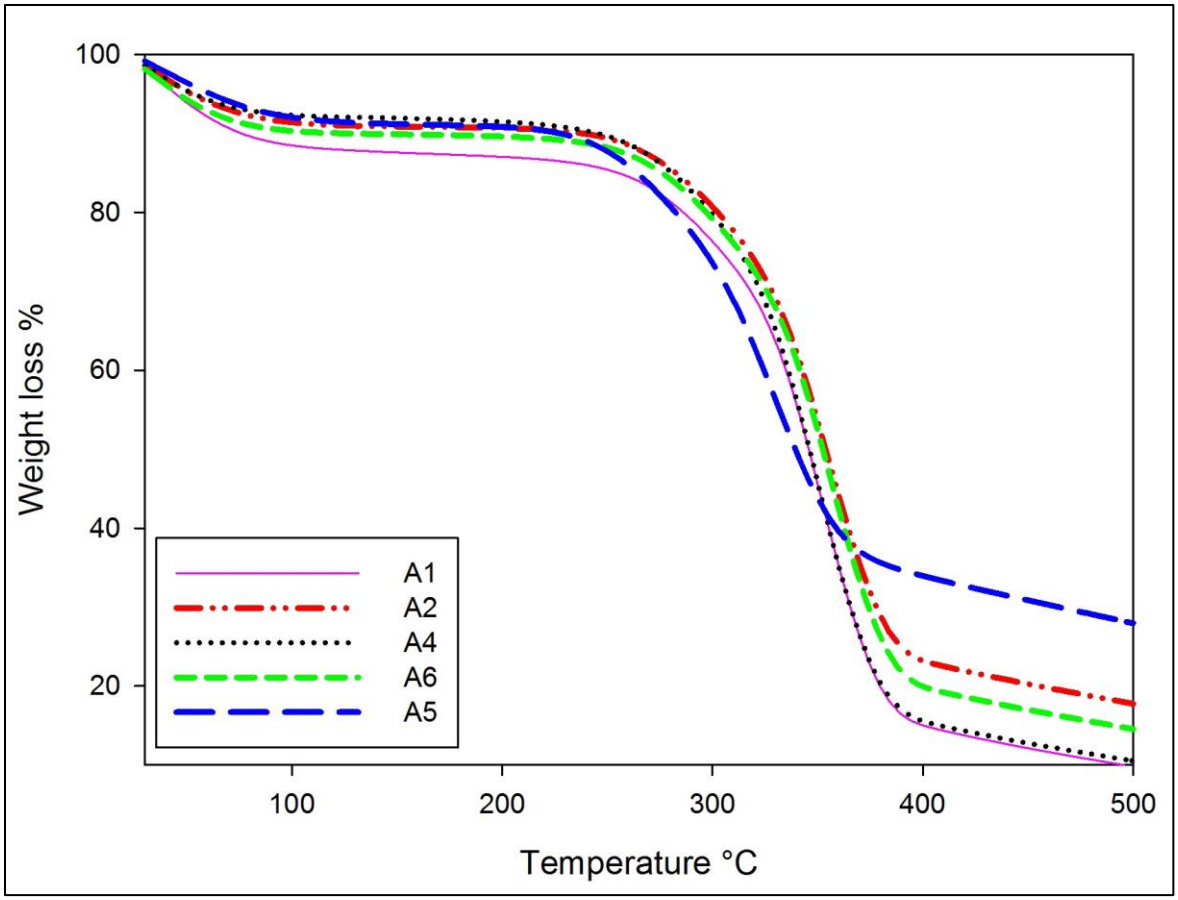

Figure 7: Percentage of weight vs. temperature curve for raw kenaf fibre and the first batch samples

Morphological structure of untreated kenaf fibre (A5) was determined using SEM machine (Figure 10). The presence of impurities on the surface of the fibre was visible. It was observed that the diameter of untreated kenaf fibre is ~180 µm. This value was used as the reference through all analysis stages to confirm the decrease in fibre diameter value. The diameter of the fibre for CNP was expected to reach 100–200 nm.

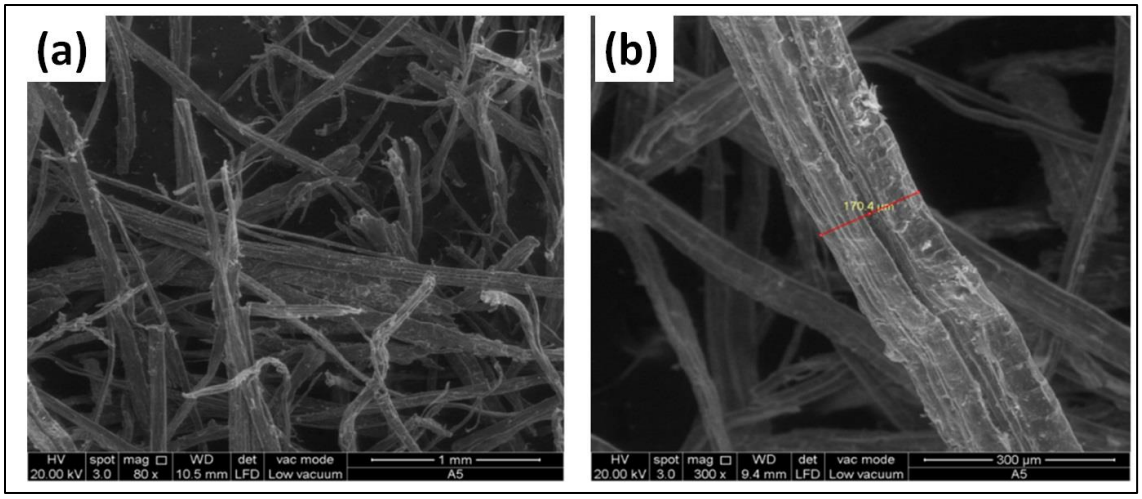

Figure 8: SEM micrographs of untreated kenaf fibre (A5); (a) 80x and (b) 300x magnification.

4.2.1.2. Influence of sonication on mercerisation and acid hydrolysis

Through trial experiments, a ratio of 4 g of ground fibre to 200 ml of distilled water was found suitable, based on the observations through the sonication process. Hence this ratio (1:50, w:v) was maintained through all treatment stages. This stage was designed to link the sonication process to both mercerisation and acid hydrolysis. Figures 9 also presents the percentage of weight loss vs. temperature curve for the samples prepared at this stage (A1, A2, A4, and A6).

A notable change in lignin content was observed. This delignification was noted as the main exothermic peak of the samples which took place at about 260 ºC. Such observation is attributed to the combination of mercerisation and hydrolysis which lead to a more efficient delignification process. At the same time, both mercerisation and acid hydrolysis decreased the thermal stability of the fibres as observed; at about 360 ºC, A5 reached only 60 % of weight loss while the other samples had reached an average of ~80 % of weight loss. This observation clearly indicated the importance of treatment process optimisation.

SEM micrographs of A1, A2, A4, and A6 were presented in Figure 11. Reduction in fibre diameter following the mercerisation process was noticeable. This was a positive response, to design further experiments to achieve the objectives of this research.

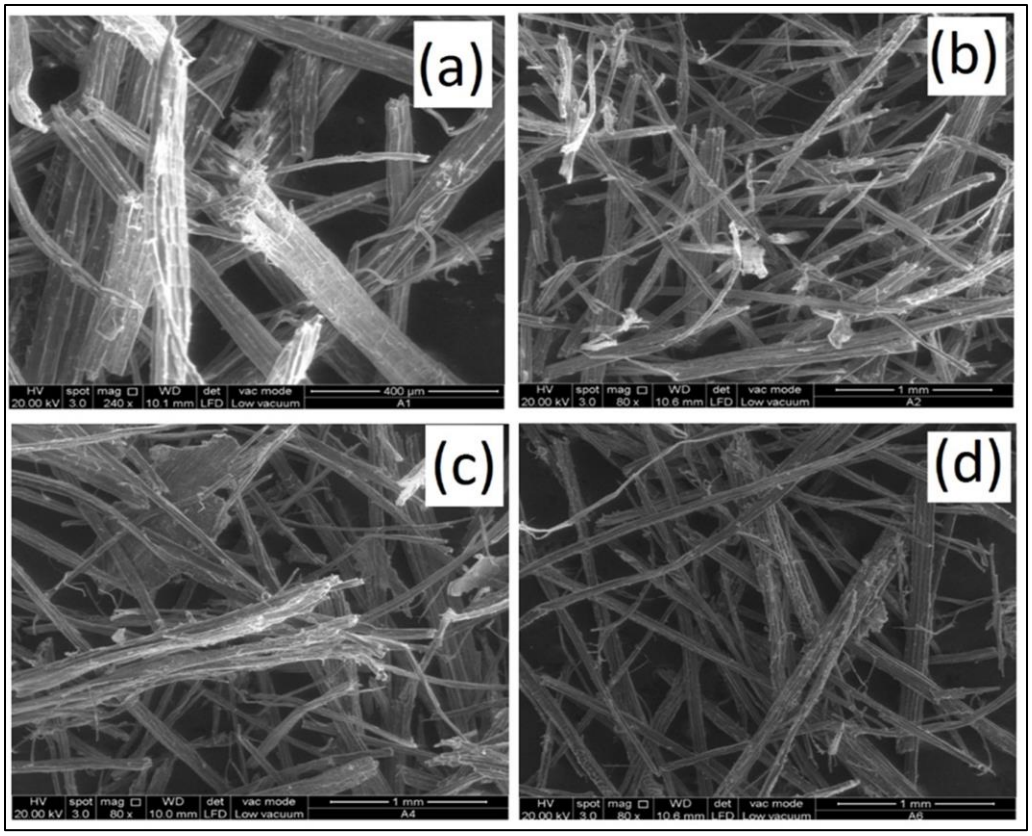

Figure 9: SEM micrographs of treated samples; (a) A1 at 240x, (b) A2 at 80x, (c) A4 at 80x, and (d) A6 at 80x of magnification.

4.2.1.3. Bleaching of kenaf fibre

The effect of bleaching on kenaf fibre was investigated. Similarly, thermal stability of the samples was characterised using the TGA technique (Figure 12). Samples showed an acceptable, and slightly higher thermal stability as compared to raw kenaf. This was linked to the removal of impurities (amorphous regions) which noticeably improved the thermal stability of the micro fibres. 6 v. % of $NaClO_2$ was observed to be the optimum amount to bleach 4 g of kenaf fibre (using 200 ml of water). The application of $NaClO_2$ resulted in acidic solution (pH of ~4). This was found favourable as it reduced the process dependability on addition of further acidic solution to complete the hydrolysis process.

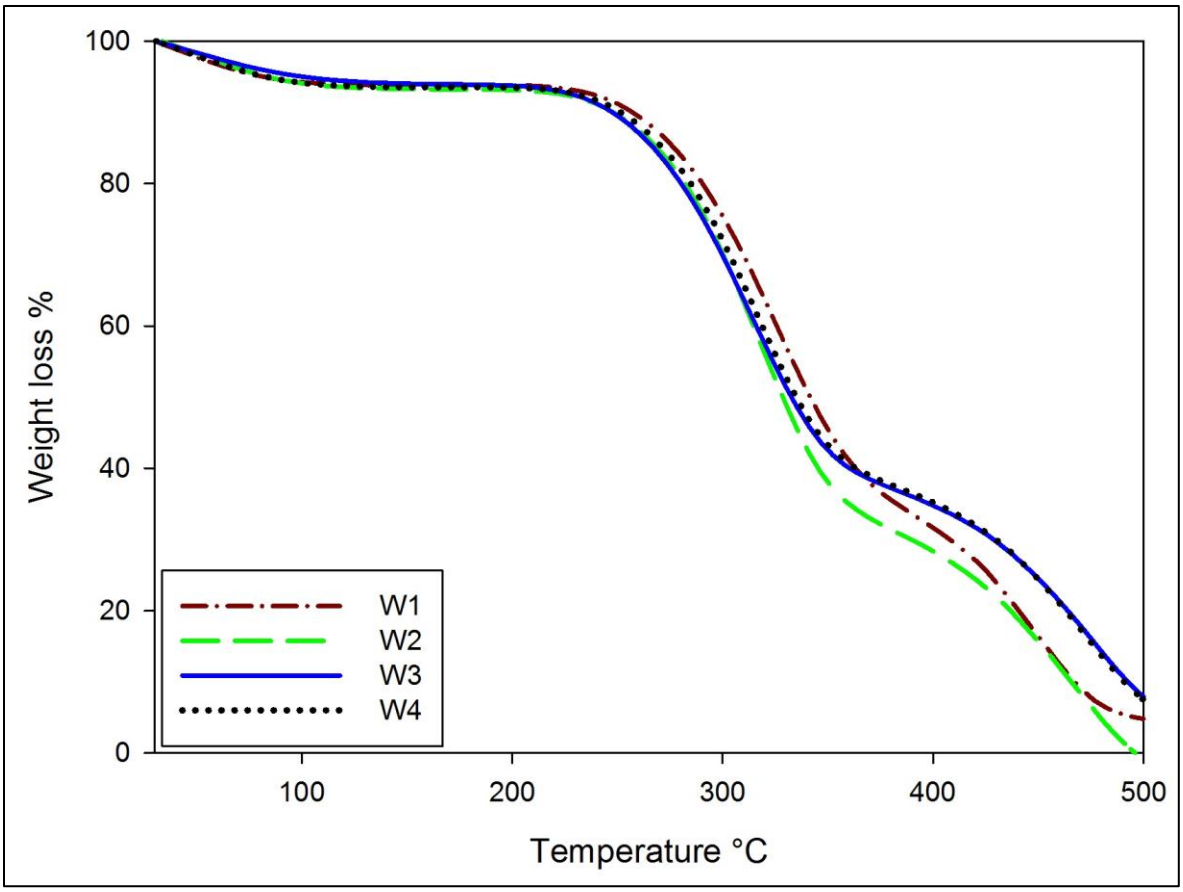

Figure 10: Percentage of weight vs. temperature curve for the bleached samples

The SEM results of the bleached samples were presented in Figure 13. Similar to the thermal analysis, the results indicate the presence of lignin as the diameter of the fibres was yet in micron size. Nevertheless, the effect of bleaching was noticeable as the fibre surface became more smooth compared to the untreated fibre. This was due to the partial removal of lignin. Hence, to derive CNP from kenaf fibre further invesitgations were carried out.

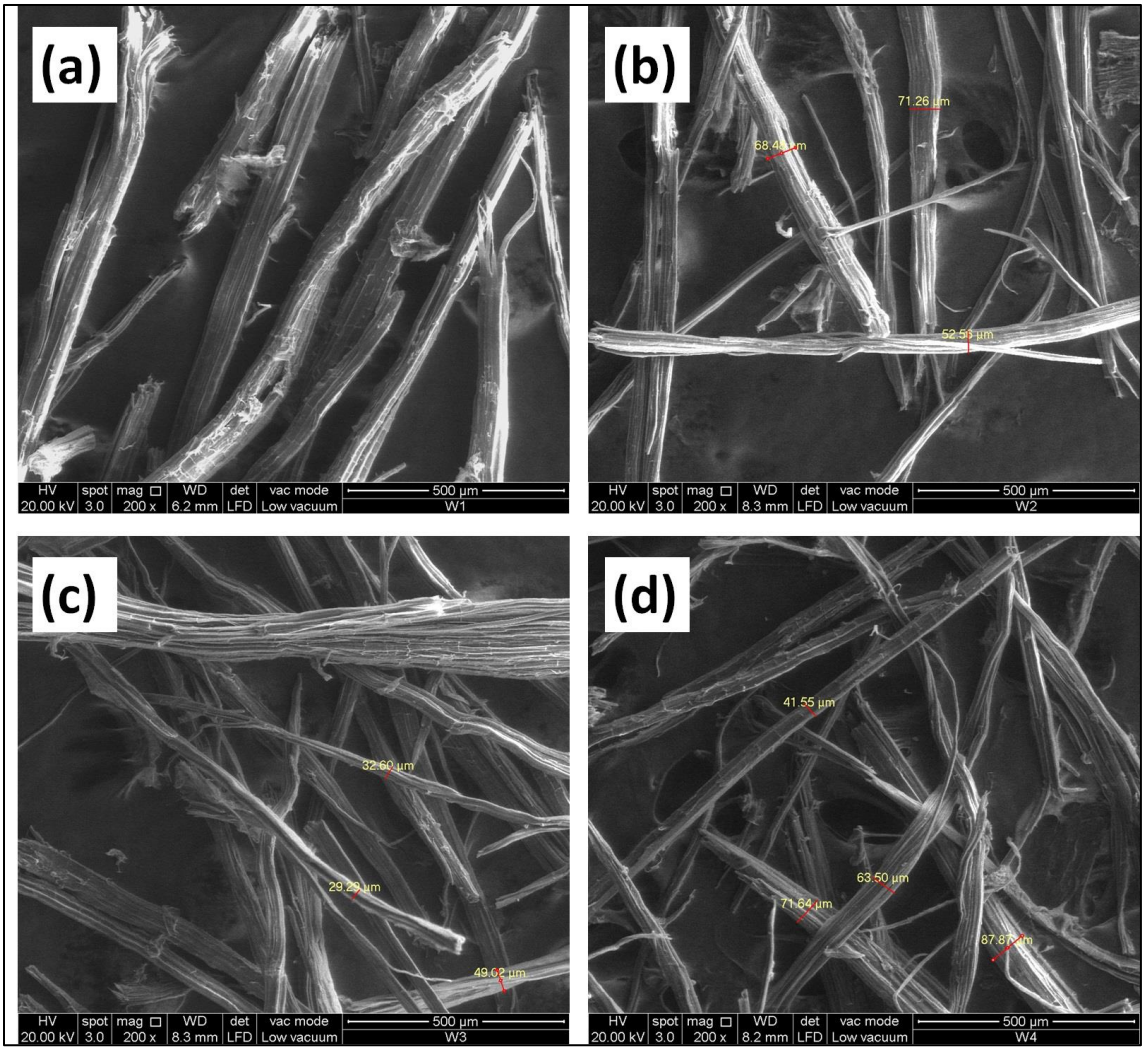

Figure 11: SEM micrographs of samples at 200x of magnification; (a) W1, (b) W2, (c) W3, and (d) W4

4.2.1.4. Influence of sonication prior to mercerisation

Influence of mercerisation process at low temperature (20 ºC) further to a cavitation process was invesitgated. WSK3 was picked as the representative from this stage of investigation (Figure 14). At this stage, in order to achieve smooth cellulose micro-fibrils, mercerisation additional to cavitation process was found be suitable. However, following the aims of this research, the proposed idea of this design was found inadequate to isolate CNP. This was further discussed through the morphological studies.

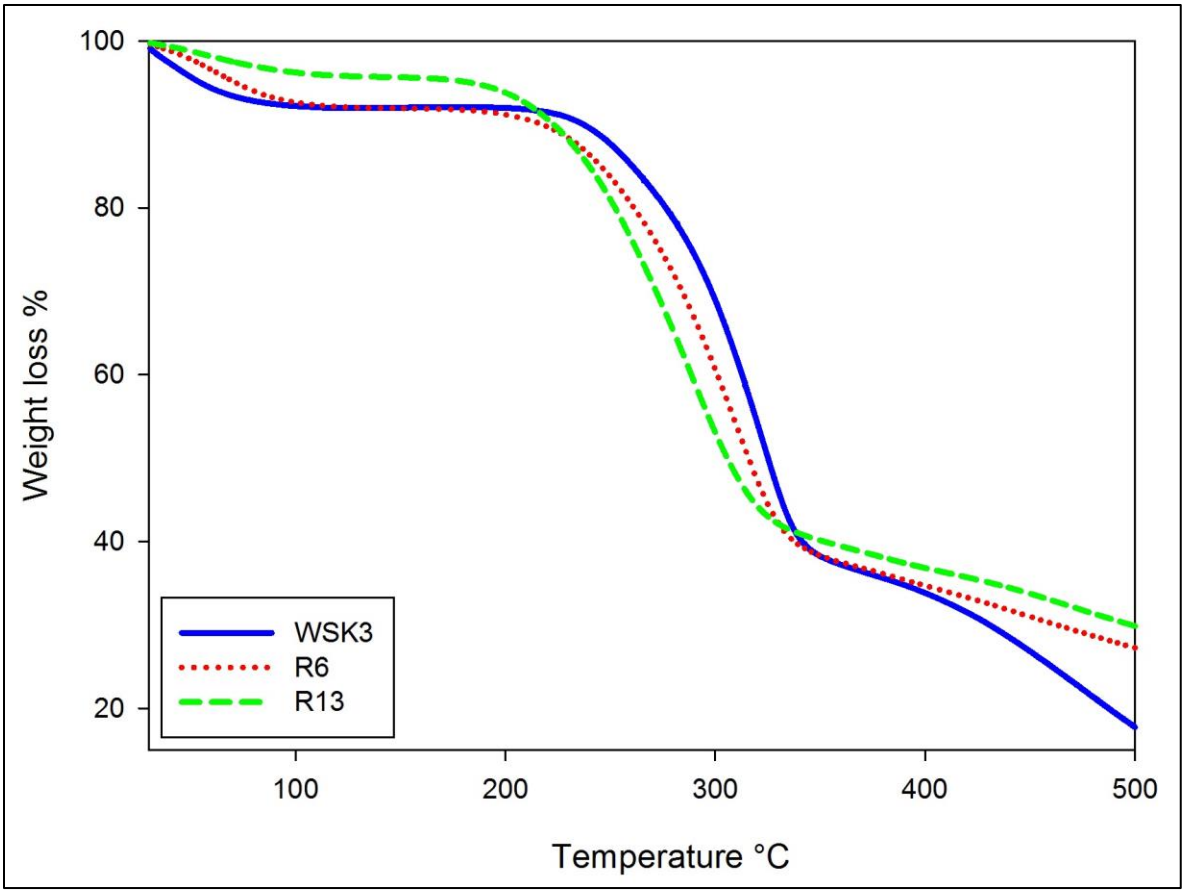

Figure 12: Percentage of weight vs. temperature curve for the sample WSK3, R6, and R13

The micrographs of WSK3 were presented in Figure 15. To achieve a homogeneous and smooth cellulose micro fibres, as discussed earlier, a mercerisation after a sonication process was found applicable. The extracted micro fibres reached an average diameter of ~15 µm. Yet, further studies were required to achieve CNP from kenaf fibre.

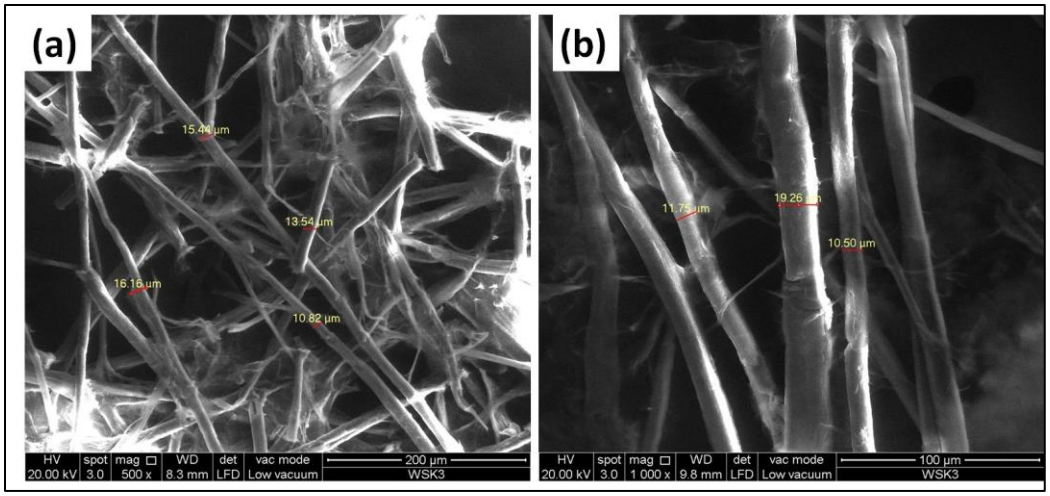

Figure 13: SEM micrographs of WSK3 at (a) 500x and (b) 1000x of magnification.

4.2.1.5. Applicability of bleaching as a replacement for acid hydrolysis

The influence of sodium hydroxide (NaOH) instead of potassium hydroxide (KOH) was determined through this stage. Figure 14, also presents the thermal stability of R6 and R13 samples. Based on environmental issues, it was thought to eliminate the application of acid. However, the presence of lignin further to the bleaching stage rejected this idea and highlighted the critical role of acid hydrolysis to achieve an acceptable delignification. Following the morphological studies, further optimisations were found necessary for extraction of CNP.

The impact of sodium hydroxide during mercerisation process was assessed. The micrographs were presented in Figure 16. A notable shrinkage in fibre diameter and removal of impurities was observed using sodium hydroxide. R6 and R13 samples, reached an average diameter of ~7 µm and ~9 µm respectively. Increase in chemical content during bleaching and mercerisation process resulted a swelling effect on fibres. Likewise, this observation showed the importance of optimisation process in such treatments. At this stage a general process for production of MCF was confirm while additional investigations were needed to conclude CNP extraction process.

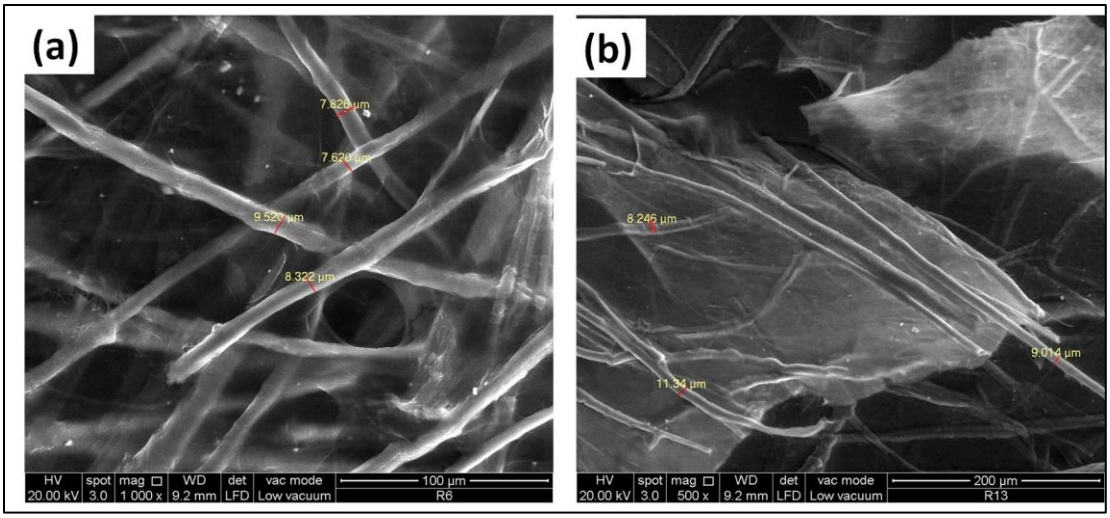

Figure 14: SEM micrographs of treated samples; (a) R6 at 1000x, and (b) R13 at 500x magnification.

4.2.1.6. Combination of sonication, mercerisation and bleaching

Following the earlier thermal analysis, the influence of various chemicals was determined. Sonication was introduced to possibly extract CNP from kenaf fibres. For further investigation, P12 was selected as the representative (Figure 17). During the treatment, the fibres were burnt and degraded due to the high acidity of the solution indicating the importance of pH level during the treatment of lignocellulosic fibres.

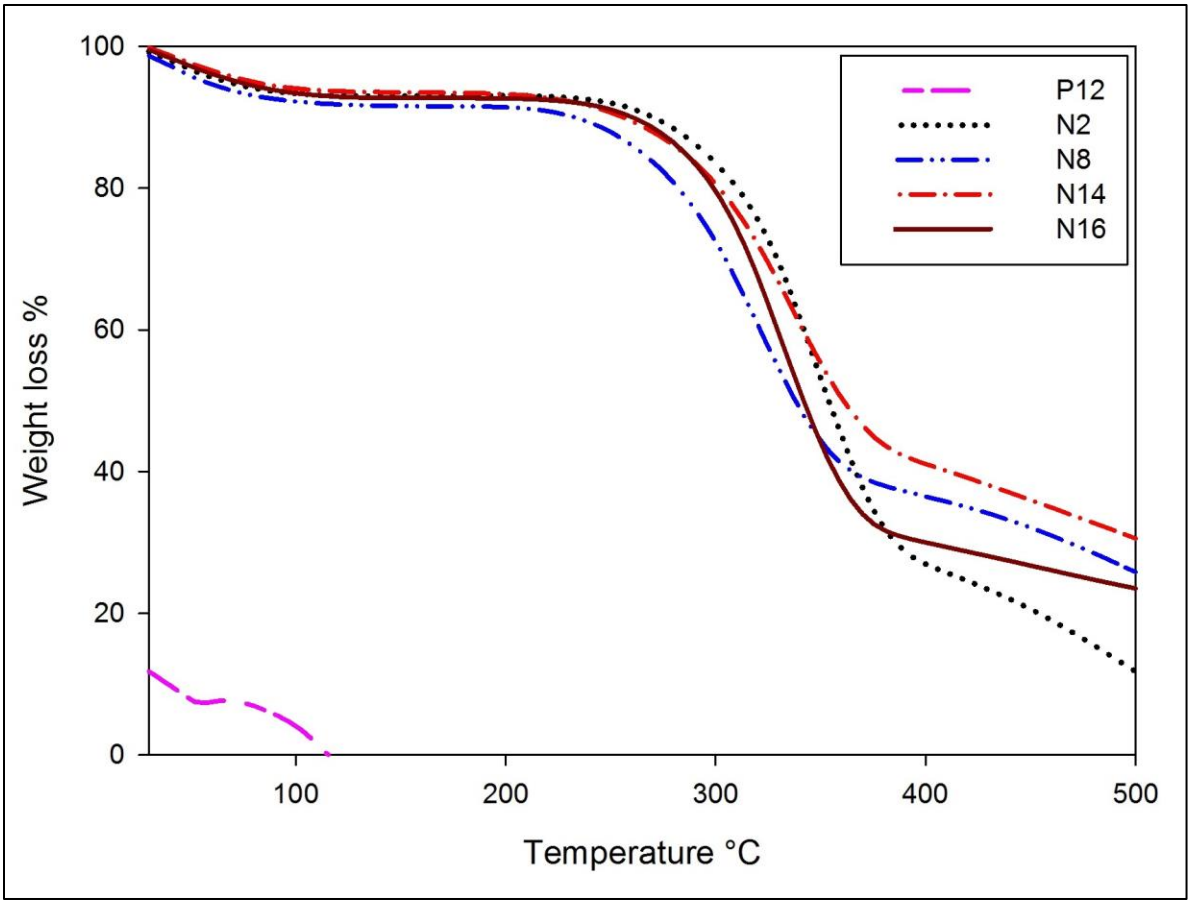

Figure 15: Percentage of weight vs. temperature curve for the sample P12, N2, N8, N14, and N16

Sonication was employed to extract CNP from MCF. The micrographs of the samples P9 and P12 were presented in Figure 18. For the first time, the SEM results indicated the presence of nanoparticles. However, the TGA results rejected the presence of any polymeric component including cellulose (Figure 17, P12). This was referred to the very low pH level (strong acidic solution) which apparently burnt the fibres. At this stage, the application of higher sonication frequency was found beneficial to reach the nano size.

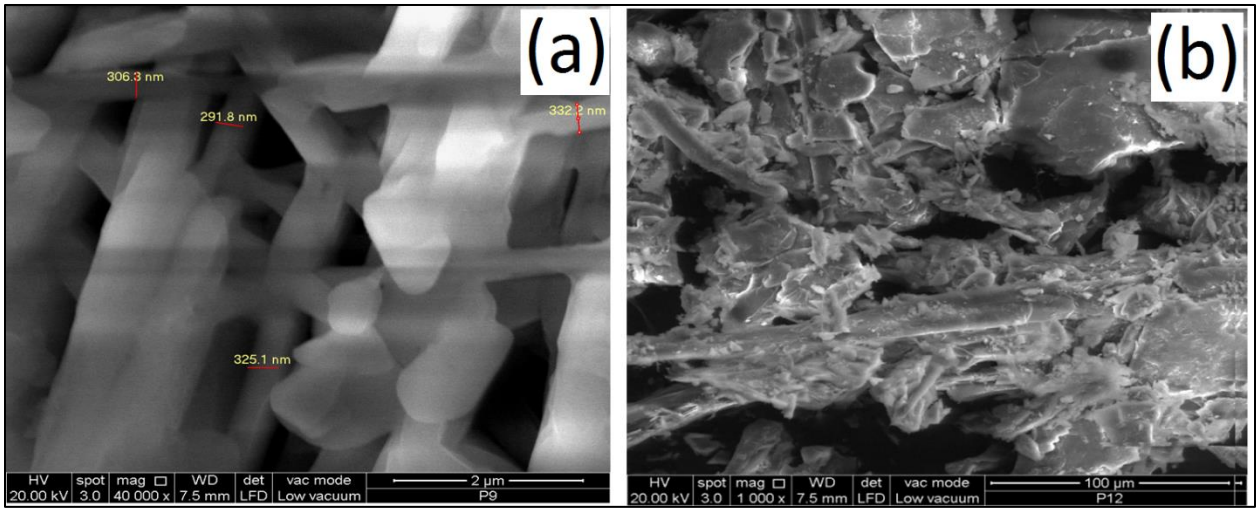

Figure 16: SEM micrographs of treated samples (a) P9 at 40000x, and (b) P12 at 1000x magnification.

4.2.1.7. Influence of treatments arrangement on the final product

The treatments arrangement was determined to improve the efficiency of the process. Moreover, the potentials of reducing the duration of extraction process, energy, and chemical consumption was explored. Figure 17 present the representatives; N2, N8, N14 and N16. Samples N8 and N2 have undergone similar treatments however during the second stage of treatment, sample N8 was involved in a bleaching process. The bleaching process resulted in extraction of CNP. Meanwhile, it should be noted that in comparison, the thermal stability of N2 was higher than N8.

Moreover, following a rearrangement in treatment orders, a notable variance in results was observed. Samples N8 and N16 had similar condition of treatment however sample N8 was first mercerised and then bleached while sample N16 was treated vice versa. The design of sample N8 resulted in perfect white CNP while the design of sample N16 exhibited brown micro-fibrils. This comparison revealed that mercerisation prior to bleaching can help to reduce the amount of employed chemicals for bleaching purposes.

The micrographs of N2, N8, N14 and N16 were presented in Figure 19. Following the addition of bleaching stage to the N8 fibres, CNP was achieved. However excess amount of $NaClO_2$, decreased its thermal stability compared to N2. At this stage, the main factors which play the most important roles through preparation of MCF and CNP were established. These factors were employed in the next stage where optimisation techniques were used to produce MCF and CNP more efficiently and ecofriendly. Figure 20 depicts the sequence of the initiated stages of extraction; grinding, mercerisation, bleaching, and sonication respectively.

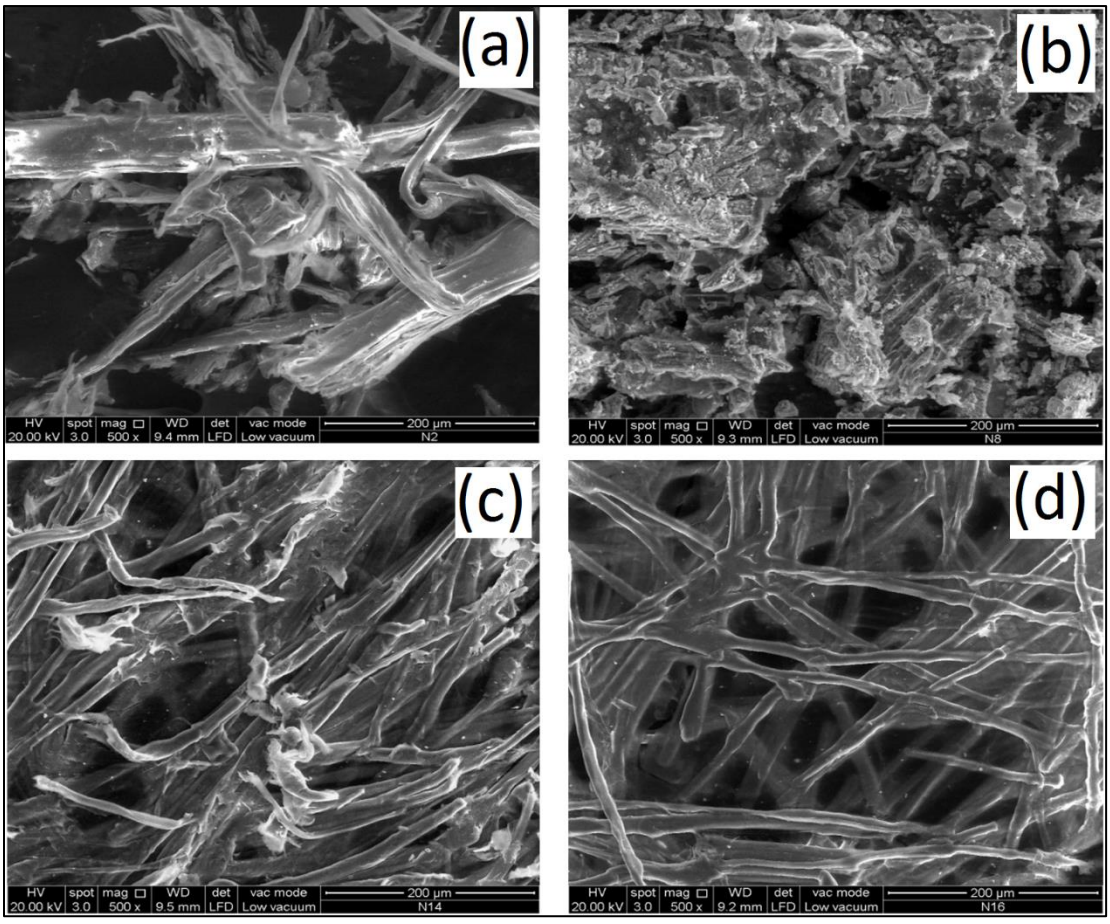

Figure 17: SEM micrographs of samples (a) N2, (b) N8, (c) N14, and (d) N16 at 500x of magnification

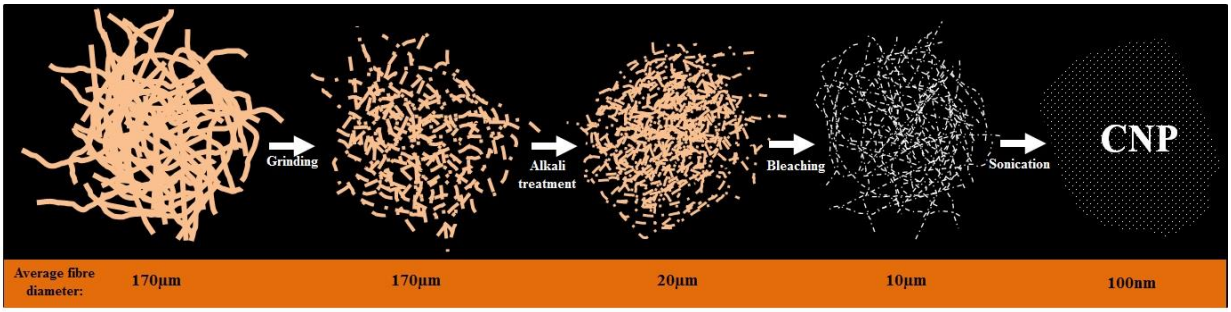

Figure 18: Extraction stages; grinding, mercerisation, bleaching, and sonication

4.2.2. Modelling and optimisation of micro cellulose fibres extraction from kenaf fibre

According to the experimental design, 20 runs were prepared and characterised respectively. Size (fibre diameter), DTG responses and independent variables for each experiment are presented in Table 23. As shown in Table 23, DTG values varied from 255–325 °C and fibre diameters varied from 10.07–55.75 µm.

Table 24: CCD design of three variables with their obtained responses

Exp. name	NaOH (g)	$NaClO_2$ (ml)	Sonication (min)	Size (µm)*	DTG (°C)
B1	0.16	4	20	14.28	316
B2	0.16	4	20	14.28	316
B3	0.08	2	10	27.03	315
B4	0.24	2	10	46.53	305
B5	0.16	2	20	55.75	311
B6	0.08	6	30	12.88	255
B7	0.16	4	30	10.07	317
B8	0.16	4	20	14.28	316
B9	0.16	4	20	14.28	316
B10	0.08	4	20	13.12	313
B11	0.08	2	30	16.83	317
B12	0.24	4	20	16.67	274
B13	0.16	4	10	13.57	315

B14	0.24	2	30	36.26	293
B15	0.16	4	20	14.30	316
B16	0.08	6	10	16.96	325
B17	0.16	4	20	14.30	316
B18	0.24	6	30	15.19	262
B19	0.24	6	10	13.81	314
B20	0.16	6	20	14.30	316

*The values are mean values of ten measurements.

The design was fitted using quadratic and 2FI models and a R^2 value of 0.89 and 0.58 were obtained for quadratic and 2FI models respectively. Therefore, quadratic model was found to be more suitable for statistical testing and was used for Analysis of Variance (ANOVA). The suitability was based on the design significance value, and Coefficient of variation (C.V). C.V percentage is a standard deviation expressed as a percentage of the mean. The lower the C.V, the smaller residuals relative to the predicted value was.

ANOVA for the fitted quadratic polynomial model of isolation of MCF based on size responses is presented in Table 24. The model F-value of 9.32 indicated that the model was significant. P-values less than 0.05 indicate model terms are significant where in this research P-value was <0.0001 favouring the design significance. Concluding equation based on coded factors was presented in Equation 4. Where A is amount of NaOH (g), B is dosage $NaClO_2$ (ml), and C is sonication time (min). Also a difference value of 0.09 showed a reasonable agreement of Adj. R^2 with R^2 value.

Table 25: Analysis of variance for the fitted quadratic polynomial model of MCF extraction (based on size)

Source	Sum of squares	Degree freedom	Mean square	F value	P value
Model	2548.48	10	283.16	9.32	0.0008
Residual	303.72	5	30.37		
Lack of fit	303.72	5	60.74	358705.8862	< 0.0001
Pure error	0.00084	19	0.00016		

Cor. total	2852.21	10

R^2 = 0.8935; R^2_{adj}=0.7977; C.V.% = 27.92.

Size = (15.74) + (4.16×A) – (10.93× B) – (2.67× C) – (4.97× A × B) + (0.67× A × C) + (2.22× B× C) – (3.02× A^2) + (17.11× B^2) – (6.10× C^2) **Eq. (4)**

The DTG responses were also fitted using quadratic and 2FI models. The models resulted R^2 values of 0.83 and 0.60 for quadratic and 2FI models respectively. Hence, ANOVA for the fitted quadratic polynomial model based on DTG responses were selected for further optimisation (Table 25). It was observed that model F-value of 7.79 was indeed significant. As well as F-value, P-value showed that the model terms were significant; significant values need to be less than 0.05. Similar to the size model, this model presented an acceptable Adj. R^2 with R^2 difference value of 0.14 (values less than 2 are desired). C.V percentage confirmed the goodness of fit of the model as it was 3.59%. According to the outcomes, final equation in terms of coded factors based on DTG results was presented in Equation 5.

Table 26: Analysis of variance for the fitted quadratic polynomial model of MCF extraction (based on DTG results)

Source	Sum of squares	Degree freedom	Mean square	F value	P value
Model	6120.86	9	680.09	5.62	0.0063
Residual	1209.93	10	120.99		
Lack of fit	1209.93	5	241.98		
Pure error	0	5	0		
Cor. total	7330.80	19			

R^2 = 0.8350; R^2_{adj}=0.6864; C.V.% = 3.59.

DTG= (314.95) – (7.70×A) – (6.90× B) – (13× C) + (3.75× A × B) + (0.5× A × C) – (14× B× C) – (19.86× A^2) + (0.14× B^2) + (2.64× C^2) **Eq. (5)**

3D interaction plots of size and DTG responses with the factors were presented in Figure 21. Figure 21a indicates that higher NaOH dosage is influential on size reduction. Meanwhile, Figure 21d points out that the increase in NaOH is only beneficial to thermal properties at around 0.16g; higher and lower values have shown lower thermal stabilities. Similarly Figures 21b and 21e express the positive role of mercerisation (using about 0.16g of NaOH) on producing higher thermal stable micro fibres. $NaClO_2$ appeared to have less impact compared to NaOH. $NaClO_2$ provides an acidic environment during the bleaching stage. This acidic stage implied a further reduction in fibre diameter accordingly. It is seen that longer durations of ultrasound can reduce thermal stability of MCF (Figures 21e and 21f). Hence, shorter periods of sonication were found suitable in applications where fibre thermal stability is a concern.

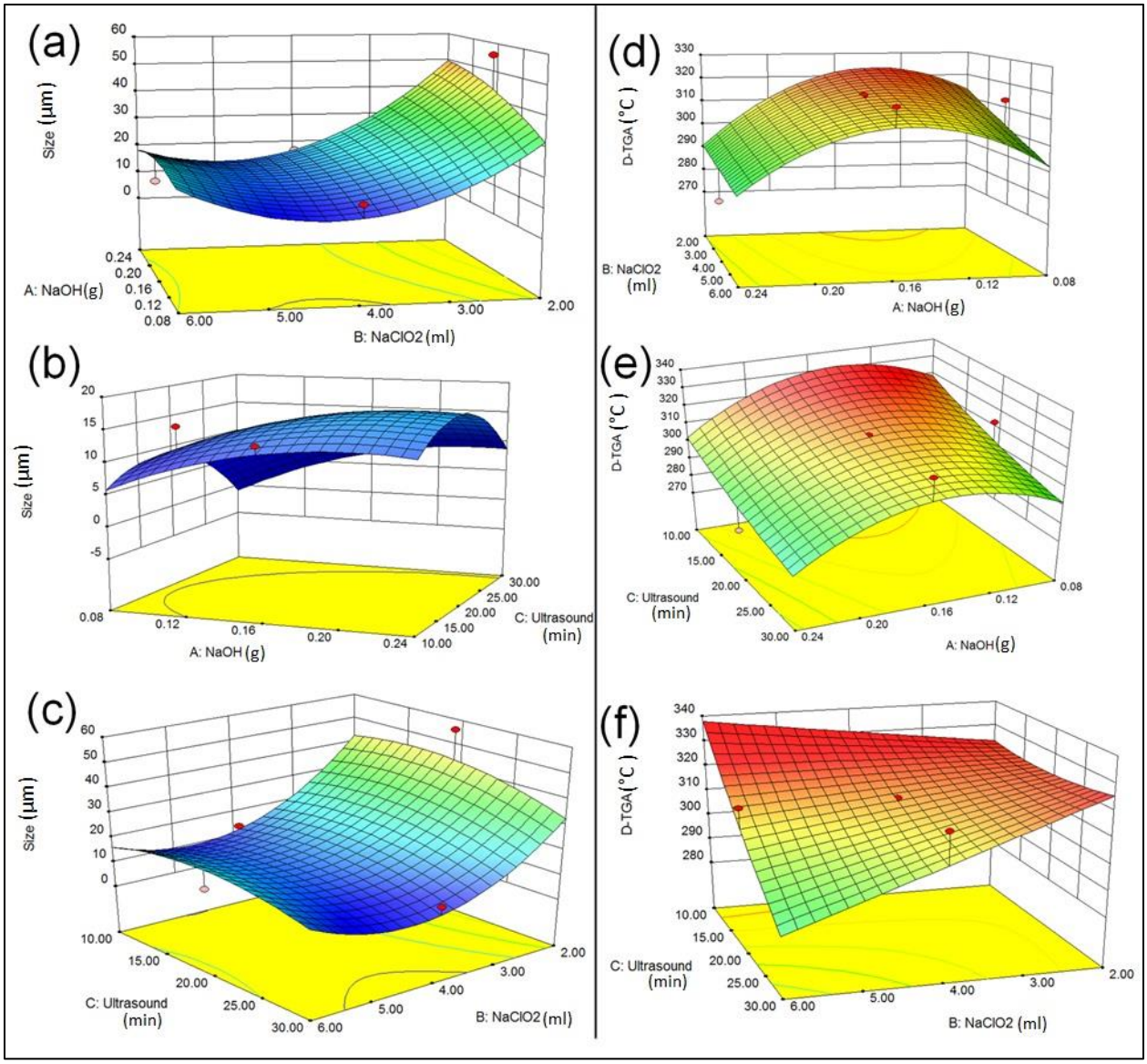

Figure 19: 3D interaction plot of design factors based on size (a-c) and DTG (d-f) responses

To obtain an optimised process, the numerical criteria were customised accordingly; size: minimise, and DTG: maximise. This was to obtain a product with the smallest particle size and the highest possible thermal stability. Based on this setting, 37 solutions were suggested by DOE with a desirability range from 0.91–1 (Appendix A1). Table 26 presents operation parameters for the selected solution with a desirability value of 1. 3D diagram of the optimum parameters, was presented in Figure 22. 0.16 g of NaOH was found the maximum amount that can be recommended to be applied in future mercerisation studies.

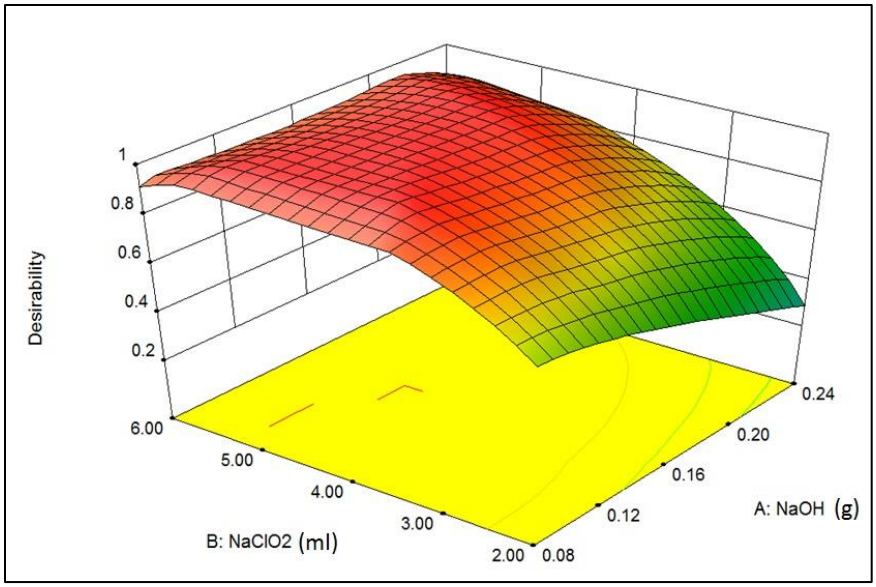

Figure 20: 3D interaction plot of $NaClO_2$ and NaOH optimum dosage

DOE predicted production of MCF with one main DTG peak at 332.71 °C and average diameter of 9.78 µm representing the cellulose content. Following the parameters given in Table 26, validation process was carried out and apparently resulted in producing an acceptable MCF with an average size of 9.33 µm (shown in Figure 23) with DTG value of 320.15 °C (shown in Figure 24). Validation results showed an error percentage 4.6 % and 3.77 % for morphological thermal properties accordingly. MCF DTG result, presented two main peaks; first peak for both samples is referred to the moisture content (30–100 °C) and second peak is referred to the cellulose content at about 320.15 °C. The DTG peak at 280 °C for untreated kenaf (raw kenaf) corresponds to the presence of hemicellulose (Figure 24b), this peak was apparently missing from the graph of MCF DTG, indicating efficient removal of hemicellulose. This further strengthens the efficiency of this design. To further confirm repeatability of the software outcome, a treatment based on 12 g of raw kenaf (3 times of the optimised condition) was carried out and similar results were observed. Confirmation in process repeatability resulted in production of 200 g of MCF.

Table 27: Selected predicted-solution parameters (with desirability of 1)

Factor	Stage 1	Stage 2	Stage 3
	Mercerisation	Bleaching	Sonication
Chemical content	NaOH (0.15 g)	$NaClO_2$ (4.67 ml)	-
Duration (min)	15	15	10
Temperature (ºC)	120	120	40
Pressure (atm)	1.7	1.7	1

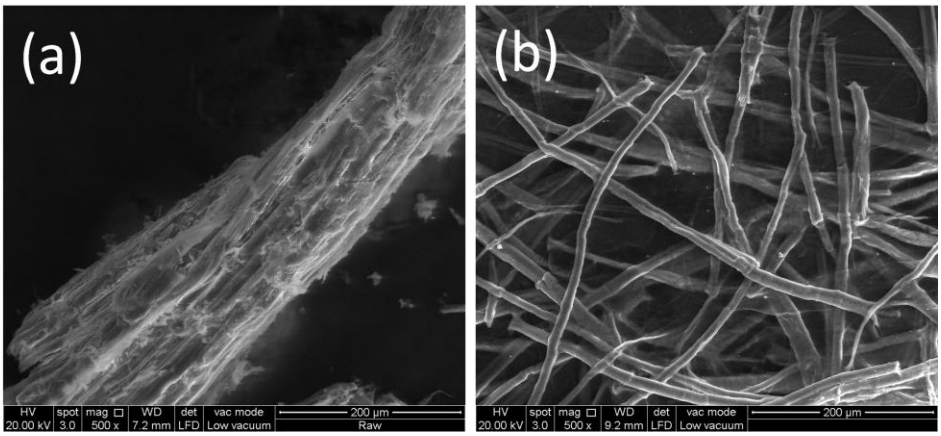

Figure 21: Morphological structure of (a) one untreated kenaf fibre, (b) optimised MCF at 500x magnification.

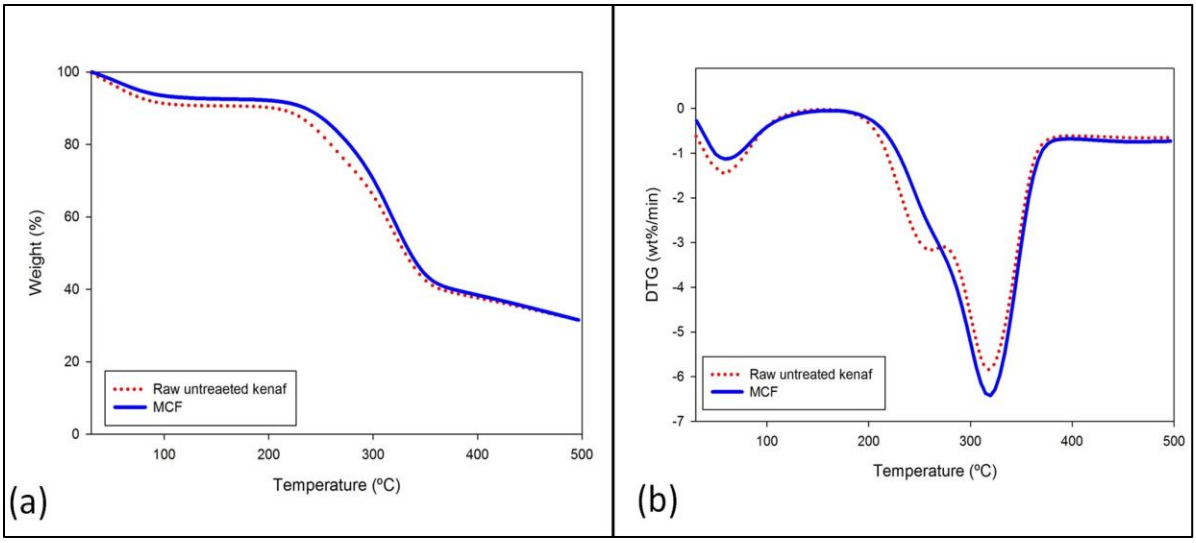

Figure 22: Optimised MCF; (a) TG and (b) DTG results through thermal analysis

Improvement in the fibre tensile strength after alkali treatment was reported by many researchers [89, 305]. NaOH is the most common reliable chemical used during this type of treatment. This could be due the ease of use and availability as well as the price of this chemical compared to other bases. To delignify kenaf fibre adequately, researchers have used different amounts of NaOH. Edeerozey et al. [306], immersed the retted kenaf fibre in NaOH solution with three different concentrations; 3, 6, and 9 wt. % of NaOH. Fibres were mercerised for 3h at room temperature and it was found that 3 wt. % of NaOH was unsuccessful to delignify the fibre surface. Meanwhile 9 % of NaOH treatment showed the finest fibre surface treatment. Kargarzadeh et al. [307] cut kenaf fibres into small pieces and conducted their treatment with a 4 wt. % NaOH solution at 80 °C for 3h under mechanical stirring at room pressure. Kenaf bast fibres were ground and treated with 4 wt. % NaOH solution at 80 ºC for 2 h [308]. In a more recent research, 25 wt. % of NaOH was used [309]; water retted kenaf bast fibres were cut to short pieces and then treated with 25 wt. % NaOH and 0.1 wt. % anthraquinone solution (liquor to fibre ratio was 7:1) at 160 °C for 2 h. In this research, the optimisation of the process resulted in applying 3.75 wt. % of NaOH to delignify kenaf fibre. As a result of using less amount of chemicals, a more thermally stable material was produced. This could be both valuable to our environment as well as to industries. To further confirm the claims SEM, FTIR, and XRD analysis were carried out.

Figure 23 depicts morphological characteristic of MCF extracted in this research. It was observed that every kenaf fibre (Figure 23a) carries lots of aligned micro fibres (Figure 23b). These micro fibres were released into solution following the treatment stages. As observed in Figure 23, diameter of raw kenaf fibre was ~180µm whilst the optimised MCF reached an average diameter of ~10 µm. This could be further employed in studies where researchers use raw kenaf fibre as a reinforcing agent to explore the effect of diameter reduction [41, 42].

The FTIR spectroscopic analysis of raw kenaf and optimised MCF was presented in Figure 25. The results show a clear influence of chemical treatments on raw kenaf fibre. Any peak in region 3700–3300 cm^{-1} presents free O–H stretching vibration of OH group in cellulose molecules [310]. As expected, both samples exhibited peaks in this region; raw kenaf at 3369.28 cm^{-1} and MCF at 3440.56 cm^{-1}. The FTIR peaks at 788.8 cm^{-1} for the raw kenaf and 796.1 cm^{-1} for MCF were attributed to C–O bending of aromatic compounds from lignin [311]. Due to the optimised chemical treatments, this rich peak has become weaker in MCF FTIR plot. FTIR peaks from 1246–950 cm^{-1} are referred to C–O–C, C–O, C–OH stretching vibration of lignin and polysaccharides from cellulose, lignin, and hemicellulose accordingly. The raw samples showed a strong peak at 1135.12 cm^{-1} while MCF displayed one weaker peak at 1123.60 cm^{-1}. FTIR peaks from 1440–1400 cm^{-1} are attributed to O–H bending of alcoholic and carboxylic functional groups from hemicellulose, cellulose [40]. Both samples showed a peak in this region while for MCF (at 1410.28 cm^{-1}) this peak was weaker as compared to raw kenaf (at 1413.44 cm^{-1}) which could be referred to the reduction of hemicellulose content. Peaks from 1510–1650 cm^{-1} are referred to C=C stretching vibration of aromatic rings from lignin and cellulose [310]. In this region, raw kenaf presented a peak at 1551.28 cm^{-1} while MCF showed a peak 1546.96 cm^{-1} which could be similarly assigned to the removal of lignin content through the treatment process.

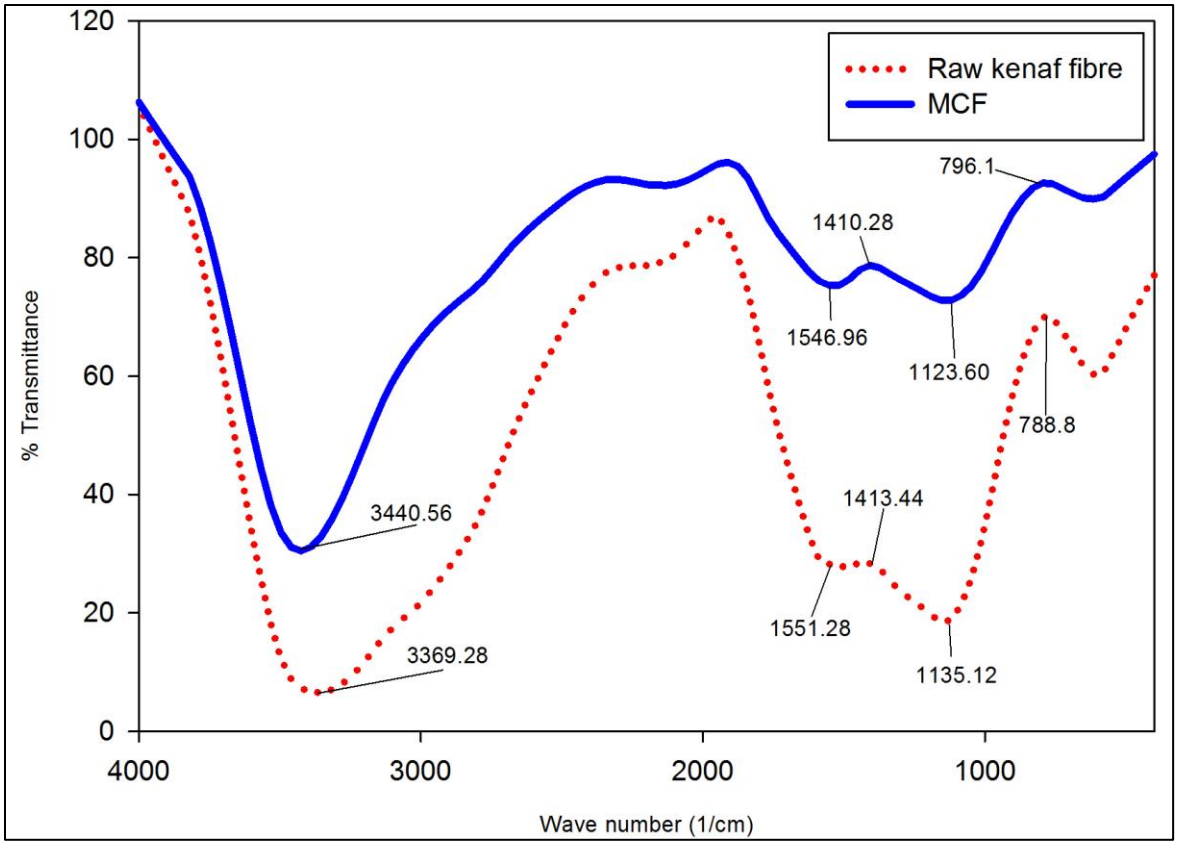

Figure 23: FTIR spectra of raw untreated kenaf and optimised MCF

Crystallinity of the final product (optimised MCF) was compared with the micro cellulose fibres extracted during our earlier investigation (based on single factorial experiments) by XRD technique. As shown in Figure 26, a notable improvement in MCF crystallinity level was observed following the optimisation done in this research.

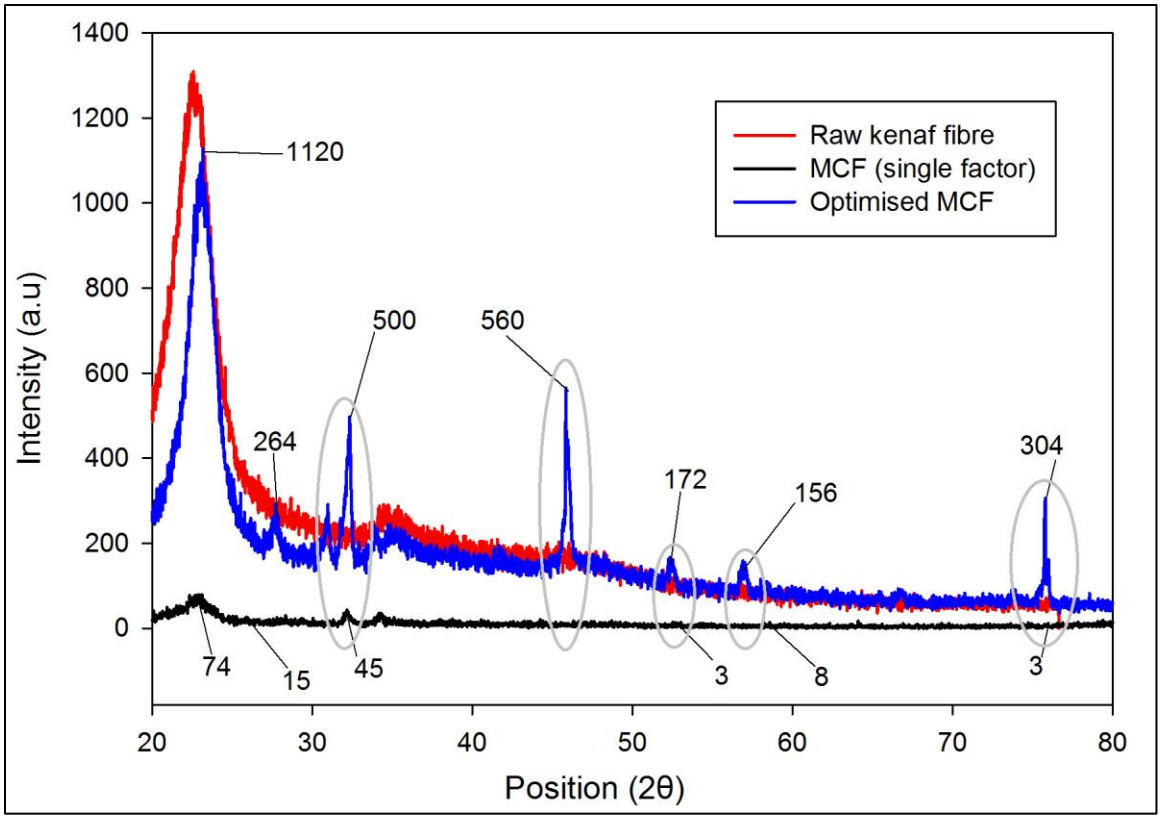

Figure 24: XRD patterns of extracted MCF based on single factor and statistical process optimisation

Crystalline peaks at 2θ value of 20° were observed. The cellulose was present in the form of cellulose I, and not cellulose II. Cellulose I X-ray diffraction pattern is generally characterised by main peak at 2θ value of 22.5° attributed to diffraction plane 0 0 2 [312-314]. As observed, the magnitudes of the crystalline peak and crystallinity index goes on increasing from the single factor MCF sample to optimised sample due to purification of cellulose and removal of amorphous lignin and hemicellulose. Clear crystalline patterns corresponding peaks of optimised MCF could be indexed. These samples indicate major peaks at 2θ values of 304°, 156°, 172°, 560°, 264, and 1120° which correspond to single factor MCF 3°, 8°, 3°, 35°, 45°, 29°, and 78° crystal patterns, respectively. Furthermore, by comparing the optimised MCF with raw kenaf fibre XRD results, another advantage in this type of optimisation was observed. As compared to the raw kenaf fibre, Figure 26 confirms that not only the crystallinity of the final product was

maintained but also improved at several regions (these regions are highlighted in the figure with grey circles).

A crystallinity index of 71.86% was obtained for the optimised MCF, which was 53.52% higher than the one prepared in the earlier trial treatments, confirming the efficient removal of the non-cellulosic amorphous polysaccharides removed by alkali and consecutive bleaching processes.

4.2.3. Modelling and optimisation of cellulose nanoparticles extraction from kenaf fibre

The responses (size quality and DTG results) of each run of the experimental design were presented in Table 27. The independent variables for each experiment are also presented. As shown in Table 27, the DTG values varied from 330–340 °C.

Table 28: CCD of three variables with their achieved responses

Exp. name	NaOH (g)	$NaClO_2$ (ml)	Sonication (min)	Size quality	DTG (°C)
Z1	0.15	4.5	25	1	335
Z2	0.15	4	25	1	337
Z3	0.1	4.5	25	1	338
Z4	0.2	5	20	3	334
Z5	0.15	4.5	25	1	335
Z6	0.15	4.5	30	1	333
Z7	0.1	4	30	1	340
Z8	0.15	5	25	1	335
Z9	0.15	4.5	20	1	337
Z10	0.2	4	30	3	330
Z11	0.1	4	20	1	336
Z12	0.15	4.5	25	1	335
Z13	0.2	4	20	2	334
Z14	0.15	4.5	25	1	335
Z15	0.2	5	30	3	330
Z16	0.15	4.5	25	1	335

Z17	0.1	5	20	1	335
Z18	0.1	5	30	2	337
Z19	0.2	4.5	25	3	335
Z20	0.15	4.5	25	1	335

Statistical testing of the quadratic model was performed using analysis of variance (ANOVA). According to the ANOVA, Quadratic polynomial model and later 2-factor interaction model (2FI) were found more suitable to analyse size quality and DTG responses respectively. The ANOVA for the fitted quadratic polynomial model of extraction of CNP based on size quality responses were presented in Table 28. The model F-value of 20.00 implies that the model is significant. P-values less than 0.05 indicate model terms are significant and apparently P-value was <0.0001, which showed that the model based on size quality response is significant. The final equation in terms of coded factors was presented as follows:

Size quality= $(0.98) + (0.70\times A) + (0.10\times B) + (0.30\times C) + (0.12\times A\times B) - (0.12\times A\times C) - (0.12\times B\times C) + (1.04\times A^2) + (0.044\times B^2) + (0.044\times C^2)$ **Eq. (6)**

Table 29: Analysis of variance for the fitted quadratic polynomial model of CNP extraction (based on size quality)

Source	Sum of squares	Degree freedom	Mean square	F value	P value
Model	12.13	9	1.34	19.99	<0.0001
Residual	0.60	9	0.06		
Lack of fit	0.60	4	0.15		
Pure error	0	5	0		
Cor. total	12.73	18			

$R^2 = 0.9524$; $R^2_{adj}=0.9047$; C.V.% = 17.01.

Furthermore, the ANOVA for the fitted 2FI model based on DTG responses is presented in Table 29. The model F value of 7.79 indicates that the model is significant. As well as the F-value, the P-value shows that the model terms are significant as its value is less than 0.050. According to

this analysis, the final equation in terms of coded factors based on DTG results is presented as follows:

DTG= (335.02) – (2.25× A) – (0.55× B) – (0.65× C) + (0.43× A× B) – (1.68× A × C) – (0.18× B × C) **Eq. (7)**

Table 30: Analysis of variance for the fitted 2FI model of CNP extraction (based on DTG responses)

Source	Sum of squares	Degree freedom	Mean square	F value	P value
Model	61.38971	6	10.23162	7.78653	0.0014
Residual	15.76818	12	1.314015		
Lack of fit	15.76818	7	2.252597		
Pure error	0	5	0		
Cor. total	77.15789	18			

R^2 = 0.7956; R^2_{adj}=0.6935; C.V.% = 0.34.

3D interaction plots of size quality and DTG responses with the factors are presented in Figure 27 respectively. Figures 27a and 27d indicate that higher NaOH dosage results in higher thermal stability and finer fibre size. Similarly Figures 27b and 27e express the role of alkali treatment on producing higher thermal stable nanoparticles. $NaClO_2$ seems to have less influence compared to NaOH.

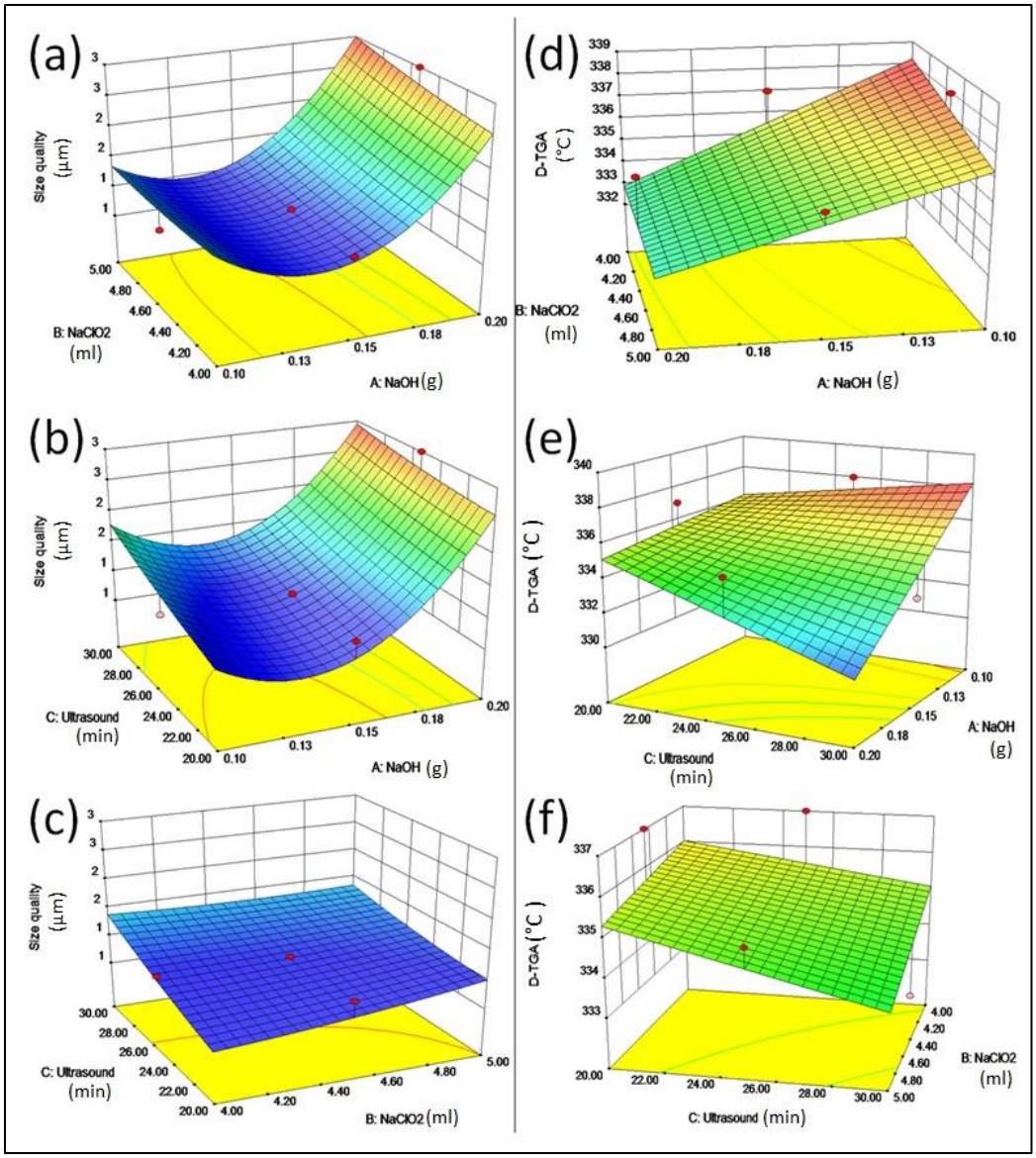

Figure 25: 3D interaction plot of size quality (a-c) and DTG (d-f) results; (a) $NaClO_2$ vs NaOH, (b) Ultrasound duration vs NaOH, (c) Ultrasound duration vs $NaClO_2$, and (d) $NaClO_2$ vs NaOH dosage interactions, (e) Ultrasound duration vs NaOH, and (f) Ultrasound duration vs $NaClO_2$

The application of ultrasound on cellulose fibres showed to be beneficial in terms of size reduction (shifting from micro to nano sized particles) however at the same time longer durations of sonication resulted in lower thermal stability (Figures 27e and 27f). Figure 27 (a-c) shows that to achieve an acceptable size quality (3), during stage 1, the minimum amount of NaOH needs to be at least 0.18 g / 4 g of fibre.

Based on the responses, 39 solutions were achieved with a desirability ranged from 40 % to 80 % (Appendix A2). Table 30 presents the operation parameters for the selected solution with a desirability value of 80.2 %. The optimum parameters 3D diagram is presented in Figure 28. As mentioned earlier, it is observed that the influence of NaOH during the alkali treatment can be only seen from the point 0.18 g and above per 4 g of fibre.

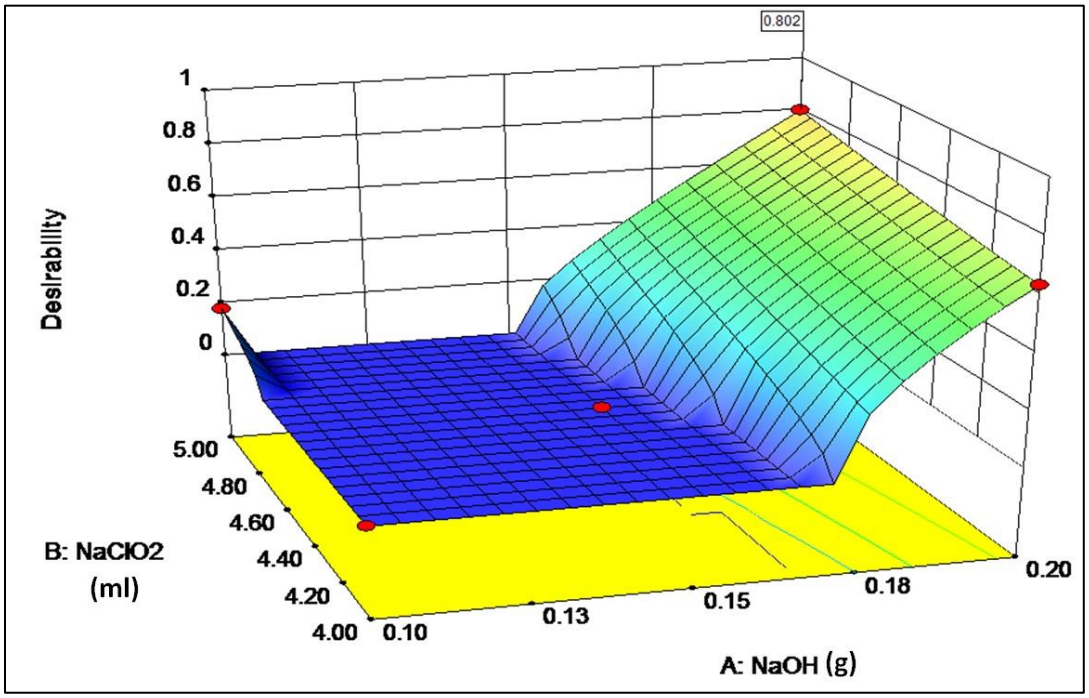

Figure 26: 3D interaction plot of $NaClO_2$ and NaOH optimum dosage

Based on the selected solution shown in table 30, the software predicted the production of cellulose nanoparticles (3) with one main peak in DTG results at 335.182 °C representing the cellulose content. Following the parameters given in table 6, the validation process was carried out and actually resulted in an acceptable nano size (diameter of ~100 nm) (Figure 30 and 31) with DTG value of 338.55 °C (Figure 29). In terms of error percentage, the validation results were in good agreement with both morphological and thermal properties results (~1 %). The DTG result, presented two main peaks the first peak is referred to the moisture content and the second peak is referred to the cellulose content accordingly.

Table 31: Selected predicted solution parameters (with 80.2% desirability)

Factor	**Stage 1** (Alkali treatment)	**Stage 2** (Bleaching)	**Stage 3** (Sonication)
Chemical content	NaOH (0.2g)	$NaClO_2$ (5ml)	-
Duration (min)	15	15	20
Temperature (ºC)	120	120	40
Pressure (atm)	1.7	1.7	1

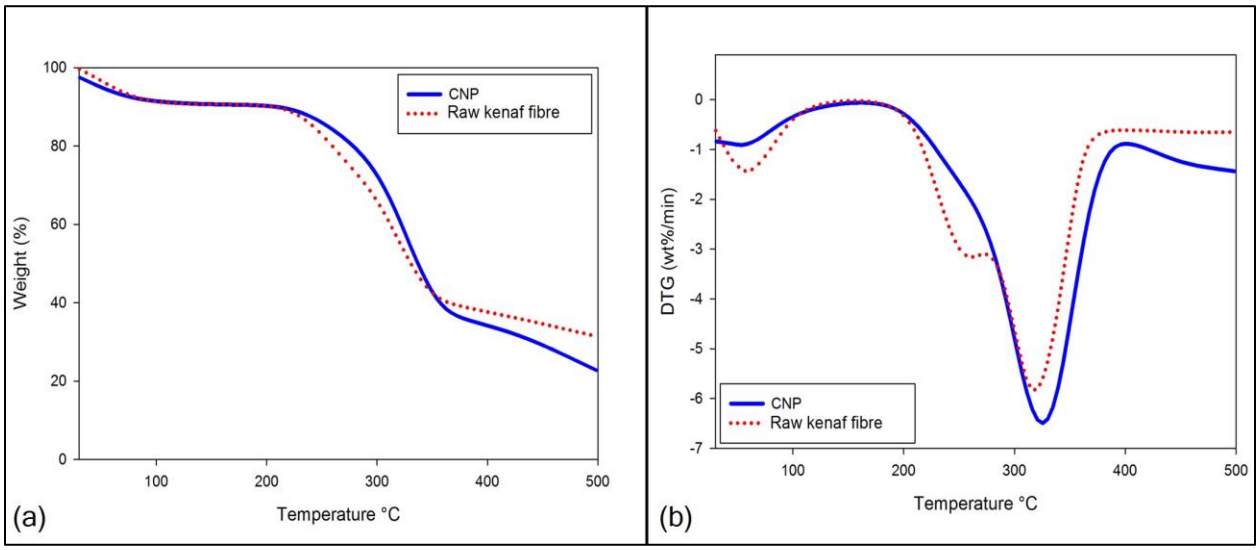

Figure 27: Optimised CNP (a) TG and (b) DTG results through thermal analysis

Through similar studies (based on kenaf fibre), researchers used 4 wt. % of NaOH during their alkali treatment [315, 316]. Similarly, 25 wt. % of NaOH was employed to delignify kenaf fibre [309]. In this research, following the optimisation outcomes, it was observed that 5 wt. % of NaOH (0.2 g of NaOH/4 g of fibre) is sufficient to delignify kenaf fibre, while maintaining the size and thermal stability. This optimised process is beneficial to both environment and industries; helping them to save a notable amount of money and energy during bulk productions. To further support this claim, the samples were characterised using SEM, TEM and FTIR.

Figures 30 and 31 depict the morphological characteristic of microfibres and nano cellulose particles extracted in this research. The diameter of raw kenaf fibre is about 180 µm while the alkali treated and bleached fibres reached an average diameter of 10 µm. It was observed that every kenaf fibre (Figure 30a) carries lots of aligned micro fibres presented in Figure 30b. Figure 30c shows a notable reduction in fibre diameter later to the sonication stage; an average diameter of ~100 nm. As comparing the structure of fibres in Figure 30b and the one fibre in Figure 31, a swelling effect is observed which is referred to the sonication stage. As observed in Figure 30c as well as Figure 30c, the dried nano particles tend to aggregate very quickly. This aggregation can be eliminated by wetting the particles.

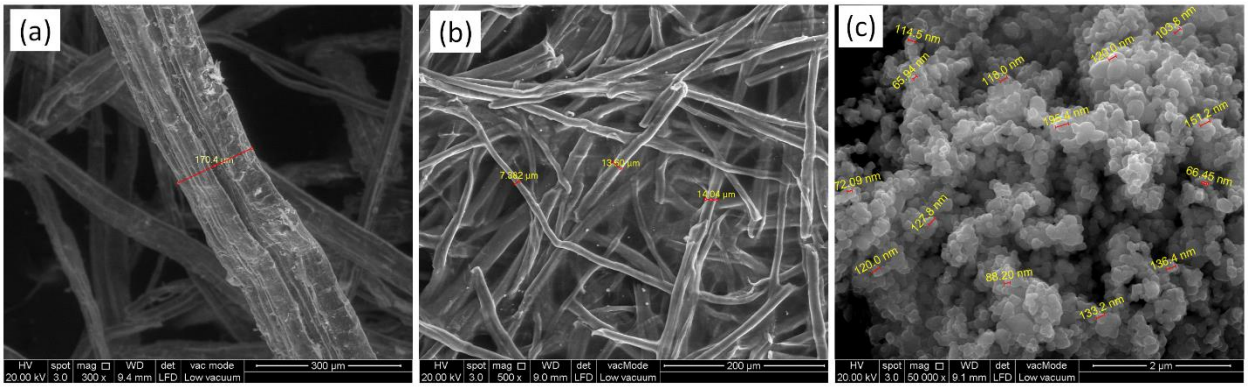

Figure 28: Morphological structure of (a) one raw kenaf fibre at 300x, (b) cellulose micro fibres at 500x, and (c) optimised CNP at 50000x of magnification.

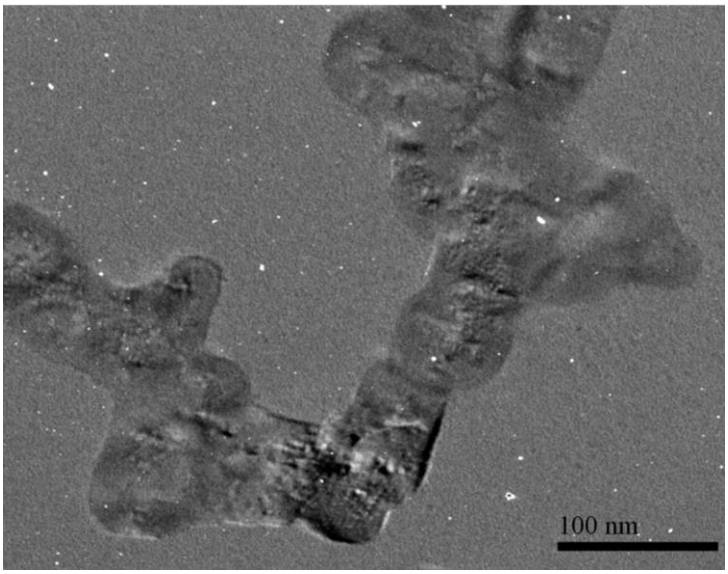

Figure 29: Transmission electron micrograph of CNP

Figure 32 presents FTIR spectroscopic analysis of raw kenaf and optimised CNP. Results revealed the chemical treatments impact on raw kenaf fibre. Any peak in the region 3700–3300 cm^{-1} presents free O–H stretching vibration of OH group in cellulose molecules [310]. Both samples exposed peaks in this area; raw kenaf at 3369.28 cm^{-1} and CNP at 3436.96 cm^{-1}. FTIR peaks from 1246–950 cm^{-1} are stated to C–O–C, C–O, C–OH stretching vibration of lignin and polysaccharides from cellulose and lignin accordingly [317]. Raw samples showed a peak at 1135.12 cm^{-1} in this area and CNP showed a much weaker peak at 1040.8 cm^{-1}. FTIR peaks from 1440–1400 cm^{-1} are referred to O–H bending of alcoholic and carboxylic functional groups from hemicellulose, cellulose [318]. Kenaf showed a strong pick in this region while CNP showed a very weak peak which was linked to the removal of hemicellulose. Peaks from 1510–1650 cm^{-1} are attributed to C=C stretching vibration of aromatic rings from lignin and cellulose [310]. In this area, raw kenaf presented a peak at 1551.28 cm^{-1} respectively, while CNP has shown a peak at 1652.08 cm^{-1}, which could be likewise assigned to the removal of lignin content through treatment processes. On the other hand, untreated kenaf showed a strong peak at 1734.73 cm^{-1} referring to C=O stretching of carbonyl group from hemicellulose. Apparently, CNP is missing this peak following the optimisation condition. The FTIR peak at 788.8 cm^{-1} for the raw kenaf is attributed to C–O bending of aromatic compounds from lignin which CNP is missing this peak

as well following the optimisation condition. At this stage, the optimised extraction of CNP was established.

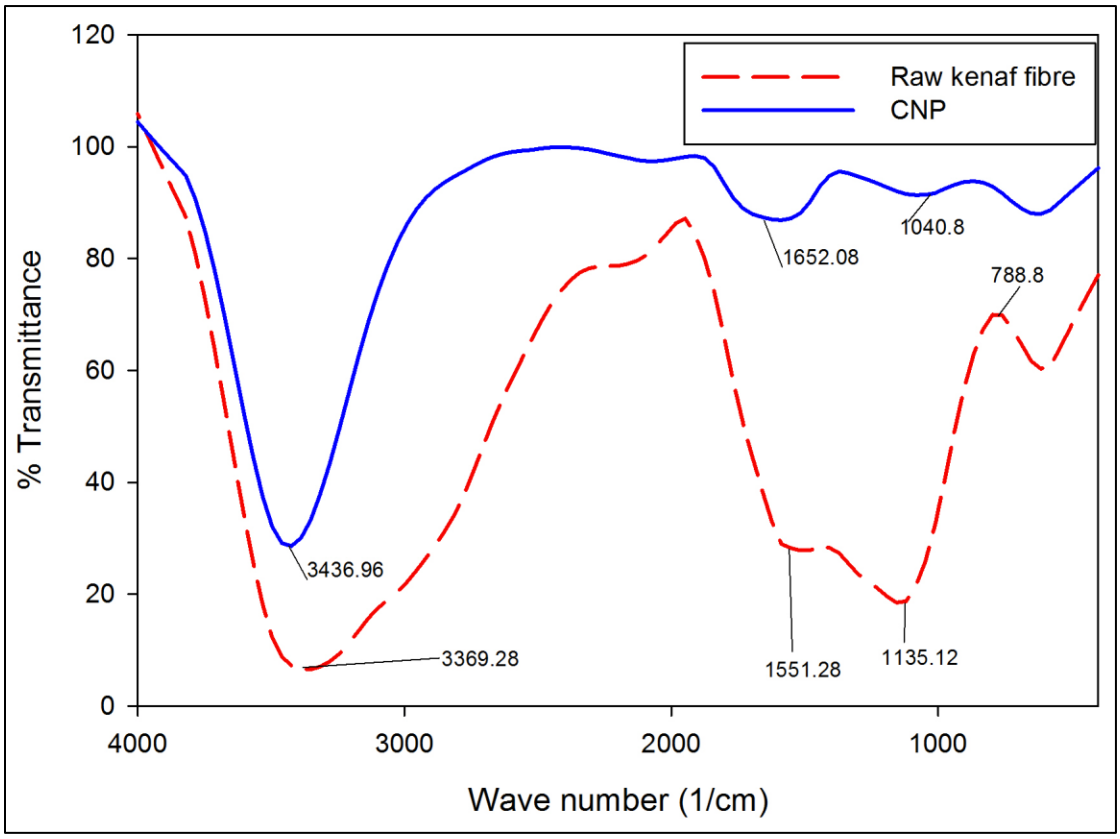

Figure 30: FTIR spectra of raw kenaf and optimised CNP

4.3. Modelling and optimisation of polylactic acid processing parameters

Table 31 summarises the achieved results; maximum stress, impact strength and young's modulus of the pure PLA. From the table, the maximum stress can be seen at 60.89 MPa, young's modulus at 776.20 MPa, and 38.47 J m^{-1} for impact strength. The quadratic model statistical testing was employed in form of Analysis of Variance (ANOVA) to achieve an optimum procedure.

Table 32: CCD design of three variables with their achieved responses

Exp. name	Speed (rpm)	Temperature (°C)	Duration (min)	Max stress (MPa)	Young's Modulus (MPa)	Impact (J m^{-1})

H1	100	180	5	57.08	611.3	30.878
H2	75	195	10	55.48	582.943	30.099
H3	50	210	5	52.25	648.478	29.804
H4	75	195	7.5	56.77	527.136	28.816
H5	100	210	5	38.08	776.205	22.367
H6	75	195	7.5	56.77	527.136	28.816
H7	75	195	7.5	56.77	527.136	28.816
H8	50	195	7.5	54.04	573.646	38.474
H9	100	180	10	56.33	651.137	32.299
H10	75	195	7.5	56.77	527.136	28.816
H11	75	180	7.5	60.89	605.713	30.476
H12	75	195	7.5	56.77	527.136	28.816
H13	75	195	5	58.12	556.089	29.787
H14	50	210	10	50.64	633.474	26.016
H15	100	210	10	41.62	650.77	23.247
H16	75	195	7.5	56.77	527.136	28.816
H17	100	195	7.5	55.77	589.227	29.889
H18	50	180	10	55.56	549.23	28.175
H19	50	180	5	55.09	638.06	29.857
H20	75	210	7.5	51.39	616.953	28.285

Model F-value was calculated as ratio of mean square regression and mean square residual. The F-value is the test for comparing the curvature variance with residual (error) variance and P-value is probability of seeing the observed F-value if the null hypothesis is true. If the null hypothesis is true, it shows that the model is a good predictor of the experimental data. Therefore, the larger F-value and the smaller P-value, corresponds to more significant coefficient.

As such, Table 32 shows the ANOVA results for the fitted quadratic polynomial model of pure PLA based on maximum stress responses. From the table, model F-value of 26.81 confirmed the model significant and stability. Furthermore, model P-value of <0.0001 complemented the model significance as it was less than 0.05, indicating the model significance. The model resulted in an acceptable adj. R^2 with R^2 difference value of 0.03 (values are preferred to be less than 0.2). Coefficient of variation (C.V) percentage is a standard deviation expressed as a percentage of the mean, where the lower the C.V, the smaller residuals relative to the predicted value was. C.V value for the fitted quadratic polynomial model was 1.96, proposing a reliable model. Concluding equation based on coded factors was presented in Equation 8.

Table 33: Analysis of variance for the fitted quadratic polynomial model of PLA processing (max stress)

Source	Sum of squares	Degree freedom	Mean square	F value	P value
Model	279.78	9	31.09	26.81	< 0.0001
Residual	9.28	8	1.16		
Lack of fit	9.28	3	3.09		
Pure error	0.00	5	0.00		
Cor. total	289.05	17			

$R^2 = 0.9679$; $R^2_{adj}=0.9318$; C.V.% = 1.96.

$$\text{Maximum stress} = (+57.30) - (1.22\times A) - (4.19\times B) - (1.00\times C) - (2.11\times A\times B) - (0.64\times A\times C) - (0.86\times B\times C) - (1.89\times A^2) - (1.95\times B^2) - (1.29\times C^2) \quad \textbf{Eq. (8)}$$

Figure 33 shows the 3D interaction plot of processing temperature, mixing speed, and duration factors with maximum stress response. A clear decline in maximum stress value can be observed as the temperature increased to 210 °C which was linked to the matrix degradation (Figures 33a and 33c). When PLA is exposed to elevated temperatures, it is known to undergo thermal degradation, leading to the formation of lactide monomers [319]. Researchers reported minimal degradation bellow 200 °C and formation of oligomers at processing temperatures above 230 °C

[320]. Meanwhile, mixing duration and speed appeared to have less influence on maximum stress value (Figure 33b).

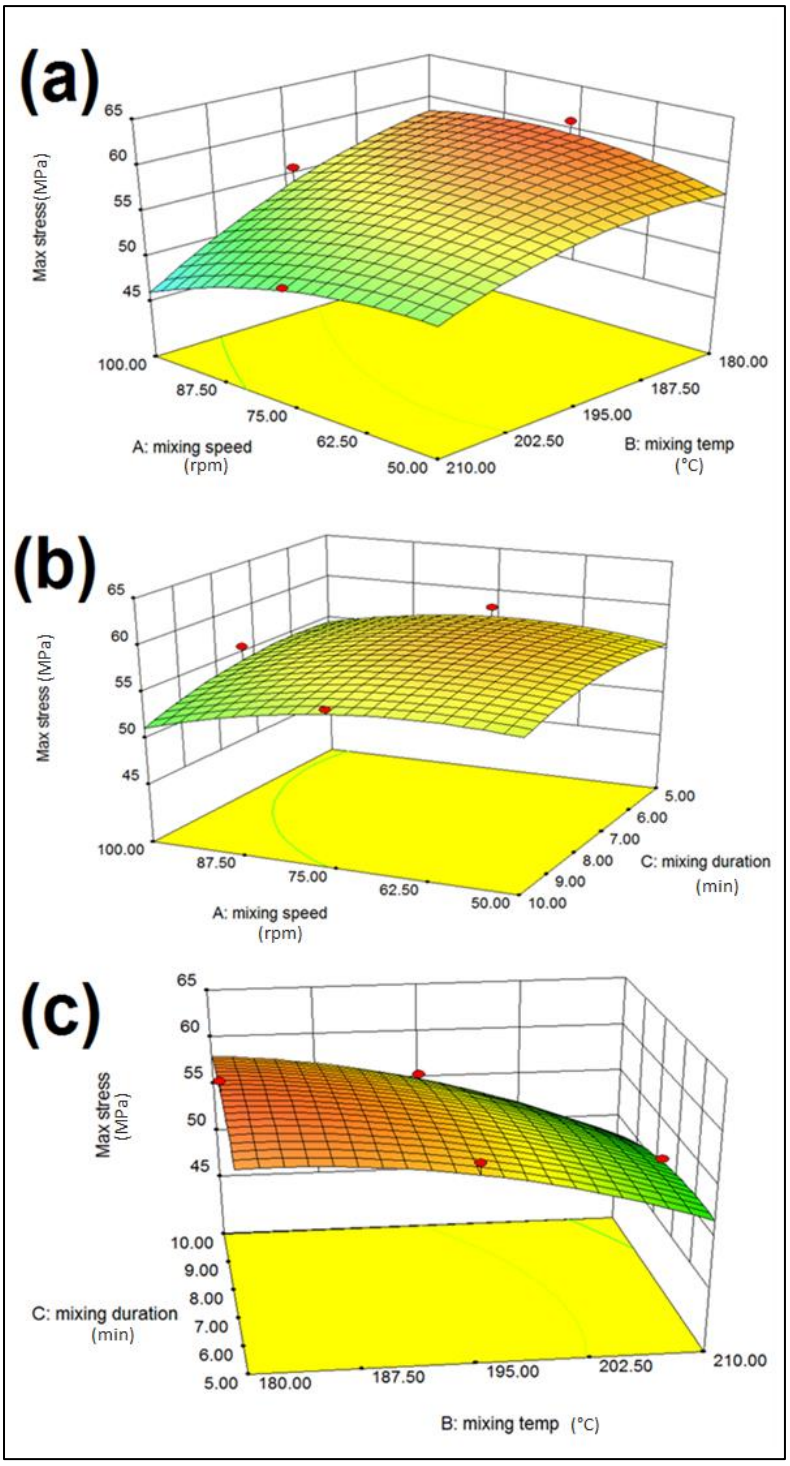

Figure 31: Response surface (3D) presenting the effect of mixing speed, mixing duration, and mixing temperature on maximum stress value.

Table 33 shows the ANOVA for the fitted quadratic polynomial model following the Young's modulus (MPa) responses. From the table, F-value of 10.07 indeed proved the significance of the model, which was further complemented by the P-value of less than 0.050. Similar to the maximum stress model, the Young's modulus model presented an acceptable adj. R^2 with R^2 difference value of 0.0913. From the R^2 value achieved, it can be concluded that the quadratic equation defines 91.89 % of the total variation of the experimental results. A C.V percentage of 3.55% also proved the significance of the model. The final equation in terms of coded factors based on DTG results was presented in Equation 9.

Table 34: Analysis of variance for the fitted quadratic polynomial model of PLA processing (Young's Modulus)

Source	Sum of squares	Degree freedom	Mean square	F value	P value
Model	38775.21	9	4308.36	10.07	0.0017
Residual	3424.23	8	428.03		
Lack of fit	3424.23	3	1141.41		
Pure error	0.000	5	0.000		
Cor. total	42199.44	17			

$R^2 = 0.9189$; $R^2_{adj} = 0.8276$; C.V.% = 3.55.

$$\text{Young's Modulus} = (+537.77) + (6.73\times A) + (7.22\times B) + (3.57\times C) - (16.05\times A \times B) + (27.06\times A \times C) + (13.35\times B\times C) + (12.84\times A^2) + (57.62\times B^2) + (15.81\times C^2) \quad \textbf{Eq. (9)}$$

Figure 34 depicts the 3D interaction graph of the three factors with young's modulus value. Processing temperature at 190 °C showed a significant effect on the young's modulus value (Figure 34a). Meanwhile, either higher or lower temperatures than 190 °C showed to be beneficial. Likewise, the previous findings, processing speed and duration appeared to have minimal effect on young's modulus values.

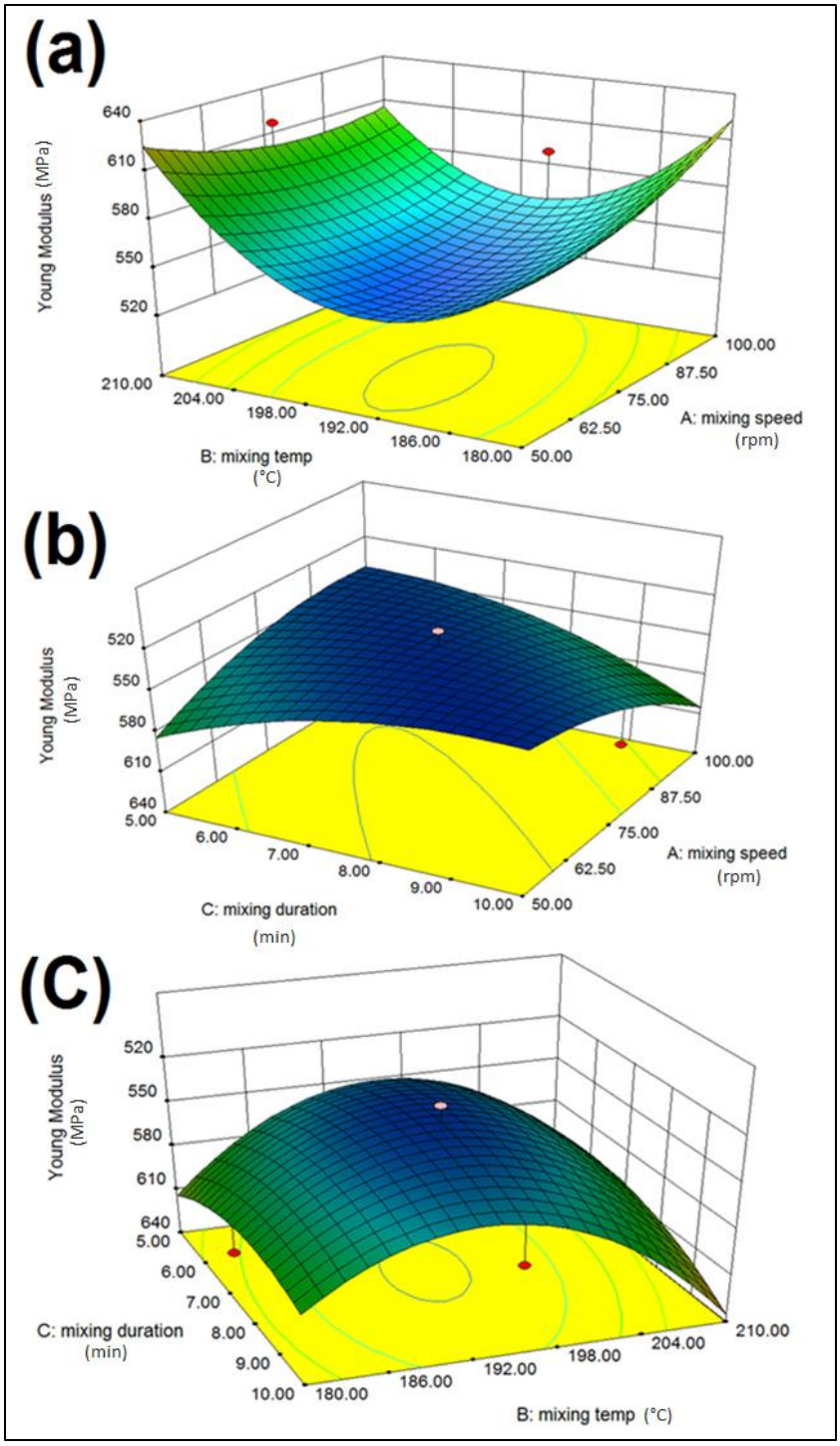

Figure 32: Response surface (3D) presenting the effect of mixing speed, mixing duration, and mixing temperature on young's modulus value

Table 34 shows the ANOVA fitted quadratic polynomial model for the impact strength. From the table, the model's F-value of 6.54 and P-value less than 0.050 proved the significance of the model. The coefficient of variation (C.V % = 3.37) of the response values further illustrated that the model has high reliability. The impact strength model presented an adequate adj. R^2 with R^2 difference value of 0.0913. The overall equation based on the coded factors was presented in Equation 10.

Table 35: Analysis of variance for the fitted quadratic polynomial model of PLA processing (Impact strength)

Source	Sum of squares	Degree freedom	Mean square	F value	P value
Model	56.33	9	6.26	6.54	0.0072
Residual	7.65	8	0.96		
Lack of fit	7.65	3	2.55		
Pure error	0.000	5	0.000		
Cor. total	63.98	17			

R^2 = 0.8804; R^2_{adj}= 0.7458; C.V.% = 3.37.

Impact strength = (+29.21) – (0.016×A) – (1.82× B) – (0.66× C) – (1.45× A × B) + (0.50× A × C) – (0.80× B× C) – (0.49× A^2) – (0.42× B^2) + (0.14× C^2) **Eq. (10)**

Figure 35 depicts the 3D interaction graphs of mixing temperature, speed, and duration interaction with impact strength value. Increase in mixing temperature from 180–210 °C appeared to clearly decrease the impact strength properties (Figures 35a and 35b). In the meantime, as observed earlier, mixing speed and duration appeared to have minor influence on impact properties as compared to the processing temperature.

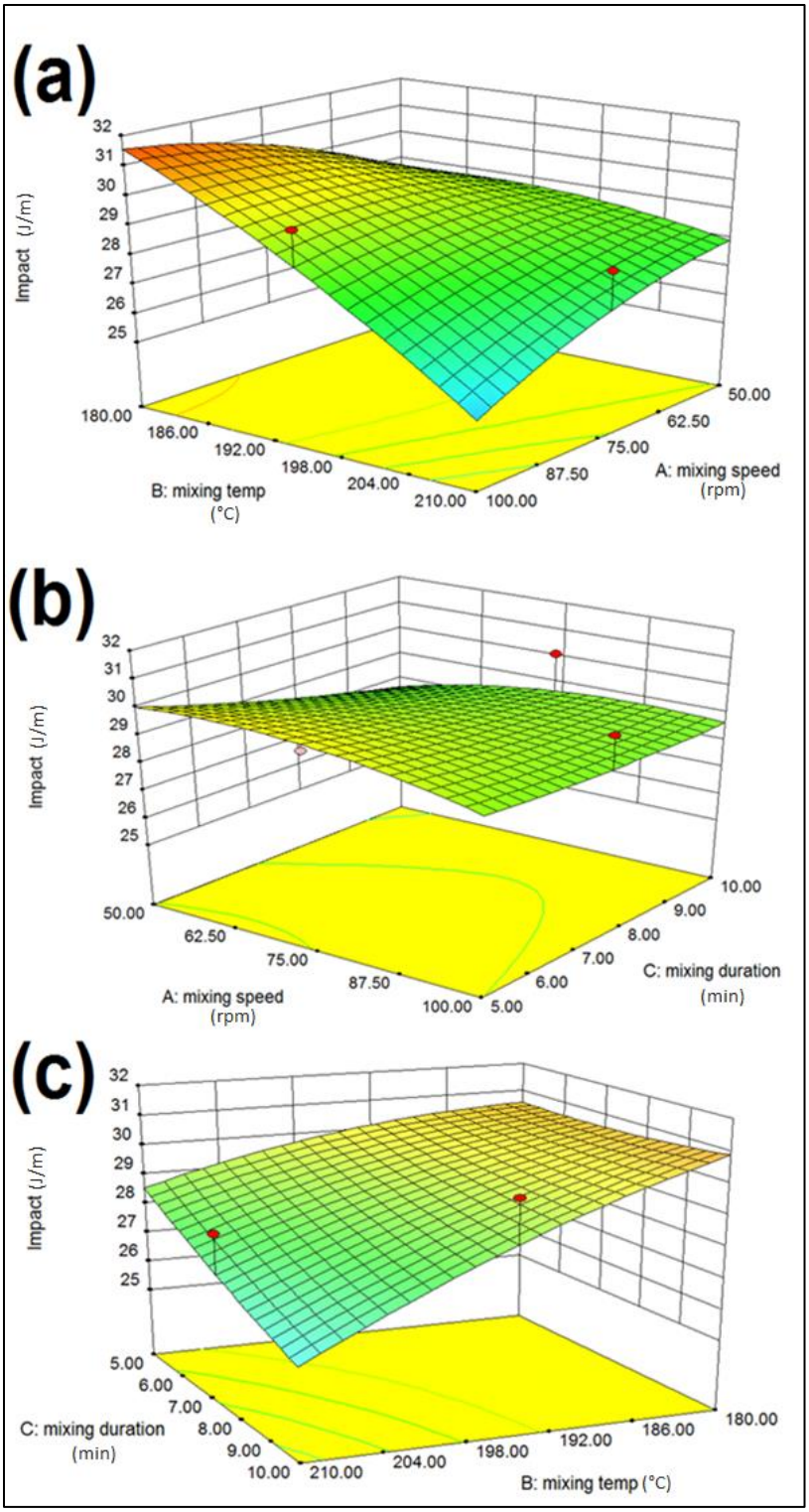

Figure 33: Response surface (3D) presenting the effect of mixing speed, mixing duration, and mixing temperature on impact strength value.

To optimise the blending parameters, the goals for mixing temperature, speed, and duration were set to “in range”. The three responses were set to “maximise”. This was to achieve the highest mechanical performance over the lowest processing temperature. As observed earlier, processing temperatures higher than 180 °C showed less desirability. Based on this setting, the software suggested 37 solutions carrying a desirability ranged from 0.67–0.92 (Appendix A3). The solution with the highest desirability value (0.92) was selected. Optimum parameters 3D diagram was presented in Figure 36.

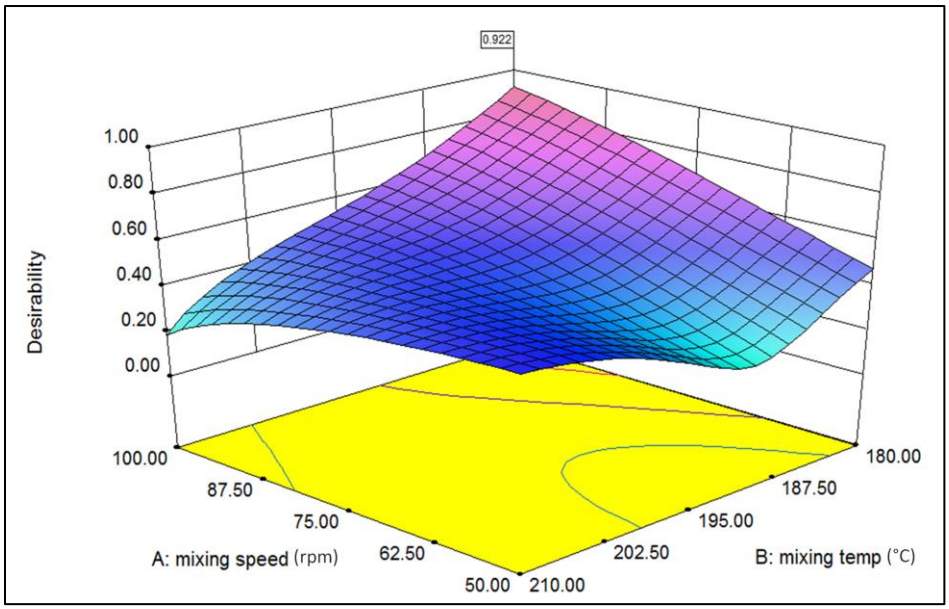

Figure 34: 3D interaction plot of optimum mixing temperature and speed

The predicted optimised factors for the blend conditions were mixing temperature of 180 °C, mixing time of 10 min and mixing speed of 100 rpm. Moreover, the predicted responses of the blend based on these predicted factors were 56.84 MPa, 651.13 MPa, and 32.23 J m^{-1} for maximum stress, young modulus, and impact strength values accordingly. Upon validation process, actual average values of 60.31 MPa, 606.54.54 MPa, and 31.65 J m^{-1} for maximum stress, young modulus, and impact strength were achieved respectively. Validation process resulted in a slightly higher stress value while lower in young modulus. In terms of error percentage, validation results agreed on -0.061 %, 0.068 %, and 0.017 % for maximum stress,

young modulus, and impact strength values accordingly. The negative error percentage indicates the higher maximum stress validation value than the predicted value.

To further investigate the role of temperature, morphological studies were carried out. Figure 37 shows tensile and notched izod impact fracture surfaces of H11, H4, and H20 samples. H11, H4, and H20 samples were prepared at same condition (blended for 7.5 min at 75 rpm) while at different temperatures (at 180, 195, 210 °C respectively). Samples prepared at 180 °C showed an enhanced interaction in-between PLA granules (Figure 37a) as compared to the samples prepared at 195 °C (Figure 37c) and 210 °C (Figure 37e). Similarly, samples prepared at higher temperature than 180 °C, showed a smoother fractured surface which could be due to the lower viscosity which achieved at higher processing temperatures. Such smoother fractured surface which was observed in notched izod impact fractured samples imply that these samples are more fragile and lesser energy needed to break as evident from impact strength results as compared to samples prepared at 180 °C.

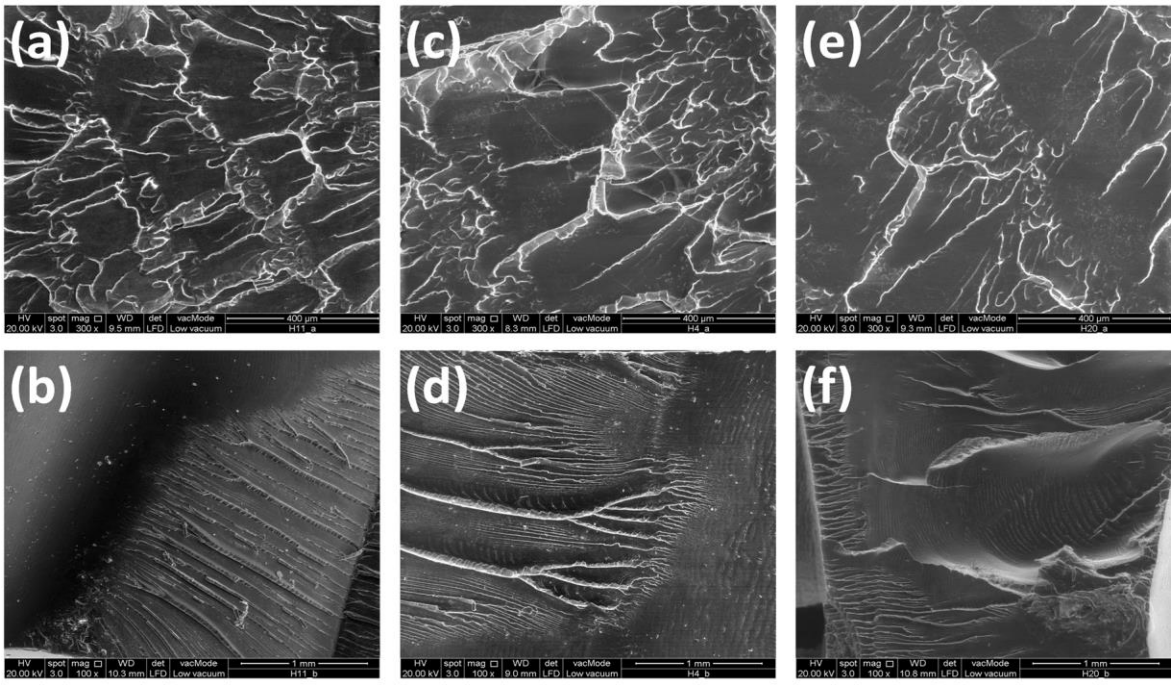

Figure 35: Morphological structure of H11((a) Tensile at 300x, and (b) Impact at 100x of magnification), H4((c) Tensile at 300x, and (d) Impact at 100x of magnification), and H20((e) Tensile at 300x, and (f) Impact at 100x magnification) samples.

During the tensile test, the failure occurs due to initiation of craze that spread catastrophically across the specimen and rapidly fractures the sample under relatively high level of stress [321]. The crazes, which dissipate the strain energy by bioplastic deformation, were clearly observed in Figures 37a, 37c, and 37e. The crazes grow in a direction perpendicular to the applied tension. It was observed that the fracture behaviour of the specimens in the tensile test changed from ductile fracture to brittleness fracture with increasing the temperature from 180 to 210 °C. A large amount of energy consumed in craze development is the major source of toughness. The samples prepared at a higher temperature than 180 °C, had relatively lower mechanical strength which was linked to the reduction in number of crazes and increasing brittleness of specimens. Similarly, the fracture surfaces of impact results show the transition to a more brittle structure at higher temperatures (Figure 37b, 37d, 37f). The flexural ductility of H4 and H20 decreased and their stiffness increased with increasing temperature.

Melt compounding technique is the least damaging to the mechanical properties of biopolymers. This is due to the procedure which is carried out in one batch. Meanwhile, extrusion is the most problematic in continuous processes, particularly in processes where the extrudate is stretched, such as film blowing [322]. Through such preparations, extrudate's viscosity plays an important role. Based on the findings in this research, higher processing temperature resulted in higher viscosity and yielded superior mobility of component. Hence, to enhance a continuous process, processing temperature higher than 180 °C up to 195 °C can be recommended.

In addition to morphological characterisation, thermal analysis was carried out to further understand the influence of processing temperature. Similarly, H11, H4, and H20 samples were selected. Figure 38 presents the effect of processing temperature on the thermal stability of the PLA. PLA is thermally unstable and exhibits rapid loss of molecular weight as the result of thermal treatment at processing temperatures. The ester linkages of PLA tend to degrade during thermal processing or under hydrolytic conditions. To further study the thermal stability of H11,

H4, and H20, different thermal degradation stages as a function of temperature were analysed (Table 35). The temperatures T_5, T_{10}, T_{50}, T_{max} and T_{90} are temperatures for 5 %, 10 %, 50 %, maximum and 90 % decomposition, respectively. Higher the values of T_5, T_{10}, T_{50}, T_{max} and T_{90}, higher will be the thermal stability of the sample. T_{max} of H11 which was prepared at 180 °C was at ~348 °C while H4 and H20 which were processed at higher temperatures were at ~359 °C and ~353 °C respectively. Thermal degradation mainly occurs through random main-chain scissions coupled with other reactions such as hydrolysis, depolymerisation, oxidative degradation, and inter and intramolecular trans-esterification reactions to mononmer and oligomeric esters [323].

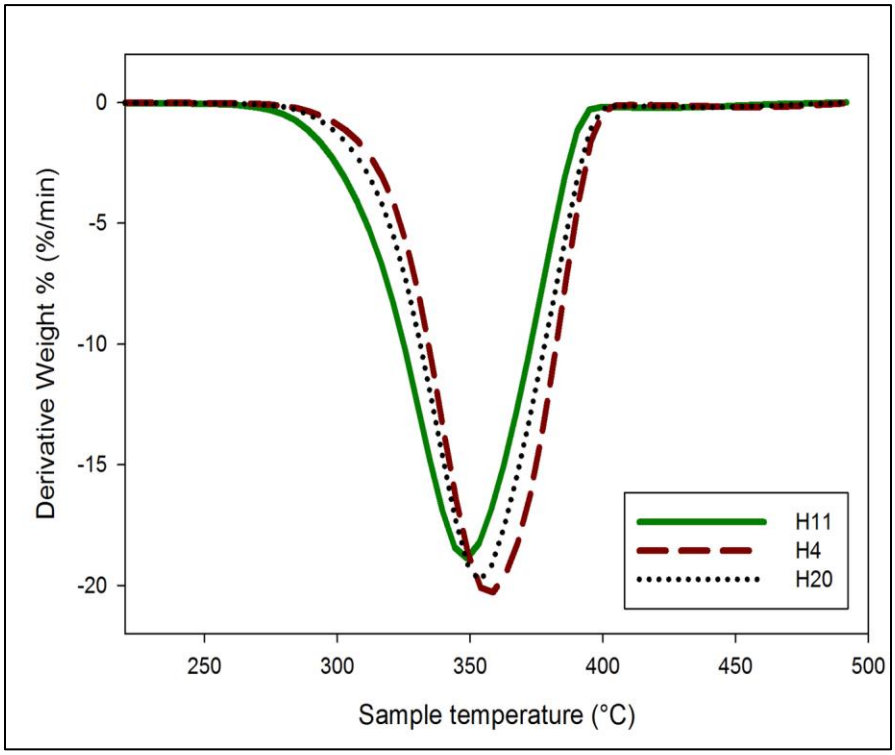

Figure 36: DTG thermogram results of H11, H4, and H20 samples

Table 36: Thermal stability data of H4, H11, and H20 obtained from TGA curves

Sample	TGA				
	T_5 (°C)	T_{10} (°C)	T_{50} (°C)	T_{max} (°C)	T_{90} (°C)
H11 (180 °C)	307.75	318.32	349.25	348.07	362.64
H4 (195 °C)	322.34	333.96	359.07	359.44	370.82
H20 (210 °C)	317.55	328.55	354.59	353.61	367.18

Thermal stability of PLA is another drawback which eventually affects its processing and performance in different applications. Low heat distortion temperature (HDT) of PLA, limits its applications in biocomposites processed at temperatures exceeding 60 °C [324]. Moreover, due to the degradation of PLA which takes place at about 180 °C, the colour of PLA changes from transparent yellow to light transparent brown which designates thermal degradation [325]. Low HDT could be the main reason that prevents PLA to replace conventional plastics for higher temperature applications.

The transparent light yellow colour of the samples compounded at 180 °C was changed to darker brownish colour for the samples processed at 210 °C. The change in colour was related to the degradation of the matrix at higher temperatures [326]. H4 presented the highest thermal stability as compared to H20 which could be referred to the PLA sensitivity at temperatures higher than 190 °C. This could be either an advantage or disadvantage based on the required application. For instance, processing temperature below 190 °C could be recommended for applications where higher thermal stability is required and above 190 °C can be suggested for thermal recycling applications [260].

4.4. Cellulose nanoparticles/polylactic acid biocomposites blend

A detailed morphology of CNP, PLA, and PN2 was presented in Figure 39. CNP had a very high surface area and showed to have a tendency to aggregate when dried (Figure 39a). Aggregation of CNP directly affects the uniform dispersion of nano particles [327]. Studies used various swelling agents to improve the particles dispersion; Phosphoric acid (H_3PO_4), Sodium hydroxide

(NaOH), dimethylsulfoxide (DMSO) [261, 328]. Recently researchers modified CNP with diethylenetriamine (DETA) curing agent and were able not to only improve the mechanical properties of biocomposite (1.42 % in modulus, 15.44 % in tensile stress, and 27.47 % in tensile strain) but also to achieve more uniform dispersion [261]. On the other hand, the voids and pores on nano particles could trap air in the biocomposite. This issue has led to various particles surface modifications prior to any application of reinforcement [329, 330]. Such modifications require suitable optimisation to avoid any damage on the particles surface. This shows the importance of particles morphology as well as surface properties during reinforcement of bioplastics.

The shearing forces during compounding would contribute to the separation of the nano particles in the matrix. Figure 39a shows large aggregates of CNP and Figure 39c clearly shows the separation process of nano particles after the compounding process. At the same time, it was observed that the addition of CNP into PLA matrix resulted in a smoother fractured surface.

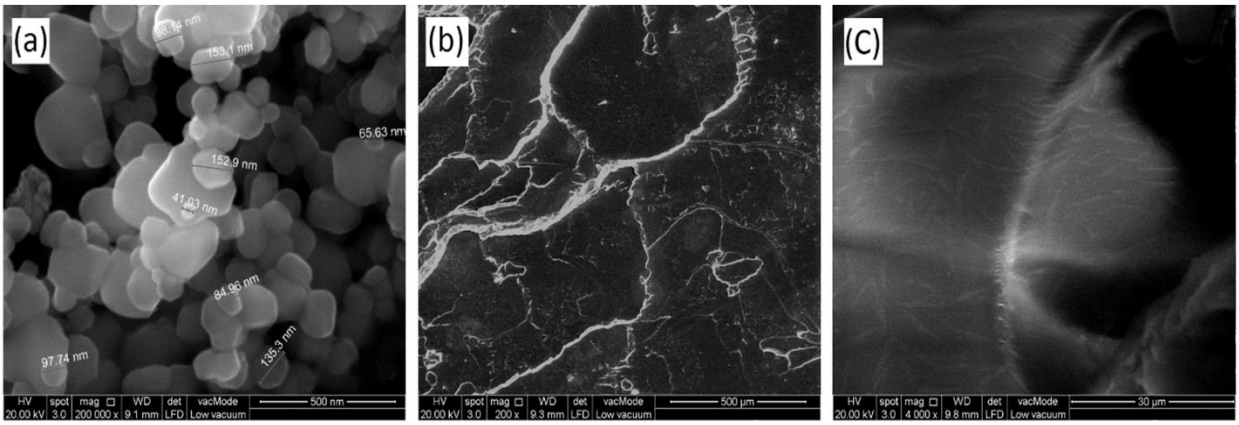

Figure 37: Scanning electron micrographs; (a) CNP at 200000x, (b) PLA at 200x, and (c) PN2 at 4000x of magnification.

The results from mechanical tests (Tensile strength, young's modulus, and impact strength) are presented in Table 36. PLA was used as reference material to observe the effect of CNP addition on mechanical properties. In general, CNP showed to have a significant effect on improving both impact and tensile strength properties of PLA. On comparing the biocomposites, the

composition of PN2 appeared to be more suitable. Reinforcement of 3 wt. % of CNP (PN2) improved tensile strength by nearly 25 %. Meanwhile, addition of 5 wt. % of CNP (PN3) significantly decreased the impact strength of PLA while slightly improved its tensile strength (tensile strength improved by ~13 % and young modulus by ~1.4 %). The increase in impact strength (PN2) can be referenced to the diameter of nanoparticles which resulted in higher aspect ratio and smooth surface. It improved the fibre/matrix interaction. Moreover, the mechanical results revealed that the addition of 5 wt. % of CNP increased the chance of nano particles aggregation and less space was left for nano particles to perform a uniform dispersion. The increase in amount of nano particles and their interaction between the matrix could be another reason for the observed young modulus results.

Table 37: PN biocomposite mechanical properties

Sample	Tensile strength (MPa)	Young's modulus (MPa)	Impact (J m^{-1})
PLA	61.49± 1.77	608.66± 10.55	31.65± 3.10
PN1	61.49± 1.95	504.71± 0.25	32.06± 1.87
PN2	74.71± 0.37	593.34± 8.11	34.67± 0.31
PN3	67.87± 0.72	590.39±17.58	18.23± 3.21

Mechanical properties of chitosan films were improved by addition of 15 wt. % CNP and 18 wt. % of glycerol as plasticiser [331]. Also by adding 5 wt. % of CNP, researchers achieved the value of ~71 MPa for tensile strength while in this research with addition of 3 wt. % of optimised CNP similar results were achieved. This comparison revealed the importance and reliability of optimisation techniques which made this research comparable to previous studies in this field. At the same time, studies were able to achieve up to about 34 % improvement in tensile strength properties by adding only 1 wt. % using solvent casting method [332]. This could be related to the filler dispersion quality improvement as well; in this way the nano particles have more time and space for better dispersion as the solution viscosity is notably lower than that of melted compounds. After all, in order to maintain the improvements in tensile strength and reclaim the impact resistance of PLA, SNR as a plasticiser was introduced to the biocomposite matrix and

PNR biocomposites were presented.

DMA was performed to investigate the stiffness of PN biocomposite at elevated temperature. PLA has two crystallisation stage; first within a range from 0–90 °C, and secondary crystallisation begins above 90 °C. In this research, the test temperature was increased from 30 °C to 120 °C at 3 °C min^{-1}. The curves of dynamic storage modulus (E') for PLA and PN1-3 samples were presented in Figure 40a. PLA showed to have the lowest E' of all biocomposites. This was directly related to the addition of CNP which improved the stiffness of PLA. Following a uniform dispersion, the stress during the test was transferred from PLA matrix to nano particles [333]. This transfer of stress reduced the mobility and deformation of the matrix [334]. The dynamic storage modulus of PN biocomposites increased with the nano particles addition to the matrix.

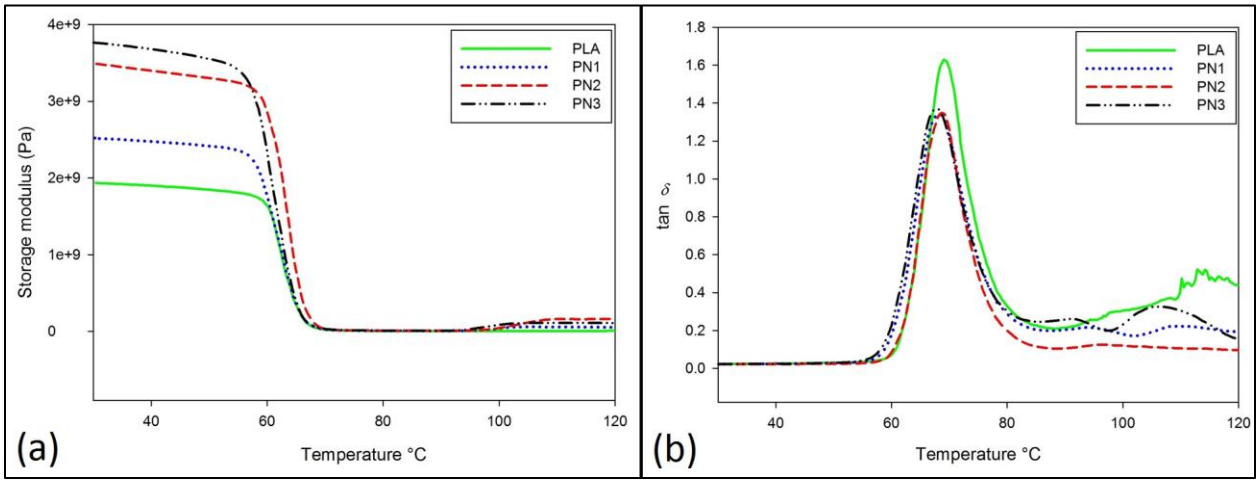

Figure 38: Effect of CNP loading on PN biocomposites; (a) dynamic storage modulus, and (b) tangent delta

Tangent delta (tan δ) as a function of temperature was also studied using Equation 11; made of storage modulus, E' and loss modulus, E''. The results for PLA and PN1-3 samples were presented in Figure 40b.

$$\tan \delta = E'' / E' \qquad \textbf{Eq. (11)}$$

The peak of tan δ curve is used to estimate the samples glass transition temperature (Tg) [335]. It was observed that PLA, PN1, PN2, PN3 samples have a Tg of 70.6 °C, 68.1 °C, 68.7 °C, 67 °C respectively. PLA has relatively high Tg and low melting temperature (T_m) as compared to other bioplastics due to its relatively lower molecular weight [319]. As comparing the curves, the increase in reinforcement of PLA with CNP hardly altered the tan δ value of biocomposites. It has been reported that the addition of CNP slightly reduced the tan δ value of PLA matrix due to the increase in the elastic response of biocomposite [336]. The damping in the stress transition region has negative influence on elasticity behaviour of samples. This incident directly affects the stress transition from matrix to nano particles which results in loss modulus value drop. Therefore, during DMA test, the introduced force for sample deformation needs to be either transferred from matrix to nano particles or will be transformed into heat [337].

Reinforcement of PLA was further explained using relative normalised storage modulus (E*) with respect to the temperature variation (Figure 41). The relative normalised storage modulus was calculated according to Equation 12:

$$E^* = (E'_C / E'_m) \qquad \textbf{Eq. (12)}$$

Where E'_C and E'_m were storage modulus of the biocomposite and the PLA matrix, respectively with temperatures at different fibre loadings. The results revealed an increase in storage modulus value following the increase in CNP loading. This improvement was more evident at higher temperatures (above 70 °C) which was due to the shift from glassy to rubbery state.

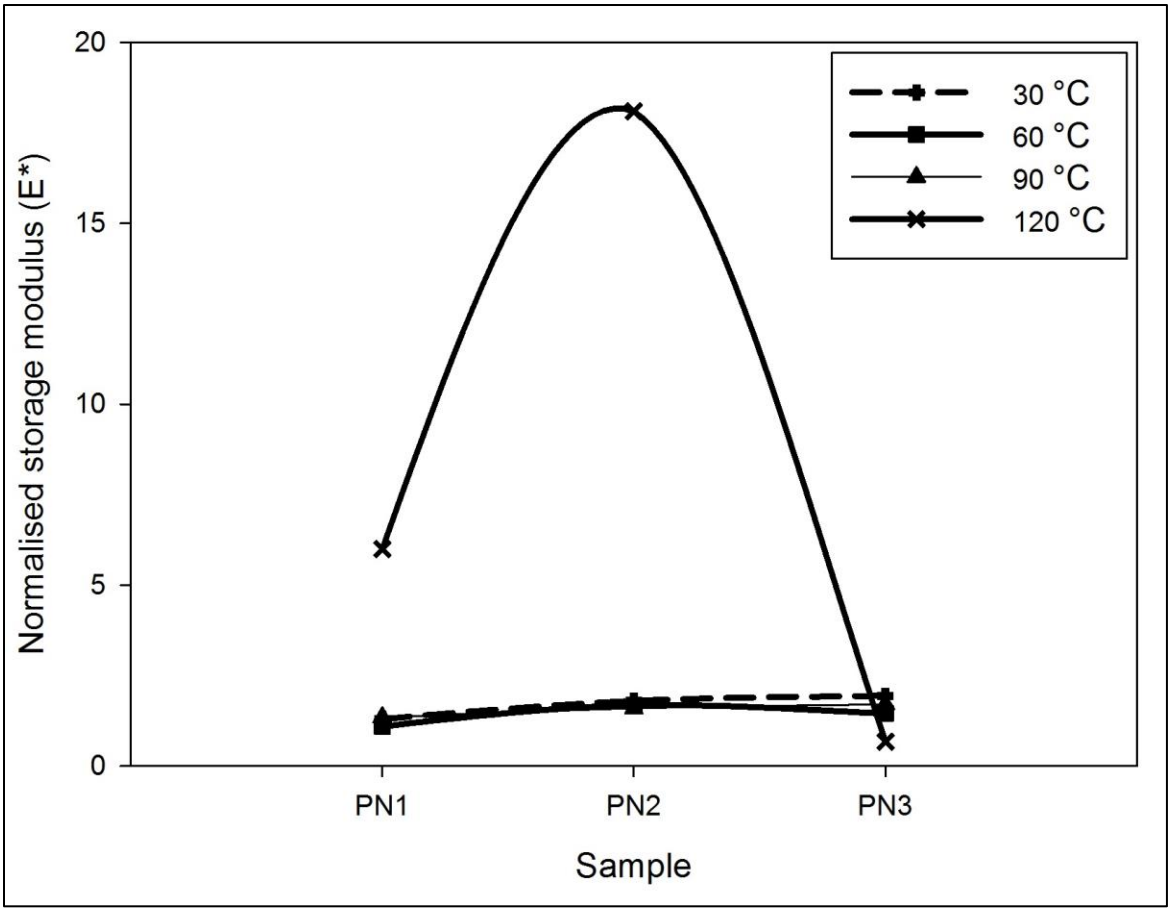

Figure 39: Normalised storage modulus of PN biocomposites

Biocomposites modulus retention variations were determined and presented in Table 37. The influence of CNP on modulus of the biocomposites was estimated using coefficient C as:

$C=((E'_G/E'_R))_{biocomposites}/((E'_G/E'_R))_{PLA}$ **Eq. (13)**

Where E'_G and E'_R were storage modulus values in glassy and rubbery regions respectively. The measured E' values at 30 °C and 120 °C (arbitrarily selected) were used as E'_G and E'_R respectively. The values were listed in Table 37 as well.

Table 38: Biocomposites modulus retention variations

Specimen	**C**	**Modulus retention %**		
		E'_{60}/E'_{30}	E'_{90}/E'_{30}	E'_{120}/E'_{30}

PLA	−	83.43	0.32	0.46
PN1	0.21	70.29	0.33	2.14
PN2	0.09	77.97	0.28	4.67
PN3	0.15	62.31	0.28	2.92

A slight decrease in modulus retention was observed following the increase in CNP loading. This was linked to the transfer of stress from the matrix to the CNP [338]. In general increase in CNP loading resulted in decrease in C value. However, this increase was more beneficial up to 3 wt. % of CNP. In comparison, composition of PN2 (with C value of 0.09) was found more reliable as lower C values, presented higher filler effectiveness. The achieved C values also revealed the significance of reinforcement of PLA with 3 wt. % of CNP as either higher or lower loading values resulted in higher C values. This highlighted the importance of nanobiofillers loading amount as excess loading reduced the dispersion quality and significantly dropped biocomposites mechanical properties.

Reinforcement of PLA with CNP increased the overall thermal stability of the matrix; PN3 > PN2 > PN1 > PLA (Figure 42). This was linked to the increase in fibre and matrix interaction. The heat deflection temperature might be influenced by the better wettability of nanoparticles and strong fibre–matrix interfacial strength. These findings are also supported by similar studies while investigating kenaf fibres reinforced PLA biocomposites [87].

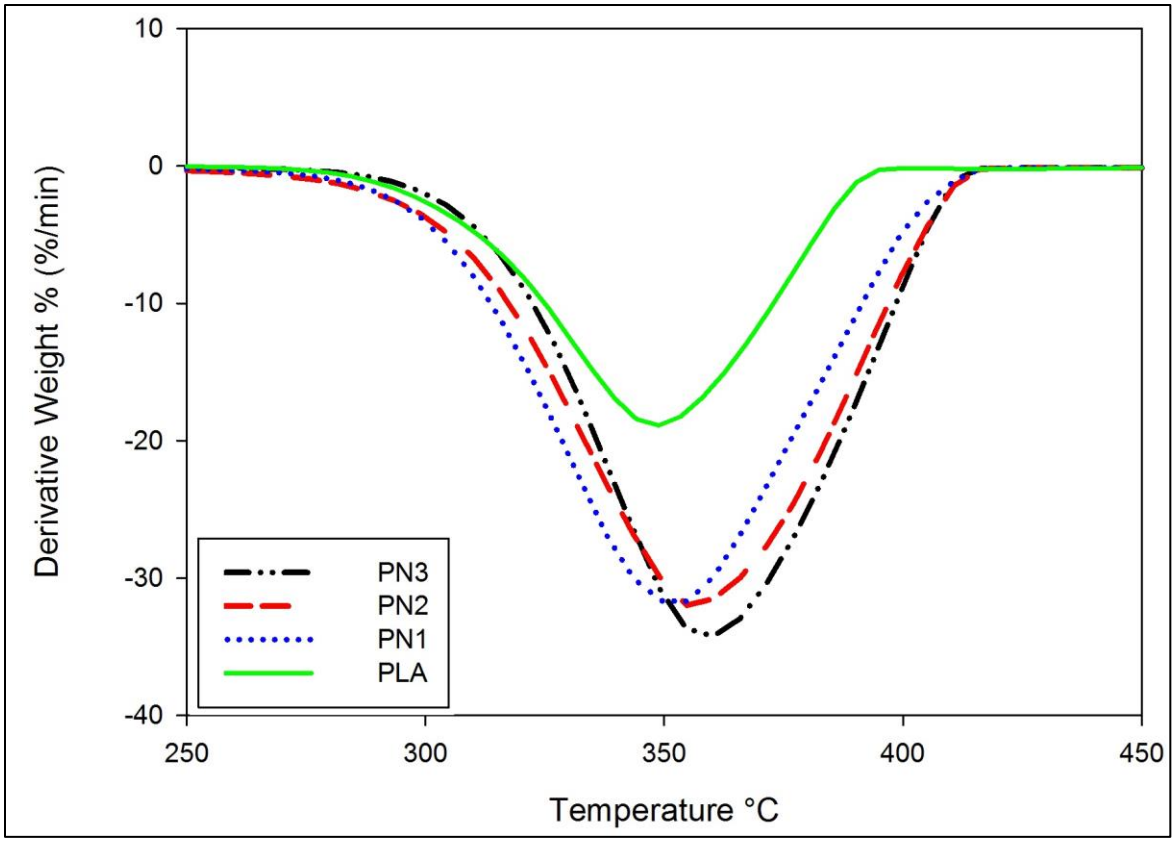

Figure 40: DTG thermogram results of PN biocomposites

All biocomposites started to degrade at ~ 320 °C. At this temperature, PN1 and PN2 showed 8 % of weight loss while PN3 showed 5 % of weight loss. This difference became more clear at higher 360 °C as PN1 faced 70 % of weight loss while PN2 and PN3 showed 55 % and 48 % of weight loss. This showed the influence of CNP on thermal stability of PLA at high temperatures. Through the processing, the transparent yellow colour of PLA matrix slightly turned to transparent brownish colour which was related to degradation of the CNP following the processing temperature (180 °C). The drop in isothermal curves at about 180 °C explained the degradation and therefore change in colour of biocomposite samples. This leaves a topic for future studies to analyse the properties of CNP individually after the compounding process.

4.5. Cellulose nanoparticles/natural rubber/polylactic acid biocomposites blend

One of the main drawbacks was CNP aggregation which result in a nonhomogeneous stress transfer from matrix to nanoparticles. Presence of SNR and selection of compounding process instead of solvent casting, were the two solutions found to this issue. As observed in Figure 43a, CNP appeared in aggregated nano spherical shapes prior to reinforcement while the same nanoparticles were found in needle shape and less aggregated after the reinforcement process (highlighted in Figure 43c). SNR made nanoparticles movement easier through the matrix and the shearing force through compounding enforced the nanoparticles to form homogenously. The white lines appeared in Figure 43b are the borders between PLA granules. The addition of SNR as a plasticiser notably reduced these lines and resulted a greater crosslinking as the granules were linked adequately. However, at higher concentrations of SNR, the excess SNR was located in between granules and apparently caused a gap between granules which notably affected tensile strength properties of biocomposites.

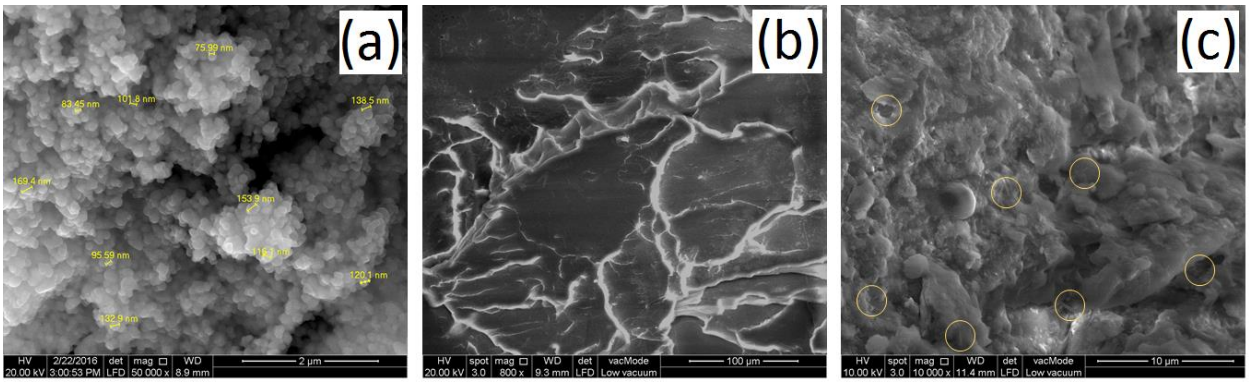

Figure 41: Scanning electron micrographs; (a) CNP at 50000x, (b) PLA at 800x, and (c) PNR at 10000x of magnification.

Mechanical tests on the biocomposites were performed and the results are presented in Table 38 respectively. As observed the addition of SNR notably decreased the tensile strength of PLA composites while at the same time remarkably improved the impact strength of PLA. With addition of 10 wt. % of SNR, ~60 % reduction if tensile strength was detected. This drawback was reported elsewhere as researchers achieved composites with high impact properties with notably weak tensile properties [250, 251]. Both studies reported ~ 35 % and ~ 37 % reduction in

tensile strength composition (based on addition of 10 wt. % of SNR to PLA) through melt compounding. Also addition of a nucleating agent was found ineffective to overcome this problem [339]. It was linked to the placement of SNR matrix in between the PLA granules. This gap in between granules made the samples to quickly give up and tear during tensile test and therefore very poor results were achieved. Nevertheless, these gaps provided a larger impact receiving area and allowed a superior force transfer from the PLA matrix to both SNR and CNP. It was assumed that incorporation of CNP will fill these gaps and recover the composites tensile strength.

Table 39: Mechanical properties of biocomposites

Sample	Tensile strength (MPa)	Young's modulus (MPa)	Impact strength (J m^{-1})
PLA	61.49±1.77	608.66±10.55	31.65±3.10
PR1	27.69±0.88	573.20±55.64	63.02±6.66
PR2	25.187±1.99	532.74±64.94	67.31±5.18
PR3	16.83±1.83	355.94±41.39	59.64±6.39
PR4	13.79±1.36	320.29±27.72	54.30±8.06
PNR	62.13±1.22	1169.47±39.45	62.34±2.79

Based on the earlier observations and current results, addition of more than 10 wt. % SNR to PLA was found to be impractical. As a result, based on the improvements in impacts resistance, PR2 composition was selected to add 3 wt. % CNP for PNR biocomposites preparation. The addition of CNP to PR2 exceptionally recovered its toughness and presented a considerable improvement in biocomposites tensile strength as compared to both all PR and PLA samples; Nearly 147 % and 1% improvement for all PR and PLA samples respectively. Moreover, impact strength of PNR was nearly double of that achieved by PLA samples. This was predictable due to SNR plasticiser characteristic. Furthermore, the introduction of 3 wt. % CNP and 10 wt. % SNR to the PLA matrix resulted in a significant improvement in young's modulus value (from 608.66 to 1169.47 MPa). This was believed to be due to the optimum presence of nano structure as well as enhanced interaction between the biocomposite components using SNR [340]. The

presence of SNR and CNP was required at the same time to maintain tensile properties of PLA while improving its impact resistant properties.

To determine the viscoelastic behaviour of biocomposites, storage modulus (E′) and tan δ curves as a function of temperature were estimated. Higher E′ values indicated the rigidity of biocomposites. The glass transition temperature (Tg) was achieved based on their damping factor. E′ value decreased through all samples with increasing temperature (Figure 44a). This was linked to the increase in viscosity and flexibility of polymer chains which reduced the rigid interface between CNP and PR2 matrix [341, 342].

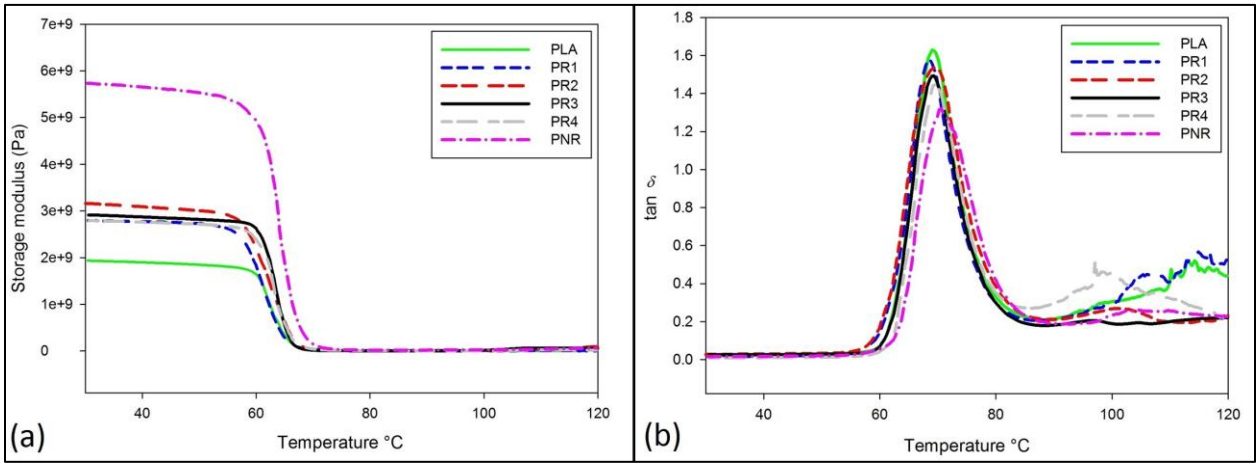

Figure 42: Biocomposites viscoelastic behaviour; (a) storage modulus, and (b) tan δ as a function of temperature

As the temperature increased to 120 °C, all PR as well as PNR compositions showed much higher storage modulus values than that of PLA. This was due to the stress transfer from PLA to both SNR and CNP while as observed, CNP showed greater capabilities in this case. Also reinforcement of rigid nano filler like CNP increases the biocomposite stiffness and thermal stability. This was observed both in dynamical and thermal analysis as PNR samples revealed superior properties. To further investigate the influence incorporation of CNP with PR2 matrix, the relative normalised storage modulus (E*) was calculated using Equation 12 and the results were presented in Figure 45. Where E'_C and E'_m were storage modulus of biocomposites and PLA matrix respectively with selected temperatures at different nano filler loadings. The values

were more pronounced at higher temperatures (above Tg). The results revealed an increase in storage modulus value for all PR samples with increase in SNR content while this improvement was best presented in PR2 samples. Therefore, PR2 was chosen to be the suitable composition to host CNP for preparation of PNR samples. PNR samples showed notably higher storage modulus values as compared to all samples including PLA. This was due to the improvement in thermal stability of the composition followed by the addition of CNP.

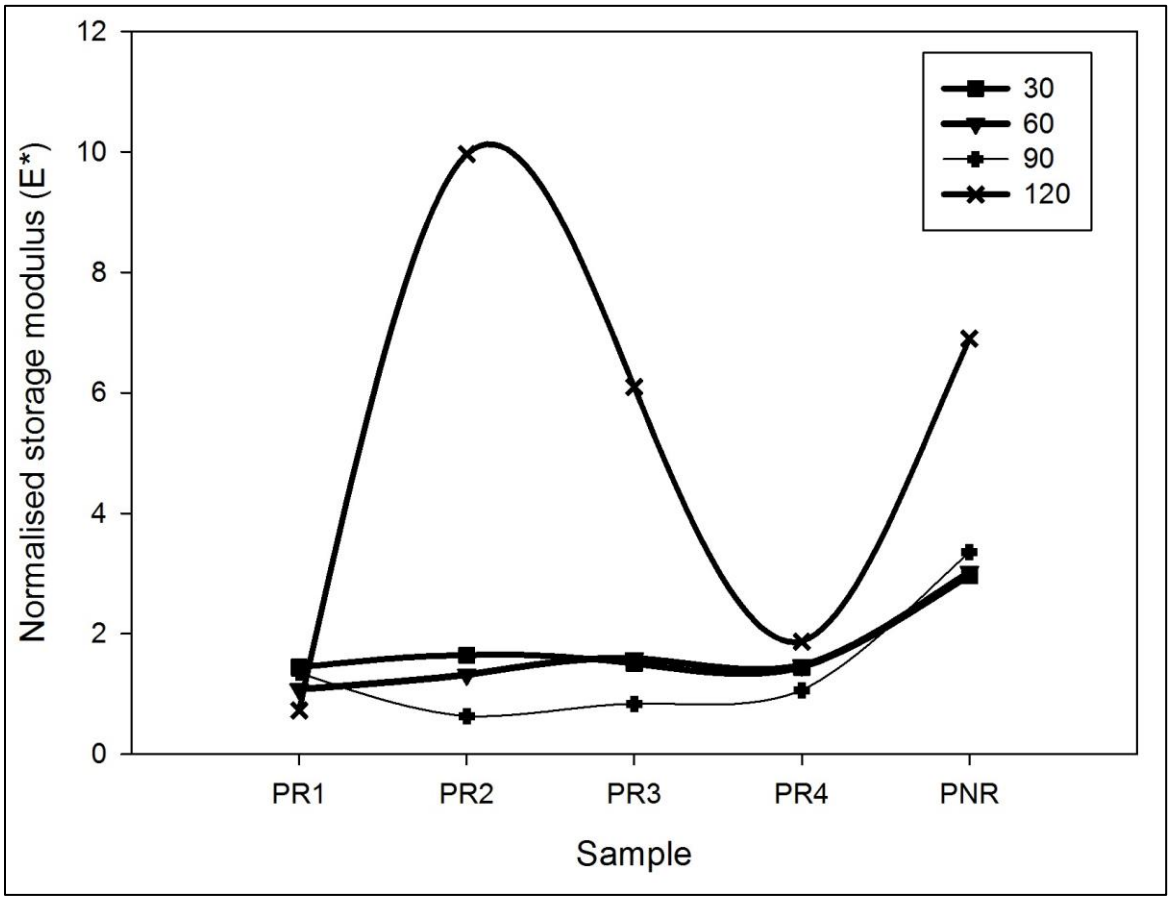

Figure 43: Normalised storage modulus of PR biocomposites with CNP

Through similar studies, samples showed higher E' values at their rubbery state as compared to glassy state [343]. Above Tg, the variance in E' values were easily distinguished due to the matrix shift from glassy state to rubbery state. The variation in biocomposites modulus retention is presented in Table 39. The influence of CNP and SNR on the modulus of the PLA matrix was determined and validated by coefficient "C" using Equation 13; where E'_G and E'_R were storage

modulus values in glassy and rubbery regions respectively. The achieved E' values at 30 °C and 120 °C (arbitrarily selected) were employed as E'_G and E'_R respectively. Lower "C" values were preferred as they were presenting higher efficiency of reinforcing PLA matrix with SNR and CNP respectively (Table 39).

Table 40: Variations of biocomposites modulus retention

Specimen	C	Modulus Retention %		
		E'_{60}/ E'_{30}	E'_{90}/ E'_{30}	E'_{120}/ E'_{30}
PLA	–	83.43	0.32	0.46
PR1	1.98	62.44	0.30	0.23
PR2	0.16	66.91	0.12	2.82
PR3	0.24	88.24	0.17	1.88
PR4	0.76	85.49	0.23	0.60
PNR	0.42	85.27	0.36	1.08

As comparing the PR samples, the addition of SNR to PLA matrix more than 10 wt. % was found less beneficial to achieve a favourable "C" value. This could be due to the increase in samples elasticity at higher SNR contents [344]. Incorporation of CNP into PR2/PLA (PR2) retained the C value at low level and slightly improved the modulus retention values.

Tan δ was determined and studied using Equation 11; where E' and E" were storage modulus and loss modulus respectively. The tan δ curves were presented in Figure 46b. Samples Tg (b-transition) was estimated based on the main peak of tan δ curve [335]. Samples had relatively close Tg values. It was observed that PLA, PR1, PR2, PR3, PR4, and PNR samples have a Tg value of 68.99 °C, 68.31 °C, 69.65 °C, 69.08 °C, 69.61 °C, and 70.80 °C respectively. The slight shift in Tg value from 69.65 °C to 70.80 °C could be linked to the reduction in rubber chain mobility [250, 345]. This was due to the incorporation of CNP as it strongly interacted and crosslinked with SNR matrix and shifted its affinity toward elastomeric phase.

Through similar earlier studies, the height of the tan δ to the motion of free main segments of molecular chains [346]. The addition of SNR and CNP, notably reduced this motion and decreased the height respectively (Figure 46b). Also in terms of damping, the increase in SNR content was found beneficial as it slightly decreased the PLA tan δ value. This value notably decreased following the introduction of CNP to PR2 matrix. This was found to be due to the nano filler toughening effect as well as increase in biocomposites elastic response [347, 348]. Also following the preparation method, it could be due to the sheared surface of nano filler particles which allow a better stress transfer [341]. Samples elasticity behaviour can be directly influenced by the damping (molecular mobility) in the stress transition region [349]. In this research, this negative influence was reduced by incorporation of CNP as the stress was transferred from matrix to the nano fillers. Similar observations were achieved for reinforced polyurethane matrix with CNP [350]. This improvement was related to the strong physical H-bonding and covalent linkages between the matrix and the nano filler.

Thermal analysis agreed on selection of PR2 as the optimum composition. As observed in Figure 46, PR2 showed to have the highest thermal stability as compared to PLA, PR1, PR3, and PR4. The addition of both SNR and CNP improved the thermal stability of PLA by ~20 °C. PNR showed lower thermal stability as compared to PR2 which was linked to the degradation of CNP content at high temperatures (higher than 300 °C). The biocomposites with SNR presented an opposite behaviour compared to the biocomposites with CNP. Higher concentration of SNR than 10 wt. % decreased the thermal stability of PLA; the excess SNR was located in between PLA granules and developed a gap between granules which affected the overall stability of PR3 and PR4 at high temperatures.

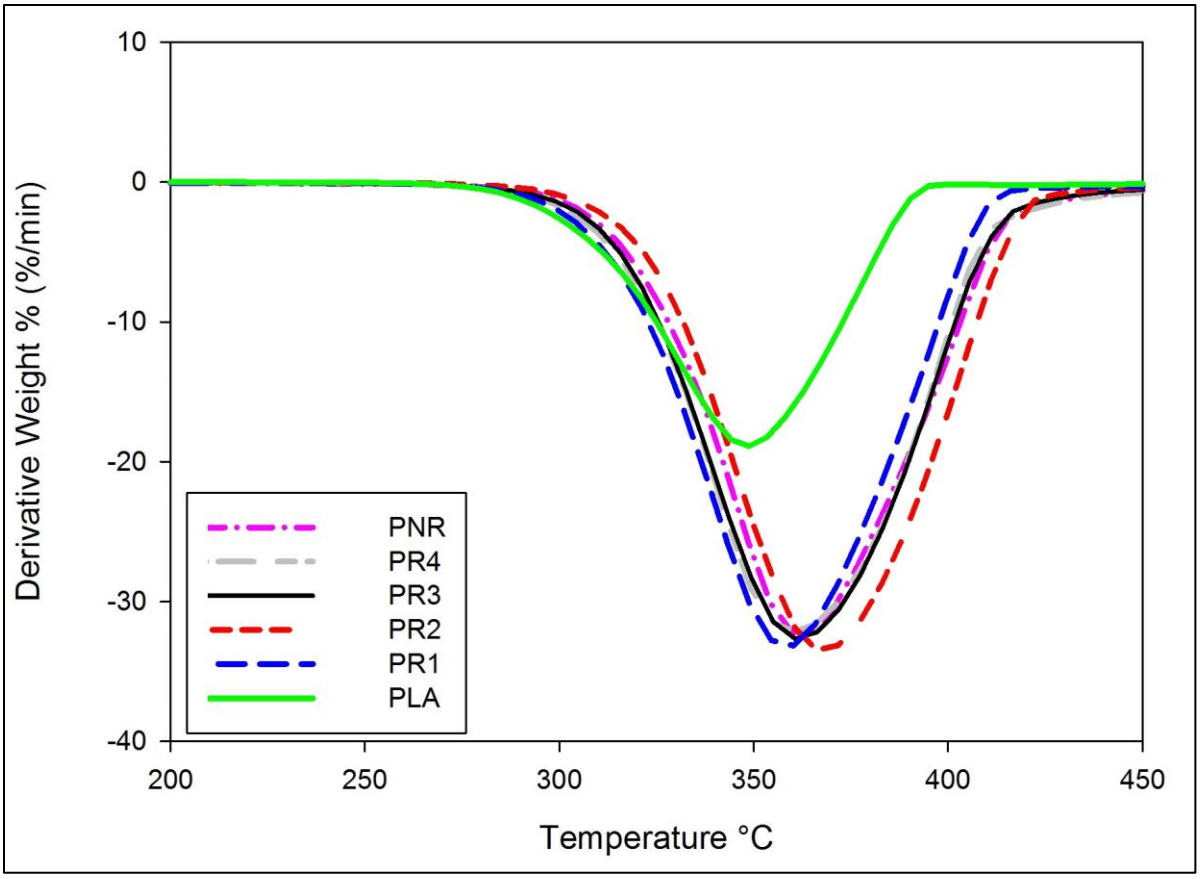

Figure 44: Experimental DTG curves for prepared biocomposites

4.6. Biodegradation, water absorption and thermal degradation of the biocomposites

Biocomposites weight loss percentage through soil burial test was achieved in a range from 0.61 % for PR2 to 3.70 % for PN3. The results were plotted and presented in Figure 47. Throughout the first 720 h of soil burial, the biocomposites barely degraded and at the same time PN2, PN3, PR1, PR4, and PNR showed a slight increase in their weight (~0.6 %); this increase was referred to water intake by biocomposites from soil. A weight loss percentage of 0.61–2.08 % was observed at the very early stages of degradation (after 1440 h). The biodegradation process was more detectable after 2160 h of soil burial where PN biocomposites faced weight loss of ~3 % while PR biocomposites showed ~1.5 % of weight loss. Basically, a higher CNP and lower SNR content resulted in a faster biodegradation process. Therefore, PN3 was biodegraded fastest of all biocomposites. This observation was linked to the minor amorphous regions of CNP which decreased the biocomposites resistant against degradation. The CNP prepared in this research

was highly crystalline. Fair biodegradation of the biocomposites with CNP confirmed this claim as amorphous structures are more easily attacked by hydrolytic enzymes which can result in much higher biodegradation rates [351]. This indicates the significant role of amorphous regions through a biodegradation process. Depending on future applications, further CNP treatment could be recommended to increase its crystallinity.

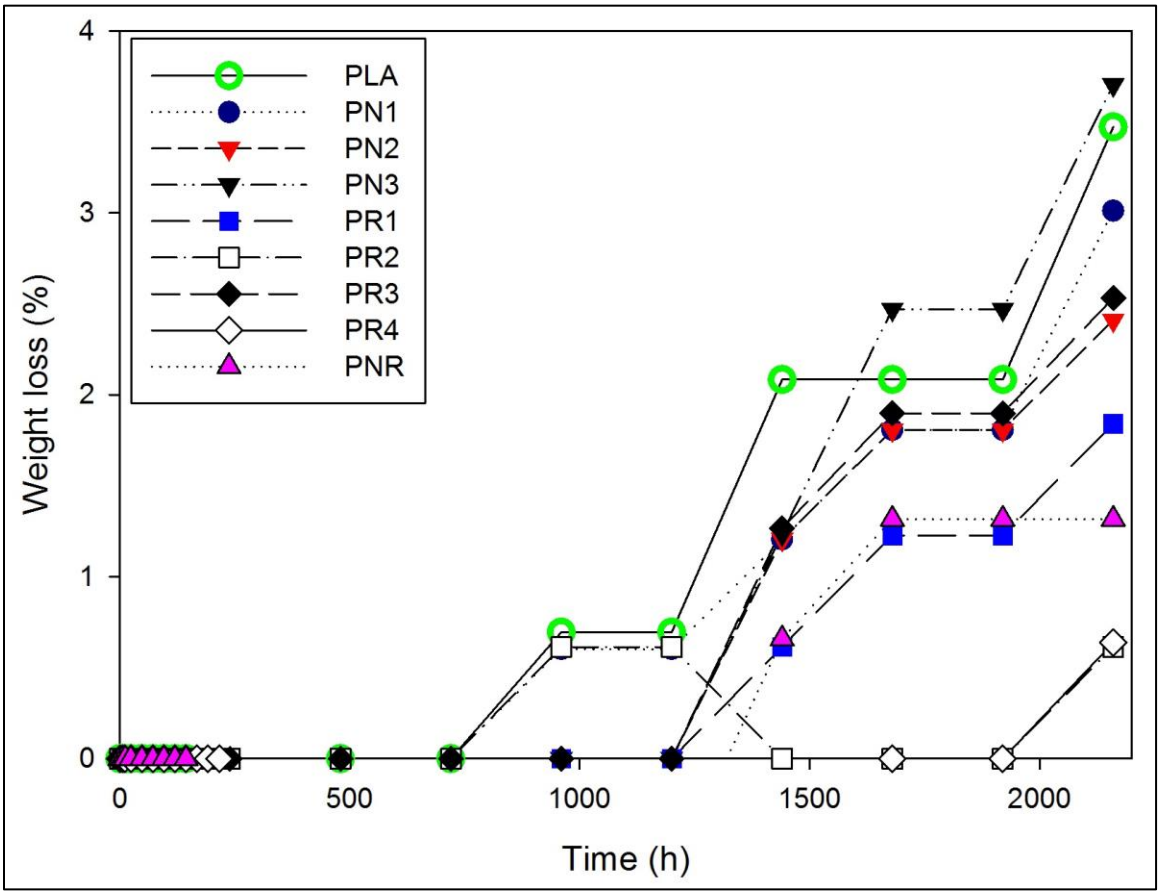

Figure 45: Weight loss percentage of biocomposites in the soil test vs time over 90 days

The degradation of PR4 was slower than that of any biocomposites. It was related to the hydrophobic nature of SNR which retained the PLA structure [352]. This was also detected in PNR and was linked not only to the nature of SNR but also to the enhanced interfacial adhesion between the PLA matrix and CNP due to the addition of SNR. Therefore, the PNR composition showed a moderate degradation as compared to both PN and PR biocomposites. PNR had weight loss of 1.3 % after 2160 h of soil burial.

Water absorption test was carried out in parallel with soil burial test. Figure 48 presented the water absorption results. During the first 72 h, most of the sample rarely appeared to absorb any amount of water. However, PR4 and PNR began notable water absorption after 12 h. They both presented the highest water uptake during this test; 3.14 % for PR4 and 4.34 % PNR after 2160 h. The biocomposites with CNP had relatively lower water absorption rate as compared to the biocomposites with SNR. This was linked to the CNP to the strong crystalline structure and preparation technique, which minimised the hydrophilic nature of the fibre. Therefore, increase in CNP content had minor influence on water absorption rate. Meanwhile increase in SNR content, increased the water uptake. This was linked to the excess amount of SNR in PR4, which resulted into formation of micro bubbles and voids in the sample. Composite materials performance is highly dependent on presence of pores as they influence the heat and mass transfer behaviour [302]. Most of the biocomposites showed maximum water absorption of ~1 % after 2160 h (except for PR4 and PNR). PN2 and PR3 had the least absorption rate repetitively. This revealed that 3 wt. % of CNP and 15 wt. % of SNR were the maximum applicable amount of reinforcement to minimise PLA water adsorption.

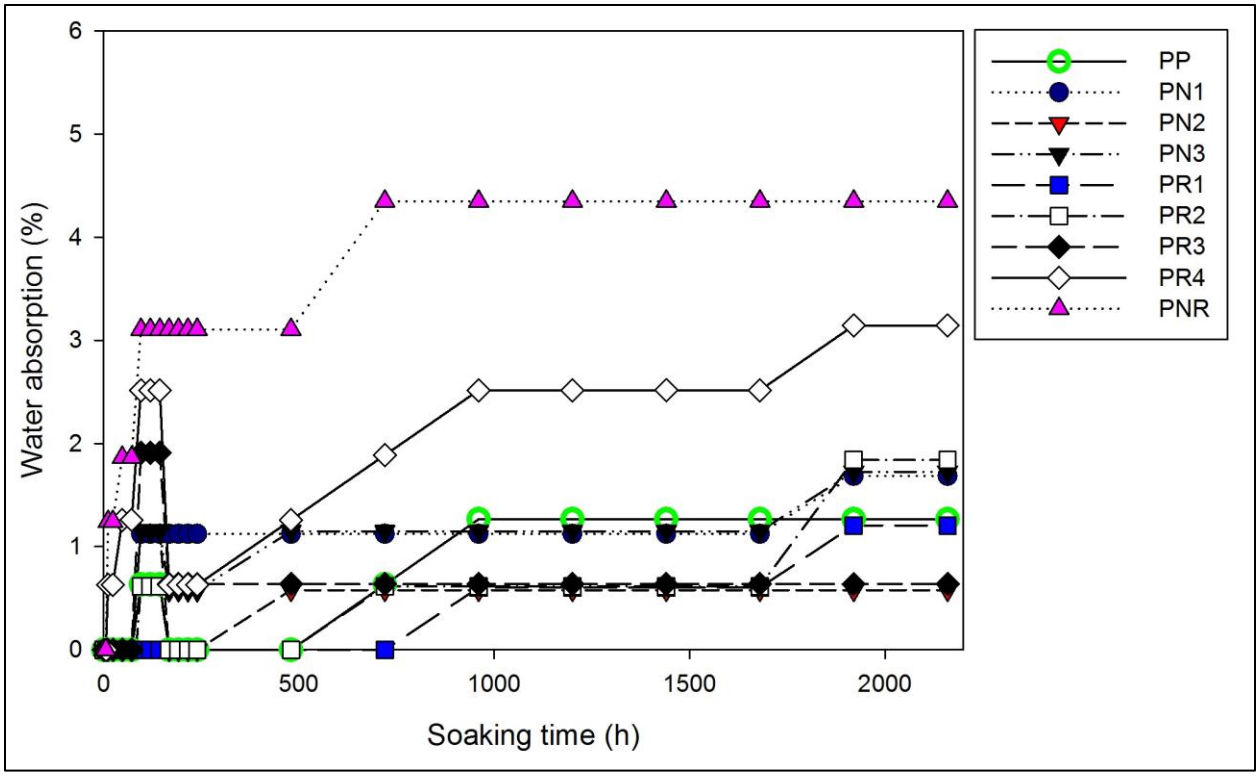

Figure 46: Water uptake as a function of exposure time in distilled water

For better understanding, Figure 49 reviews the changes of the relative biocomposites through thermal degradation. All biocomposites started to degrade at ~320 °C. At this temperature, PN1 and PN2 showed 8 % of weight loss while PN3 showed 5 % of weight loss. This difference became more clear at higher 360 °C as PN1 faced 70 % of weight loss while PN2 and PN3 showed 55 % and 48 % of weight loss. This showed the influence of CNP on thermal stability of PLA at high temperatures. Meanwhile, the biocomposites with SNR presented an opposite behaviour compared to the biocomposites with CNP. Higher concentration of SNR than 10 wt. % decreased the thermal stability of PLA; the excess SNR was located in between PLA granules and developed a gap between granules which affected the overall stability of PR3 and PR4 at high temperatures. At higher temperatures of degradation, cellulose fibres contributed a higher portion of weight loss as compared to SNR and as a result PR2 showed the highest thermal stability amongst all biocomposites. Thermal studies in conjunction with soil burial and water absorption test agreed on optimum PNR compositions (addition of 3 wt. % of CNP and 10 wt. % of SNR). Reinforcement PLA with both SNR and CNP improved its thermal stability by ~20 °C.

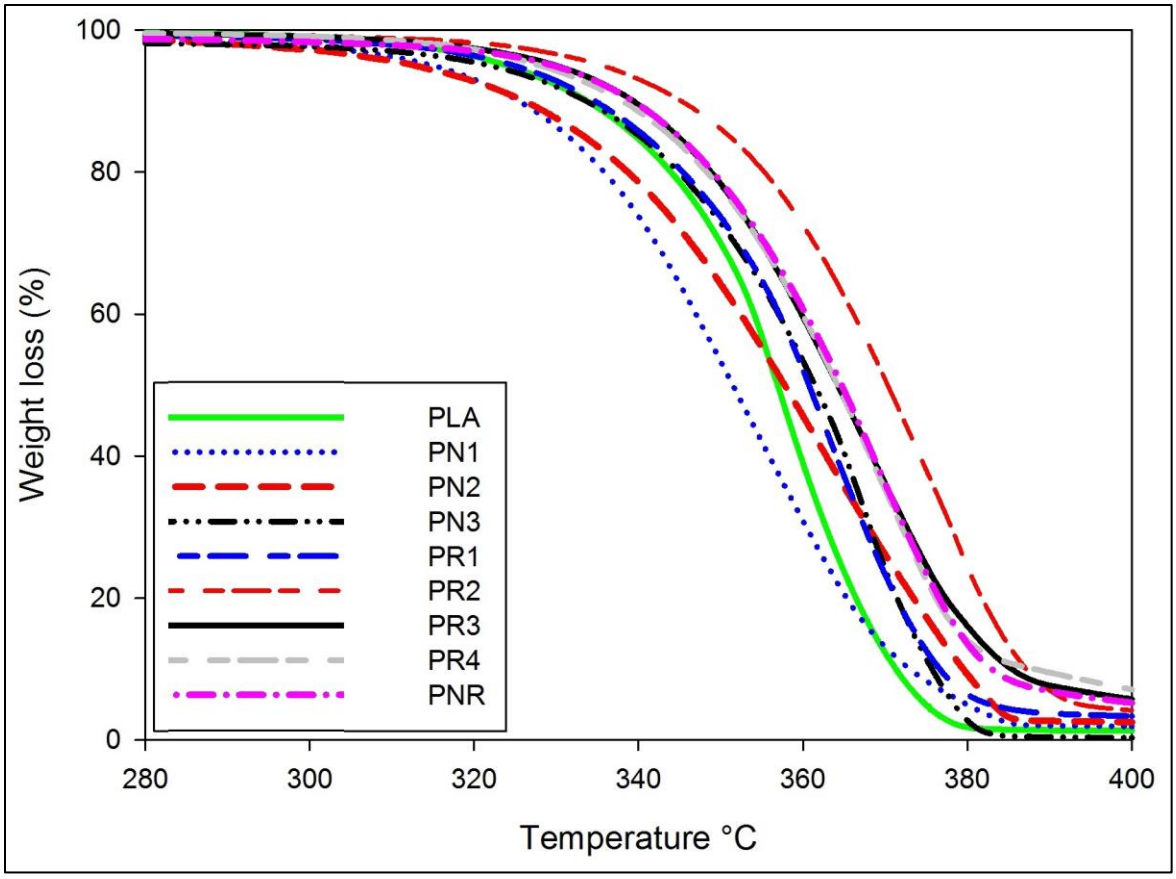

Figure 47: Thermogravimetric curves of PLA and its biocomposites

The effects of biodegradation on the surface of all biocomposites after 2160 h of soil burial was analysed using SEM micrographs and selectively presented in Figure 50. Partial biodegradation of PLA matrix was observed which was due to microbial action rather than physical discharge. Randomly stretched and expanded cracks and holes confirmed the biodegradation process [353]. Biocomposites with higher rates of biodegradation (PLA, PN3, and PR3) presented quite more number of cracks. In addition to the cracks, the shrinkage of biocomposites was found another reason to accelerate the exposure of CNP to moisture and its surrounding area [297]. Much fewer numbers of cracks and crack spaces were observed on PNR surface as compared to PLA which was related to the reinforcement which notably decreased its biodegradation rate. PNR was found to be a suitable fertiliser coating material due to its suitable biodegradation process. Moderate biodegradation of PNR can stabilise and control the fertiliser nutrients release in the soil. Master-batch preparation of PNR/fertiliser was recommended for future studies.

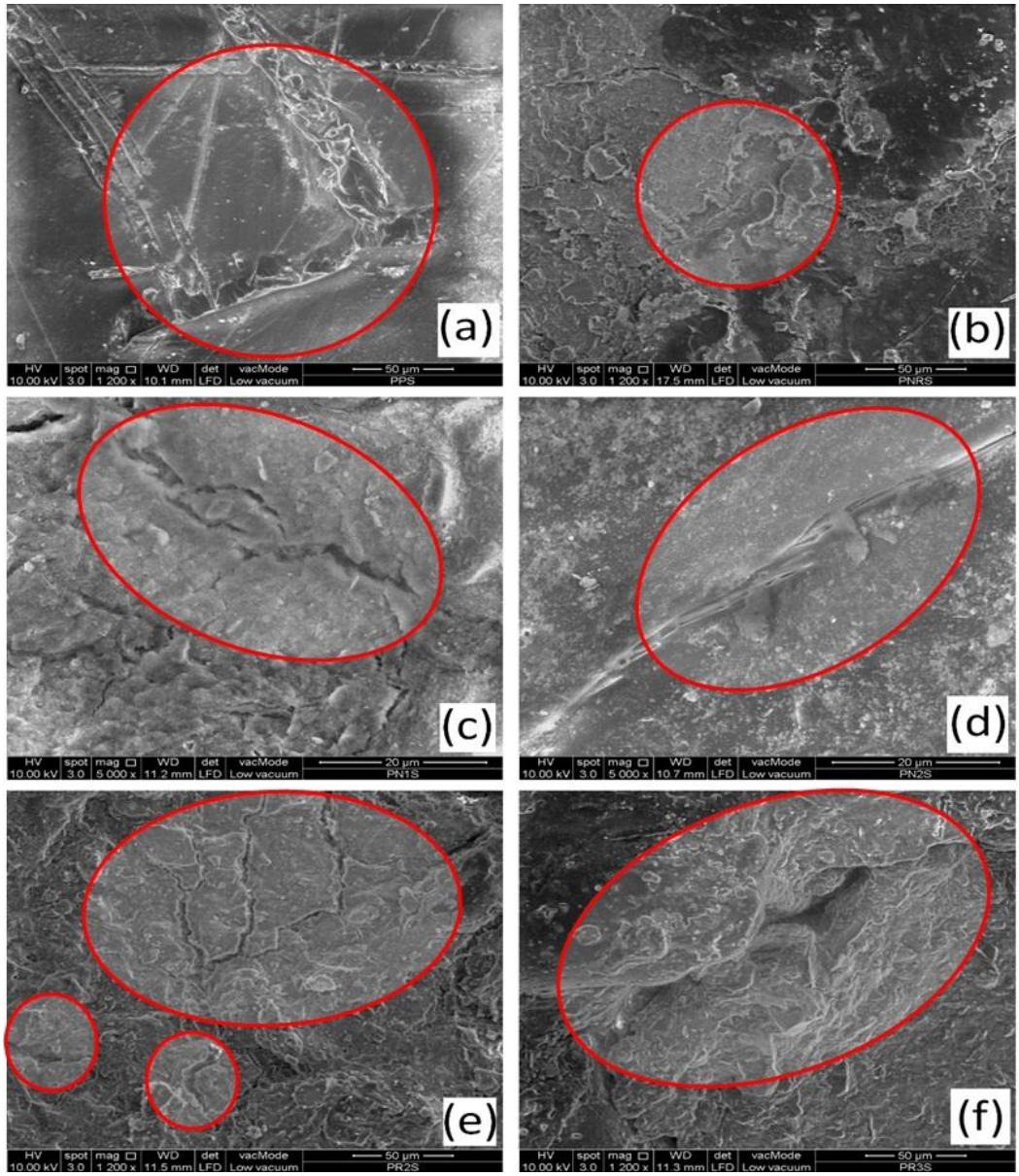

Figure 48: Scanning electron micrographs after 2160 h of soil burial; (a) PLA at 1200x, (b) PNR at 1200x, (c) PN1 at 5000x, (d) PN2 at 5000x, (e) PR2 at 1200x, (f) PR3 at 1200x of magnification.

As a biomaterial, it was necessary to determine the time required for complete biodegradation of PNR and its water absorption rate. The soil burial and the water absorption test results were best fitted to cubic polynomial model (Equation 14); Y was weight-loss %/water-absorption % factor; X was time factor; Y_0, a, b and c were the four coefficients of the cubic model. Applicability of

the polynomial model was determined by regression coefficient R^2. The results were presented in Table 40.

$$Y = Y_0 + aX + bX^2 + cX^3 \qquad \textbf{Eq. (14)}$$

Table 41: Results of the cubic polynomial regression model for soil burial test

Test type	Biocomposite	Y_0	a	b	c	R^2
Soil	PNR	0.150	-0.0045	0.0000052	-0.0000000013	0.85
	PLA	-0.028	-0.0019	0.0000032	-0.00000000078	0.92
Water	PNR	1.190	0.0096	-0.0000083	0.0000000021	0.81
	PLA	0.089	0.00028	0.00000099	-0.00000000041	0.79

Based on the cubic equations, it was found that ~3062 h and ~3863 h of soil burial is required for complete (100 %) biodegradation of PNR and PLA respectively. The predicted periods were found quick as compared to similar studies. This was linked to the test condition which was conducted at high humidity. Biodegradation rate of PNR was found to be at ~0.15 % h^{-1} and this value for PLA was at ~0.03 % h^{-1}. This meant that, as a fertiliser coating material, PNR would last for nearly 3072 h in soil and perform a moderate biodegradation rate at ~0.15 % h^{-1}; biodegradation of PNR allows fertiliser nutrient release in the soil. Water absorption rate was 1.2 % h^{-1} and 0.08 % h^{-1} for PNR and PLA respectively. Slightly higher biodegradation and water absorption rates were linked to the presence of amorphous regions [354, 355]. CNP accelerated and SNR moderated the biodegradation of PLA biocomposites. This further confirmed the optimum composition of PNR biocomposites.

CHAPTER 5

CONCLUSIONS AND FUTURE RESEARCH

5.1. Introduction

This thesis has expressed the possibility of efficiently reinforcing polylactic acid (PLA) biocomposites. An emphasis has been placed on the role of extracted cellulose nanoparticles (CNP) in PLA matrix. This study was aimed at improving the thermal and mechanical properties of PLA by blending with CNP. This thesis also went a step forward by optimising the extraction process of CNP from kenaf fibre, and processing parameters of PLA. Moreover, for the first time, the influence of natural rubber as plasticiser in CNP/PLA blend was identified.

5.2. Principal findings

Cellulose nano particles were extracted from kenaf fibre and successfully used as a reinforcing filler in SNR/PLA (PR) biocomposites. Kenaf fibres showed to be an interesting source of raw material for the production of CNP. For various types of treatment, an optimum solid-liquid ratio of 1:50 (w:v) (fibre:distilled water) was found significant. Chemical treatment performed with sodium chlorite and sodium hydroxide removed the non-cellulosic components of untreated fibre and resulted in fibres with a low content of lignin and a high content of cellulose. Application of sonication for at least 15 min was found necessary to shift from the micro size to the nano size. Mercerisation process prior to the bleaching process was found more beneficial to isolate smooth white particles. Moreover, succeeding to a mercerisation process, the addition of only 2 v. % of $NaClO_2$ was found sufficient for an acceptable bleaching process and extraction process. Production of CNP was found through four extraction techniques; steam explosion, mercerisation, bleaching, and sonication. Statistical and experimental optimisation was found essential to balance the correlation between the mercerisation and bleaching process.

Extraction of MCF from kenaf fibre was successfully optimised using response surface methodology. Significant impact of NaOH and sonication was observed on reducing the fibre diameter and agglomeration, which affected the thermal stability. Optimal extraction conditions for MCF were found as 0.15 g of NaOH at first stage, 4.67 ml of $NaClO_2$ at second stage, and 10

min of sonication during the third stage. Following the optimised parameters, MCF reached an acceptable diameter size of ~10 µm, which was in agreement with the predicted values. The main peak in DTG results of MCF was observed at 320.15 °C which was also confirmed by the predicted values. Further, FTIR shows an acceptable removal of non-cellulosic components from the final product. Finally, the XRD results demonstrated the effectiveness of optimisation as the optimised MCF presented a crystallinity index value of 71.86 %, 53.52 % improvement compared to single factor analysis.

Ultrasonic-assisted extraction of CNP from kenaf fibre was optimised using response surface methodology. The results showed that NaOH played the main role in the extraction of cellulose from the fibres. However, to attain nano size fibres sonication was found to be beneficial. This optimisation indicated that longer sonication time could affect fibre's thermal stability and reduce the degradation point. The optimal extraction conditions for the CNP were as follows: 0.2 g of NaOH/4 g of fibre at first stage, 5 ml of $NaClO_2$/4 g of fibre at second stage, and 20 min of sonication period during the third stage. Following these conditions, the CNP reached an acceptable nano size (~100 nm), which was agreed with the predicted value. Also the main peak in DTG results of CNP pointed out a value of 338.55 °C which was confirmed by the predicted values. This was further ascertain by FTIR plots which shows the removal of non-cellulosic components in the final product.

Processing parameters of PLA were optimised using a statistic model. A range of temperature starting from 180 °C to 210 °C was selected. It was observed that process temperature plays the most important role as compared to mixing duration and speed. Samples prepared at higher temperatures than 180 °C performed lower mechanical properties while having smoother fractured surface. Moreover, the quadratic polynominal model showed to be suitable to optimise preparation parameters. The optimal blending condition for PLA was achieved at 180 °C, 10 min and 100 rpm. Validation process confirms the optimal predicted values. The optimised parameters resulted in maximum stress, young modulus, and impact strength values of 60.31 MPa, 606.54.54 MPa, and 31.65 J m^{-1} respectively. To achieve an acceptable mechanical performance, preparation of PLA composites at temperatures higher than 180 °C is not recommended. However, it needs to be mentioned that based on the application, a brittle PLA

can be prepared at temperatures higher than 180 °C. Higher processing temperature was concluded to be beneficial in terms of thermal stability properties.

CNP showed to have the potential to reinforce PLA matrices. The melt compounding technique was found beneficial and solvent casting method was recommended for future studies. Aggregation was the only drawback of CNP. The nano particles uniform dispersion showed to play the main role during matrix reinforcement. The shearing forces through compounding process was contributed to the separation of the nano particles in the matrix. The brownish colour of biocomposites was found to be related to the degradation of nano particles at high temperature. Overall the addition of 3 wt. % of CNP was more acceptable as compared to the other two compositions. Addition of CNP improved the elongation properties of PLA while reverse results were observed through impact properties.

PR biocomposites were reinforced with 3 wt. % of CNP through melt compounding technique. This technique was found more beneficial as compared to solvent casting method. The three components (CNP, SNR, and PLA) showed to be highly compatible. PR2 carrying 10 wt. % of SNR was found the optimum composition to add 3 wt. % of CNP. The presence of SNR resulted a homogeneous dispersion of CNP. The presence of SNR and CNP together was found essential to retain tensile properties of PLA while improving its impact resistant properties. Addition of CNP enhanced the viscoelastic behaviour of PR2 composites. The damping effect was reduced following the addition of CNP.

Indoor biodegradation, thermal degradation, and water absorption process of PLA biocomposites was investigated. The results were best fitted to cubic polynomial model. PNR biocomposites showed to be potentially biodegradable in natural condition. Cracks and shrinkage in biocomposites surface accelerated the exposure of CNP to moisture and its surrounding area. Amorphous regions in CNP showed to play the main role to accelerate PNR biodegradation. Increase in biodegradation rate was also linked to the test condition which was carried out at high humidity. CNP accelerated and SNR moderated the biodegradation of PNR biocomposites. PNR performed an acceptable water resistance following the optimised composition. 3 wt. % of CNP and 10 wt. % of SNR was concluded to be the maximum applicable amount of reinforcement to

minimise PLA water adsorption. Excess amount of SNR in PR4 biocomposites affected its morphology and resulted into higher water absorption capacity. Improvement in PLA thermal stability was achieved following incorporation of both CNP and SNR.

5.3. Recommendation for future studies

Optimised extraction processes of MCF and CNP were found ecofriendly and cost effective. Their applicability to extract MCF and CNP from other natural fibres could be recommended for future studies. Moreover, future studies could be directed toward finding the CNP capability to reinforce other bioplastics such as polyhydroxyalkanoates (PHA), polyhydroxy butyrate (PHB), polycaprolactones (PCL), and poly(butylene succinate) (PBS). To commercialise the product of this research (PNR), further analysis on rheological, UV aging, and weathering properties are needed. Furthermore, comparison of two processing techniques (solvent casting and melt compounding) to prepare PNR could open new gates for research. Another factor that needs further attention, is the influence of biocomposite viscosity on the processing quality, speed and cycle time. Also, the influence of the application of ultrasonic technology during compounding process could be another important topic worthy of further study.

BIBLIOGRAPHY

1. Robinson, B.H., *E-waste: an assessment of global production and environmental impacts.* Science of the total environment, 2009. **408**(2): p. 183-191.
2. Vijayendra, S. and T. Shamala, *Film forming microbial biopolymers for commercial applications—a review.* Critical reviews in biotechnology, 2014.
3. Briassoulis, D., C. Dejean, and P. Picuno, *Critical review of norms and standards for biodegradable agricultural plastics Part II: Composting.* Journal of Polymers and the Environment, 2010. **18**(3): p. 364-383.
4. Pérez, J., et al., *Biodegradation and biological treatments of cellulose, hemicellulose and lignin: an overview.* International Microbiology, 2002. **5**(2): p. 53-63.
5. Hendriks, A.T.W.M. and G. Zeeman, *Pretreatments to enhance the digestibility of lignocellulosic biomass.* Bioresource Technology, 2009. **100**(1): p. 10-18.
6. Balat, M., H. Balat, and C. Öz, *Progress in bioethanol processing.* Progress in Energy and Combustion Science, 2008. **34**(5): p. 551-573.
7. Yan, Z., et al., *Impact of lignin removal on the enzymatic hydrolysis of fermented sweet sorghum bagasse.* Applied Energy, 2015.
8. Deepa, B., et al., *Utilization of various lignocellulosic biomass for the production of nanocellulose: a comparative study.* Cellulose, 2015. **22**(2): p. 1075-1090.
9. Wang, Y.-n., Y.-x. Weng, and L. Wang, *Characterization of interfacial compatibility of polylactic acid and bamboo flour (PLA/BF) in biocomposites.* Polymer Testing, 2014. **36**: p. 119-125.
10. Auras, R., B. Harte, and S. Selke, *An overview of polylactides as packaging materials.* Macromolecular bioscience, 2004. **4**(9): p. 835-864.
11. Mwaikambo, L.Y. and M.P. Ansell, *Chemical modification of hemp, sisal, jute, and kapok fibers by alkalization.* Journal of Applied Polymer Science, 2002. **84**(12): p. 2222-2234.
12. Abdullah-Al-Mamun, M., et al., *Physical and mechanical properties of flat pressed polypropylene bonded composite made from bamboo (Bambusa balcooa Roxb.).* Journal of the Indian Academy of Wood Science, 2015. **12**(2): p. 145-148.
13. Lu, H., et al., *Morphological, crystalline, thermal and physicochemical properties of cellulose nanocrystals obtained from sweet potato residue.* Food Research International, 2013. **50**(1): p. 121-128.
14. Abdul Khalil, H.P.S., A.H. Bhat, and A.F. Ireana Yusra, *Green composites from sustainable cellulose nanofibrils: A review.* Carbohydrate Polymers, 2012. **87**(2): p. 963-979.
15. Ahmed, K.S. and S. Vijayarangan, *Tensile, flexural and interlaminar shear properties of woven jute and jute-glass fabric reinforced polyester composites.* Journal of Materials Processing Technology, 2008. **207**(1–3): p. 330-335.

16. Gírio, F.M., et al., *Hemicelluloses for fuel ethanol: A review.* Bioresource Technology, 2010. **101**(13): p. 4775-4800.

17. Nar, M., et al., *Superior plant based carbon fibers from electrospun poly-(caffeyl alcohol) lignin.* Carbon, 2016. **103**: p. 372-383.

18. Laurichesse, S. and L. Avérous, *Chemical modification of lignins: Towards biobased polymers.* Progress in Polymer Science, (0).

19. Matsushita, Y., *Conversion of technical lignins to functional materials with retained polymeric properties.* Journal of Wood Science, 2015. **61**(3): p. 230-250.

20. Ghaffar, S.H. and M. Fan, *Structural analysis for lignin characteristics in biomass straw.* Biomass and Bioenergy, 2013. **57**(0): p. 264-279.

21. Kalia, S., B.S. Kaith, and I. Kaur, *Pretreatments of natural fibers and their application as reinforcing material in polymer composites—A review.* Polymer Engineering & Science, 2009. **49**(7): p. 1253-1272.

22. Serrano, A., et al., *Study on the technical feasibility of replacing glass fibers by old newspaper recycled fibers as polypropylene reinforcement.* Journal of Cleaner Production, 2014. **65**(0): p. 489-496.

23. Belgacem, M.N. and A. Pizzi, *Lignocellulosic Fibers and Wood Handbook: Renewable Materials for Today's Environment*. 2016: John Wiley & Sons.

24. Mohanty, A.K., M. Misra, and G. Hinrichsen, *Biofibres, biodegradable polymers and biocomposites: An overview.* Macromolecular Materials and Engineering, 2000. **276-277**(1): p. 1-24.

25. Ohkita, T. and S.-H. Lee, *Crystallization behavior of poly(butylene succinate)/corn starch biodegradable composite.* Journal of Applied Polymer Science, 2005. **97**(3): p. 1107-1114.

26. Munawar, S.S., et al., *Effects of alkali, mild steam, and chitosan treatments on the properties of pineapple, ramie, and sansevieria fiber bundles.* Journal of wood science, 2008. **54**(1): p. 28-35.

27. Akil, H.M., et al., *Kenaf fiber reinforced composites: A review.* Materials & Design, 2011. **32**(8–9): p. 4107-4121.

28. Ashori, A. and A. Nourbakhsh, *Performance properties of microcrystalline cellulose as a reinforcing agent in wood plastic composites.* Composites Part B: Engineering, 2010. **41**(7): p. 578-581.

29. Renner, K., et al., *Micromechanical deformation processes in PP/wood composites: Particle characteristics, adhesion, mechanisms.* Composites Part A: Applied Science and Manufacturing, 2010. **41**(11): p. 1653-1661.

30. Yang, H.S., et al., *Thermal properties of lignocellulosic filler-thermoplastic polymer bio-composites.* Journal of Thermal Analysis and Calorimetry, 2005. **82**(1): p. 157-160.

31. Cao, Y., S. Shibata, and I. Fukumoto, *Mechanical properties of biodegradable composites reinforced with bagasse fibre before and after alkali treatments.* Composites Part A: Applied Science and Manufacturing, 2006. **37**(3): p. 423-429.

32. Luz, S.M., et al., *Cellulose and cellulignin from sugarcane bagasse reinforced polypropylene composites: Effect of acetylation on mechanical and thermal properties.* Composites Part A: Applied Science and Manufacturing, 2008. **39**(9): p. 1362-1369.

33. Huang, Z., et al., *Effect of mechanical activation pretreatment on the properties of sugarcane bagasse/poly(vinyl chloride) composites.* Composites Part A: Applied Science and Manufacturing, 2012. **43**(1): p. 114-120.

34. Habibi, Y., et al., *Processing and characterization of reinforced polyethylene composites made with lignocellulosic fibers from Egyptian agro-industrial residues.* Composites Science and Technology, 2008. **68**(7–8): p. 1877-1885.

35. Yao, F., et al., *Rice straw fiber-reinforced high-density polyethylene composite: Effect of fiber type and loading.* Industrial Crops and Products, 2008. **28**(1): p. 63-72.

36. Yao, F., et al., *Rice straw fiber reinforced high density polyethylene composite: Effect of coupled compatibilizating and toughening treatment.* Journal of Applied Polymer Science, 2011. **119**(4): p. 2214-2222.

37. Chong, E.L., et al., *Reinforcement of natural rubber/high density polyethylene blends with electron beam irradiated liquid natural rubber-coated rice husk.* Radiation Physics and Chemistry, 2010. **79**(8): p. 906-911.

38. Kim, H.-S., et al., *Thermal properties of bio-flour-filled polyolefin composites with different compatibilizing agent type and content.* Thermochimica Acta, 2006. **451**(1–2): p. 181-188.

39. Premalal, H.G.B., H. Ismail, and A. Baharin, *Comparison of the mechanical properties of rice husk powder filled polypropylene composites with talc filled polypropylene composites.* Polymer Testing, 2002. **21**(7): p. 833-839.

40. Yang, H.-S., et al., *Effect of different compatibilizing agents on the mechanical properties of lignocellulosic material filled polyethylene bio-composites.* Composite Structures, 2007. **79**(3): p. 369-375.

41. Tajeddin, B., R.A. Rahman, and L.C. Abdulah, *The effect of polyethylene glycol on the characteristics of kenaf cellulose/low-density polyethylene biocomposites.* International Journal of Biological Macromolecules, 2010. **47**(2): p. 292-297.

42. Salleh, F.M., et al., *Effects of extrusion temperature on the rheological, dynamic mechanical and tensile properties of kenaf fiber/HDPE composites.* Composites Part B: Engineering, 2014. **58**: p. 259-266.

43. Alemdar, A. and M. Sain, *Biocomposites from wheat straw nanofibers: Morphology, thermal and mechanical properties.* Composites Science and Technology, 2008. **68**(2): p. 557-565.

44. Han, G., et al., *Effect of pressurized steam treatment on selected properties of wheat straws.* Industrial Crops and Products, 2009. **30**(1): p. 48-53.

45. Le Digabel, F., et al., *Properties of thermoplastic composites based on wheat-straw lignocellulosic fillers.* Journal of Applied Polymer Science, 2004. **93**(1): p. 428-436.

46. Van de Weyenberg, I., et al., *Influence of processing and chemical treatment of flax fibres on their composites.* Composites Science and Technology, 2003. **63**(9): p. 1241-1246.

47. Islam, M.S., K.L. Pickering, and N.J. Foreman, *Influence of alkali treatment on the interfacial and physico-mechanical properties of industrial hemp fibre reinforced polylactic acid composites.* Composites Part A: Applied Science and Manufacturing, 2010. **41**(5): p. 596-603.

48. Thomsen, A.B., et al., *Effects of chemical–physical pre-treatment processes on hemp fibres for reinforcement of composites and for textiles.* Industrial Crops and Products, 2006. **24**(2): p. 113-118.

49. Wan Nadirah, W.O., et al., *Cell Wall Morphology, Chemical and Thermal Analysis of Cultivated Pineapple Leaf Fibres for Industrial Applications.* Journal of Polymers and the Environment, 2012. **20**(2): p. 404-411.

50. Devi, L.U., S.S. Bhagawan, and S. Thomas, *Mechanical properties of pineapple leaf fiber-reinforced polyester composites.* Journal of Applied Polymer Science, 1997. **64**(9): p. 1739-1748.

51. Jawaid, M., H.P.S. Abdul Khalil, and O.S. Alattas, *Woven hybrid biocomposites: Dynamic mechanical and thermal properties.* Composites Part A: Applied Science and Manufacturing, 2012. **43**(2): p. 288-293.

52. Zabihzadeh, S.M., et al., *Physical and Mechanical Properties of Rapeseed Waste-filled LLDPE Composites.* Journal of Thermoplastic Composite Materials, 2011. **24**(4): p. 447-458.

53. Alsaeed, T., B.F. Yousif, and H. Ku, *The potential of using date palm fibres as reinforcement for polymeric composites.* Materials & Design, 2013. **43**(0): p. 177-184.

54. Arrakhiz, F.Z., et al., *Mechanical and thermal properties of natural fibers reinforced polymer composites: Doum/low density polyethylene.* Materials & Design, 2013. **43**(0): p. 200-205.

55. Feng, Y., et al., *Preparation and mechanical properties of high-performance short ramie fiber-reinforced polypropylene composites.* Journal of Applied Polymer Science, 2011. **122**(3): p. 1564-1571.

56. Silva, R.V. and E.M.F. Aquino, *Curaua Fiber: A New Alternative to Polymeric Composites.* Journal of Reinforced Plastics and Composites, 2007.

57. Ratna Prasad, A.V. and K. Mohana Rao, *Mechanical properties of natural fibre reinforced polyester composites: Jowar, sisal and bamboo.* Materials & Design, 2011. **32**(8–9): p. 4658-4663.

58. Fernandes, E.M., J.F. Mano, and R.L. Reis, *Hybrid cork–polymer composites containing sisal fibre: Morphology, effect of the fibre treatment on the mechanical properties and tensile failure prediction.* Composite Structures, 2013. **105**(0): p. 153-162.

59. Wong, K.J., et al., *Fracture characterisation of short bamboo fibre reinforced polyester composites.* Materials & Design, 2010. **31**(9): p. 4147-4154.

60. Gunning, M.A., et al., *Mechanical and biodegradation performance of short natural fibre polyhydroxybutyrate composites.* Polymer Testing, 2013. **32**(8): p. 1603-1611.

61. Taşdemır, M., H. Biltekin, and G.T. Caneba, *Preparation and characterization of LDPE and PP—Wood fiber composites.* Journal of Applied Polymer Science, 2009. **112**(5): p. 3095-3102.

62. Balakrishnan, P., et al., *Natural fibre and polymer matrix composites and their applications in aerospace engineering.* Advanced Composite Materials for Aerospace Engineering: Processing, Properties and Applications, 2016: p. 365.

63. Jiang, L., et al., *Study of Poly(3-hydroxybutyrate-co-3-hydroxyvalerate) (PHBV)/Bamboo Pulp Fiber Composites: Effects of Nucleation Agent and Compatibilizer.* Journal of Polymers and the Environment, 2008. **16**(2): p. 83-93.

64. Feng, D., D.F. Caulfield, and A.R. Sanadi, *Effect of compatibilizer on the structure-property relationships of kenaf-fiber/polypropylene composites.* Polymer Composites, 2001. **22**(4): p. 506-517.

65. Ranganathan, N., et al., *Impact toughness, viscoelastic behavior, and morphology of polypropylene–jute–viscose hybrid composites.* Journal of Applied Polymer Science, 2016. **133**(7).

66. Tabar, M.M., et al., *Using silicon dioxide (SiO2) nano-powder as reinforcement for walnut shell flour/HDPE composite materials.* Journal of the Indian Academy of Wood Science, 2015. **12**(1): p. 15-21.

67. Nishiyama, Y., *Structure and properties of the cellulose microfibril.* Journal of Wood Science, 2009. **55**(4): p. 241-249.

68. Satterthwaite, J.D., et al., *Effect of resin-composite filler particle size and shape on shrinkage-stress.* Dental Materials, 2012. **28**(6): p. 609-614.

69. Niu, Z., Y. Chen, and J. Feng, *Preparation, structure, and property of wood flour incorporated polypropylene composites prepared by a solid-state mechanochemical method.* Journal of Applied Polymer Science, 2016. **133**(10).

70. Wong, T.-t., et al., *UV resistibility of a nano-ZnO/glass fibre reinforced epoxy composite.* Materials & Design, 2014. **56**(0): p. 254-257.

71. Arjmandi, R., et al., *Effects of Micro-and Nano-cellulose on Tensile and Morphological Properties of Montmorillonite Nanoclay Reinforced Polylactic Acid Nanocomposites*, in *Nanoclay Reinforced Polymer Composites*. 2016, Springer. p. 103-125.

72. Essabir, H., et al., *Bio-composites based on polypropylene reinforced with Almond Shells particles: Mechanical and thermal properties.* Materials & Design, 2013. **51**(0): p. 225-230.

73. Ismail, H., S. Shuhelmy, and M.R. Edyham, *The effects of a silane coupling agent on curing characteristics and mechanical properties of bamboo fibre filled natural rubber composites.* European Polymer Journal, 2002. **38**(1): p. 39-47.

74. Hietala, M., et al., *The effect of pre-softened wood chips on wood fibre aspect ratio and mechanical properties of wood–polymer composites.* Composites Part A: Applied Science and Manufacturing, 2011. **42**(12): p. 2110-2116.

75. Doh, G.-H., et al., *Mechanical properties and creep behavior of liquefied wood polymer composites (LWPC).* Composite Structures, 2005. **68**(2): p. 225-233.

76. Bledzki, A.K., P. Franciszczak, and A. Meljon, *High performance hybrid PP and PLA biocomposites reinforced with short man-made cellulose fibres and softwood flour.* Composites Part A: Applied Science and Manufacturing, 2015. **74**(0): p. 132-139.

77. Fávaro, S.L., et al., *Chemical, morphological, and mechanical analysis of rice husk/post-consumer polyethylene composites.* Composites Part A: Applied Science and Manufacturing, 2010. **41**(1): p. 154-160.

78. Yang, H.-S., et al., *Rice-husk flour filled polypropylene composites; mechanical and morphological study.* Composite Structures, 2004. **63**(3–4): p. 305-312.

79. Ahankari, S.S., A.K. Mohanty, and M. Misra, *Mechanical behaviour of agro-residue reinforced poly(3-hydroxybutyrate-co-3-hydroxyvalerate), (PHBV) green composites: A comparison with traditional polypropylene composites.* Composites Science and Technology, 2011. **71**(5): p. 653-657.

80. Bendahou, A., et al., *Short Palm Tree Fibers Polyolefin Composites: Effect of Filler Content and Coupling Agent on Physical Properties.* Macromolecular Materials and Engineering, 2008. **293**(2): p. 140-148.

81. Romanzini, D., et al., *Influence of fiber content on the mechanical and dynamic mechanical properties of glass/ramie polymer composites.* Materials & Design, 2013. **47**(0): p. 9-15.

82. Jarukumjorn, K. and N. Suppakarn, *Effect of glass fiber hybridization on properties of sisal fiber–polypropylene composites.* Composites Part B: Engineering, 2009. **40**(7): p. 623-627.

83. Haque, R., et al., *Fibre-matrix adhesion and properties evaluation of sisal polymer composite.* Fibers and Polymers, 2015. **16**(1): p. 146-152.

84. Rahman, M.R., et al., *Mechanical properties of polypropylene composites reinforced with chemically treated abaca.* Composites Part A: Applied Science and Manufacturing, 2009. **40**(4): p. 511-517.

85. Vilela, C., et al., *Novel sustainable composites prepared from cork residues and biopolymers.* Biomass and Bioenergy, 2013. **55**(0): p. 148-155.

86. Herrera-Franco, P.J. and A. Valadez-González, *Mechanical properties of continuous natural fibre-reinforced polymer composites.* Composites Part A: Applied Science and Manufacturing, 2004. **35**(3): p. 339-345.

87. Huda, M.S., et al., *Effect of fiber surface-treatments on the properties of laminated biocomposites from poly(lactic acid) (PLA) and kenaf fibers.* Composites Science and Technology, 2008. **68**(2): p. 424-432.

88. Bledzki, A.K. and J. Gassan, *Composites reinforced with cellulose based fibres.* Progress in Polymer Science, 1999. **24**(2): p. 221-274.

89. Das, M., A. Pal, and D. Chakraborty, *Effects of mercerization of bamboo strips on mechanical properties of unidirectional bamboo–novolac composites.* Journal of applied polymer science, 2006. **100**(1): p. 238-244.

90. Naushad, M., et al., *Mechanical and damage tolerance behavior of short sisal fiber reinforced recycled polypropylene biocomposites.* Journal of Composite Materials, 2016: p. 0021998316658945.

91. Kabir, M.M., et al., *Mechanical properties of chemically-treated hemp fibre reinforced sandwich composites.* Composites Part B: Engineering, 2012. **43**(2): p. 159-169.

92. Aziz, S.H. and M.P. Ansell, *The effect of alkalization and fibre alignment on the mechanical and thermal properties of kenaf and hemp bast fibre composites: Part 1 – polyester resin matrix.* Composites Science and Technology, 2004. **64**(9): p. 1219-1230.

93. Threepopnatkul, P., N. Kaerkitcha, and N. Athipongarporn, *Effect of surface treatment on performance of pineapple leaf fiber–polycarbonate composites.* Composites Part B: Engineering, 2009. **40**(7): p. 628-632.

94. Agrawal, R., et al., *Activation energy and crystallization kinetics of untreated and treated oil palm fibre reinforced phenol formaldehyde composites.* Materials Science and Engineering: A, 2000. **277**(1–2): p. 77-82.

95. Khalid, M., et al., *Comparative study of polypropylene composites reinforced with oil palm empty fruit bunch fiber and oil palm derived cellulose.* Materials & Design, 2008. **29**(1): p. 173-178.

96. Abdul Khalil, H.P.S., et al., *Exploring isolated lignin material from oil palm biomass waste in green composites.* Materials & Design, 2011. **32**(5): p. 2604-2610.

97. Razak, N.W.A. and A. Kalam, *Effect of OPEFB Size on the Mechanical Properties and Water Absorption Behaviour of OPEFB/PPnanoclay/PP Hybrid Composites.* Procedia Engineering, 2012. **41**(0): p. 1593-1599.

98. Gomes, A., K. Goda, and J. Ohgi, *Effects of Alkali Treatment to Reinforcement on Tensile Properties of Curaua Fiber Green Composites.* JSME International Journal Series A Solid Mechanics and Material Engineering, 2004. **47**(4): p. 541-546.

99. Schmidt, T.M., et al., *Permeability of Hybrid Reinforcements and Mechanical Properties of their Composites Molded by Resin Transfer Molding.* Journal of Reinforced Plastics and Composites, 2009. **28**(23): p. 2839-2850.

100. Kalaprasad, G., et al., *Effect of fibre length and chemical modifications on the tensile properties of intimately mixed short sisal/glass hybrid fibre reinforced low density polyethylene composites.* Polymer International, 2004. **53**(11): p. 1624-1638.

101. Seki, Y., *Innovative multifunctional siloxane treatment of jute fiber surface and its effect on the mechanical properties of jute/thermoset composites.* Materials Science and Engineering: A, 2009. **508**(1–2): p. 247-252.

102. Sever, K., *The Improvement of Mechanical Properties of Jute Fiber/LDPE Composites by Fiber Surface Treatment.* Journal of Reinforced Plastics and Composites, 2010. **29**(13): p. 1921-1929.

103. Srivastav, A.K., M.K. Behera, and B.C. Ray, *Loading Rate Sensitivity of Jute/Glass Hybrid Reinforced Epoxy Composites: Effect of Surface Modifications.* Journal of Reinforced Plastics and Composites, 2007. **26**(9): p. 851-860.

104. Fiore, V., G. Di Bella, and A. Valenza, *The effect of alkaline treatment on mechanical properties of kenaf fibers and their epoxy composites.* Composites Part B: Engineering, 2015. **68**: p. 14-21.

105. Manikandan, V., et al., *Investigation of the effect of surface modifications on the mechanical properties of basalt fibre reinforced polymer composites.* Composites Part B: Engineering, 2012. **43**(2): p. 812-818.

106. Lenka, S., P.L. Nayak, and M.K. Mishra, *Grafting vinyl monomers onto cellulose. I. Graft copolymerization of methyl methacrylate onto cellulose using quinquevalent vanadium ion.* Journal of Applied Polymer Science, 1980. **25**(7): p. 1323-1333.

107. Ibrahim, M.M., E.M. Flefel, and W.K. El-Zawawy, *Cellulose membranes grafted with vinyl monomers in homogeneous system.* Journal of Applied Polymer Science, 2002. **84**(14): p. 2629-2638.

108. Ibrahim, N., et al., *Graft Copolymerization of Acrylamide onto Oil Palm Empty Fruit Bunch (OPEFB) Fiber.* Journal of Polymer Research, 2005. **12**(3): p. 173-179.

109. Abu-Ilaiwi, F.A., et al., *Optimized conditions for the grafting reaction of poly(methyl acrylate) onto rubberwood fiber.* Polymer International, 2004. **53**(4): p. 386-391.

110. Rider, A.N. and D.R. Arnott, *Boiling water and silane pre-treatment of aluminium alloys for durable adhesive bonding.* International Journal of Adhesion and Adhesives, 2000. **20**(3): p. 209-220.

111. Khan, A., et al., *Effect of Silane Treatment on the Mechanical and Interfacial Properties of Calcium Alginate Fiber Reinforced Polypropylene Composite.* Journal of Composite Materials, 2010. **44**(24): p. 2875-2886.

112. Abdelmouleh, M., et al., *Short natural-fibre reinforced polyethylene and natural rubber composites: Effect of silane coupling agents and fibres loading.* Composites Science and Technology, 2007. **67**(7–8): p. 1627-1639.

113. Jaszkiewicz, A., A. Meljon, and A. Bledzki, *Mechanical and thermomechanical properties of PLA/Man-made cellulose green composites modified with functional chain extenders—A comprehensive study.* Polymer Composites, 2016.

114. Xie, Y., et al., *Silane coupling agents used for natural fiber/polymer composites: A review.* Composites Part A: Applied Science and Manufacturing, 2010. **41**(7): p. 806-819.

115. Xie, Y., et al., *Silane coupling agents used for natural fiber/polymer composites: A review.* Composites Part A: Applied Science and Manufacturing, 2010. **41**(7): p. 806-819.

116. Hill, C.A.S. and H.P.S. Abdul Khalil, *Effect of fiber treatments on mechanical properties of coir or oil palm fiber reinforced polyester composites.* Journal of Applied Polymer Science, 2000. **78**(9): p. 1685-1697.

117. Haque, M. and C. Hill, *Chemical modification of model compounds, wood flour and fibre with acetic anhydride.* Journal of the Institute of Wood Science, 2000. **15**(3): p. 109-115.

118. Bertoti, A.R., S. Luporini, and M.C.A. Esperidião, *Effects of acetylation in vapor phase and mercerization on the properties of sugarcane fibers.* Carbohydrate Polymers, 2009. **77**(1): p. 20-24.

119. Khalil, H.P.S.A., et al., *The effect of acetylation on interfacial shear strength between plant fibres and various matrices.* European Polymer Journal, 2001. **37**(5): p. 1037-1045.

120. Alawar, A., A.M. Hamed, and K. Al-Kaabi, *Characterization of treated date palm tree fiber as composite reinforcement.* Composites Part B: Engineering, 2009. **40**(7): p. 601-606.

121. Mukherjee, T., et al., *Improved dispersion of cellulose microcrystals in polylactic acid (PLA) based composites applying surface acetylation.* Chemical Engineering Science, 2013. **101**(0): p. 655-662.

122. Hamed, O.A., et al., *Cellulose acetate from biomass waste of olive industry.* Journal of wood science, 2015. **61**(1): p. 45-52.

123. Ashori, A., et al., *Solvent-free acetylation of cellulose nanofibers for improving compatibility and dispersion.* Carbohydrate polymers, 2014. **102**: p. 369-375.

124. Martin-Sampedro, R., et al., *Integration of a kraft pulping mill into a forest biorefinery: Pre-extraction of hemicellulose by steam explosion versus steam treatment.* Bioresource Technology, 2014. **153**(0): p. 236-244.

125. Bogolitsyn, K.G., et al., *Application of steam explosion as a method of wood matrix thermochemical activation.* Journal of the Indian Academy of Wood Science: p. 1-8.

126. Ahvazi, B., et al., *Chemical Pulping of Steam-Exploded Mixed Hardwood Chips.* Journal of wood chemistry and technology, 2007. **27**(2): p. 49-63.

127. Rahikainen, J.L., et al., *Inhibitory effect of lignin during cellulose bioconversion: The effect of lignin chemistry on non-productive enzyme adsorption.* Bioresource Technology, 2013. **133**(0): p. 270-278.

128. Kemppainen, K., et al., *Hot water extraction and steam explosion as pretreatments for ethanol production from spruce bark.* Bioresource Technology, 2012. **117**(0): p. 131-139.

129. Mussatto, S., *Biomass Pretreatment With Acids.* Biomass Fractionation Technologies for a Lignocellulosic Feedstock Based Biorefinery, 2016: p. 169.

130. Kurosumi, A., et al., *Novel extraction method of antioxidant compounds from Sasa palmata (Bean) Nakai using steam explosion.* Process Biochemistry, 2007. **42**(10): p. 1449-1453.

131. Asada, C., et al., *Effect of steam explosion pretreatment with ultra-high temperature and pressure on effective utilization of softwood biomass.* Biochemical engineering journal, 2012. **60**: p. 25-29.

132. Chen, G. and H. Chen, *Extraction and deglycosylation of flavonoids from sumac fruits using steam explosion.* Food chemistry, 2011. **126**(4): p. 1934-1938.

133. Chen, H., et al., *New process of maize stalk amination treatment by steam explosion.* Biomass and Bioenergy, 2005. **28**(4): p. 411-417.

134. Liu, Z.-H., et al., *Evaluation of storage methods for the conversion of corn stover biomass to sugars based on steam explosion pretreatment.* Bioresource Technology, 2013. **132**(0): p. 5-15.

135. Ibrahim, M.M., et al., *Banana fibers and microfibrils as lignocellulosic reinforcements in polymer composites.* Carbohydrate Polymers, 2010. **81**(4): p. 811-819.

136. Sindhu, R., P. Binod, and A. Pandey, *Biological pretreatment of lignocellulosic biomass–An overview.* Bioresource technology, 2016. **199**: p. 76-82.

137. Zhang, Z., et al., *Sonication enhanced cornstarch separation.* Starch-Stärke, 2005. **57**(6): p. 240-245.

138. Tatsumi, D., S. Ishioka, and T. Matsumoto, *Effect of fiber concentration and axial ratio on the rheological properties of cellulose fiber suspensions.* Nihon Reoroji Gakkaishi, 2002. **30**(1): p. 27-32.

139. Delannay, F., et al., *Processing and properties of metal matrix composites reinforced with continuous fibres for the control of thermal expansion, creep resistance and fracture toughness.* Le Journal de Physique IV, 1993. **3**(C7): p. C7-1675-C7-1684.

140. Subhedar, P.B. and P.R. Gogate, *Intensification of enzymatic hydrolysis of lignocellulose using ultrasound for efficient bioethanol production: a review.* Industrial & Engineering Chemistry Research, 2013. **52**(34): p. 11816-11828.

141. Mishra, S.P., et al., *Ultrasound-catalyzed TEMPO-mediated oxidation of native cellulose for the production of nanocellulose: effect of process variables.* BioResources, 2010. **6**(1): p. 121-143.

142. Chen, X., Q. Guo, and Y. Mi, *Bamboo fiber-reinforced polypropylene composites: A study of the mechanical properties.* Journal of Applied Polymer Science, 1998. **69**(10): p. 1891-1899.

143. Cho, M.-J. and B.-D. Park, *Tensile and thermal properties of nanocellulose-reinforced poly(vinyl alcohol) nanocomposites.* Journal of Industrial and Engineering Chemistry, 2011. **17**(1): p. 36-40.

144. Siró, I. and D. Plackett, *Microfibrillated cellulose and new nanocomposite materials: a review.* Cellulose, 2010. **17**(3): p. 459-494.

145. Karimi, S., et al., *Kenaf bast cellulosic fibers hierarchy: A comprehensive approach from micro to nano.* Carbohydrate Polymers, 2014. **101**(0): p. 878-885.

146. Jonoobi, M., et al., *Different preparation methods and properties of nanostructured cellulose from various natural resources and residues: a review.* Cellulose, 2015. **22**(2): p. 935-969.

147. Nishino, T., et al., *Kenaf reinforced biodegradable composite.* Composites Science and Technology, 2003. **63**(9): p. 1281-1286.

148. Webber III, C.L. and V.K. Bledsoe, *Kenaf yield components and plant composition.* Trends in new crops and new uses, 2002: p. 348-357.

149. Nayeri, M.D., et al., *Effects of temperature and time on the morphology, pH, and buffering capacity of bast and core kenaf fibres.* BioResources, 2013. **8**(2): p. 1801-1812.

150. Bakhtiar, B., et al., *Kenaf (Hibiscus cannabinus) response to fertilizer application.* Journal of Agricultural Research (Pakistan), 1990.

151. Kuchinda, N., et al., *The effects of nitrogen and period of weed interference on the fibre yield of kenaf (Hisbiscus cannabinus L.) in the northern Guinea Savanna of Nigeria.* Crop Protection, 2001. **20**(3): p. 229-235.

152. Hill, C. and H. Abdul Khalil, *Effect of fiber treatments on mechanical properties of coir or oil palm fiber reinforced polyester composites.* Journal of Applied Polymer Science, 2000. **78**(9): p. 1685-1697.

153. Guo, F., et al., *Pyrolysis kinetics of biomass (herb residue) under isothermal condition in a micro fluidized bed.* Energy Conversion and Management, 2015. **93**: p. 367-376.

154. Dong, Y., et al., *Polylactic acid (PLA) biocomposites reinforced with coir fibres: Evaluation of mechanical performance and multifunctional properties.* Composites Part A: Applied Science and Manufacturing, 2014. **63**: p. 76-84.

155. Datta, R. and M. Henry, *Lactic acid: recent advances in products, processes and technologies—a review.* Journal of Chemical Technology and Biotechnology, 2006. **81**(7): p. 1119-1129.

156. Chieng, B.W., et al., *Mechanical, Thermal, and Morphology Properties of Poly (lactic acid) Plasticized With Poly (ethylene glycol) and Epoxidized Palm Oil Hybrid Plasticizer.* Polymer Engineering & Science, 2016.

157. Chieng, B.W., et al. *Plasticized and Nanofilled Poly (Lactic Acid) Nanocomposites: Mechanical, Thermal and Morphology Properties*. in *Materials Science Forum*. 2016. Trans Tech Publ.

158. Mehta, R., et al., *Synthesis of poly (lactic acid): a review.* Journal of Macromolecular Science, Part C: Polymer Reviews, 2005. **45**(4): p. 325-349.

159. Kong, I., K. Tshai, and M.E. Hoque, *Manufacturing of Natural Fibre-Reinforced Polymer Composites by Solvent Casting Method*, in *Manufacturing of Natural Fibre Reinforced Polymer Composites*. 2015, Springer. p. 331-349.

160. Bulota, M. and T. Budtova, *PLA/algae composites: Morphology and mechanical properties.* Composites Part A: Applied Science and Manufacturing, 2015. **73**: p. 109-115.

161. Herrera, N., et al., *Plasticized polylactic acid nanocomposite films with cellulose and chitin nanocrystals prepared using extrusion and compression molding with two cooling rates: Effects on mechanical, thermal and optical properties.* Composites Part A: Applied Science and Manufacturing.

162. Yang, X., et al., *Two Step Extrusion Process: From Thermal Recycling of PHB to Plasticized PLA by Reactive Extrusion Grafting of PHB Degradation Products onto PLA Chains.* Macromolecules, 2015. **48**(8): p. 2509-2518.

163. Fox, D.M., et al., *Flame retarded poly(lactic acid) using POSS-modified cellulose. 2. Effects of intumescing flame retardant formulations on polymer degradation and composite physical properties.* Polymer Degradation and Stability, 2014. **106**: p. 54-62.

164. Asaithambi, B., G. Ganesan, and S. Ananda Kumar, *Bio-composites: Development and mechanical characterization of banana/sisal fibre reinforced poly lactic acid (PLA) hybrid composites.* Fibers and Polymers, 2014. **15**(4): p. 847-854.

165. Robles, E., et al., *Surface-modified nano-cellulose as reinforcement in poly(lactic acid) to conform new composites.* Industrial Crops and Products, 2015. **71**: p. 44-53.

166. Nair, P.P., K. George, and N. Jayakrishnan, *Studies on mechanical behavior high impact polystyrene/vinyl clay nanocomposites: Comparison between in situ polymerization and melt mixing.* Polymer Composites, 2015.

167. Rasti, B., et al., *Optimization on preparation condition of polyunsaturated fatty acids nanoliposome prepared by Mozafari method.* Journal of liposome research, 2014. **24**(2): p. 99-105.

168. Mor-Yossef, Y., *Unconditionally stable time marching scheme for Reynolds stress models.* Journal of Computational Physics, 2014. **276**: p. 635-664.

169. Abo-Hamad, W. and A. Arisha, *Simulation-optimisation methods in supply chain applications: a review.* Irish Journal of Management, 2011. **30**(2): p. 95.

170. Thakur, V.K. and M.K. Thakur, *Processing and characterization of natural cellulose fibers/thermoset polymer composites.* Carbohydrate Polymers, 2014. **109**(0): p. 102-117.

171. Memon, A. and A. Nakai, *Mechanical Properties of Jute Spun Yarn/PLA Tubular Braided Composite by Pultrusion Molding.* Energy Procedia, 2013. **34**(0): p. 818-829.

172. Silva, F.J.G., et al., *Optimising the energy consumption on pultrusion process.* Composites Part B: Engineering, 2014. **57**(0): p. 13-20.

173. Yun, M.S. and W.I. Lee, *Analysis of bubble nucleation and growth in the pultrusion process of phenolic foam composites.* Composites Science and Technology, 2008. **68**(1): p. 202-208.

174. Matuana, L.M., et al., *Surface characterization of esterified cellulosic fibers by XPS and FTIR Spectroscopy.* Wood Science and Technology, 2001. **35**(3): p. 191-201.

175. Keener, T.J., R.K. Stuart, and T.K. Brown, *Maleated coupling agents for natural fibre composites.* Composites Part A: Applied Science and Manufacturing, 2004. **35**(3): p. 357-362.

176. Kelly, A.L., et al., *High shear strain rate rheometry of polymer melts.* Journal of Applied Polymer Science, 2009. **114**(2): p. 864-873.

177. Bariani, P.F., M. Salvador, and G. Lucchetta, *Development of a test method for the rheological characterization of polymers under the injection molding process conditions.* Journal of Materials Processing Technology, 2007. **191**(1–3): p. 119-122.

178. Vera-Sorroche, J., et al., *The effect of melt viscosity on thermal efficiency for single screw extrusion of HDPE.* Chemical Engineering Research and Design, (0).

179. Serizawa, S., K. Inoue, and M. Iji, *Kenaf-fiber-reinforced poly(lactic acid) used for electronic products.* Journal of Applied Polymer Science, 2006. **100**(1): p. 618-624.

180. Huda, M.S., et al., *"Green" composites from recycled cellulose and poly(lactic acid): Physico-mechanical and morphological properties evaluation.* Journal of Materials Science, 2005. **40**(16): p. 4221-4229.

181. Huda, M.S., et al., *Wood-fiber-reinforced poly(lactic acid) composites: Evaluation of the physicomechanical and morphological properties.* Journal of Applied Polymer Science, 2006. **102**(5): p. 4856-4869.

182. Huda, M.S., et al., *Chopped glass and recycled newspaper as reinforcement fibers in injection molded poly(lactic acid) (PLA) composites: A comparative study.* Composites Science and Technology, 2006. **66**(11–12): p. 1813-1824.

183. Kim, S.Y., et al., *Measurement of residual stresses in film insert molded parts with complex geometry.* Polymer Testing, 2009. **28**(5): p. 500-507.

184. Shokrieh, M., *Residual Stresses in Composite Materials*. 2014: Woodhead Publishing, Limited. 408.

185. White, J.R., *On the layer removal analysis of residual stress.* Journal of Materials Science, 1985. **20**(7): p. 2377-2387.

186. Carpenter, H.W., R.G. Reid, and R. Paskaramoorthy, *Extension of the layer removal technique for the measurement of residual stresses in layered anisotropic cylinders.* International Journal of Mechanics and Materials in Design, 2014: p. 1-12.

187. Kim, C., et al., *Measurement of residual stresses in injection molded polymeric part by applying layer-removal and incremental hole-drilling methods.* Fibers and Polymers, 2007. **8**(4): p. 443-446.

188. Park, S.H., S.G. Lee, and S.H. Kim, *Isothermal crystallization behavior and mechanical properties of polylactide/carbon nanotube nanocomposites.* Composites Part A: Applied Science and Manufacturing, 2013. **46**(0): p. 11-18.

189. Garancher, J.P. and A. Fernyhough, *Expansion and dimensional stability of semi-crystalline polylactic acid foams.* Polymer Degradation and Stability, 2014. **100**(0): p. 21-28.

190. Batra, R.C., G. Gopinath, and J.Q. Zheng, *Material parameters for pressure-dependent yielding of unidirectional fiber-reinforced polymeric composites.* Composites Part B: Engineering, 2012. **43**(6): p. 2594-2604.

191. Nechwatal, A., K.-P. Mieck, and T. Reußmann, *Developments in the characterization of natural fibre properties and in the use of natural fibres for composites.* Composites Science and Technology, 2003. **63**(9): p. 1273-1279.

192. Folkes, M.J. and D.A.M. Russell, *Orientation effects during the flow of short-fibre reinforced thermoplastics.* Polymer, 1980. **21**(11): p. 1252-1258.

193. Lee, K., et al., *Confocal microscopy measurement of the fiber orientation in short fiber reinforced plastics.* Fibers and Polymers, 2001. **2**(1): p. 41-50.

194. Pujadas, P., et al., *Fibre distribution in macro-plastic fibre reinforced concrete slab-panels.* Construction and Building Materials, 2014. **64**(0): p. 496-503.

195. Zabihzadeh, S.M., et al., *Physical and mechanical properties of rapeseed waste-filled LLDPE composites.* Journal of Thermoplastic Composite Materials, 2010: p. 0892705710388591.

196. Malkapuram, R., V. Kumar, and Y.S. Negi, *Recent development in natural fiber reinforced polypropylene composites.* Journal of Reinforced Plastics and Composites, 2008.

197. Wambua, P., J. Ivens, and I. Verpoest, *Natural fibres: can they replace glass in fibre reinforced plastics?* composites science and technology, 2003. **63**(9): p. 1259-1264.

198. Holbery, J. and D. Houston, *Natural-fiber-reinforced polymer composites in automotive applications.* Jom, 2006. **58**(11): p. 80-86.

199. Hargitai, H., I. Rácz, and R.D. Anandjiwala, *Development of HEMP Fiber Reinforced Polypropylene Composites.* Journal of Thermoplastic Composite Materials, 2008. **21**(2): p. 165-174.

200. Abu-Sharkh, B.F. and H. Hamid, *Degradation study of date palm fibre/polypropylene composites in natural and artificial weathering: mechanical and thermal analysis.* Polymer Degradation and Stability, 2004. **85**(3): p. 967-973.

201. El-Sabbagh, A., *Effect of coupling agent on natural fibre in natural fibre/polypropylene composites on mechanical and thermal behaviour.* Composites Part B: Engineering, 2014. **57**(0): p. 126-135.

202. Yap, S.P., et al., *Flexural toughness characteristics of steel–polypropylene hybrid fibre-reinforced oil palm shell concrete.* Materials & Design, 2014. **57**(0): p. 652-659.

203. Părpăriţă, E., et al., *Structure–morphology–mechanical properties relationship of some polypropylene/lignocellulosic composites.* Materials & Design, 2014. **56**(0): p. 763-772.

204. Arrakhiz, F.Z., et al., *Tensile, flexural and torsional properties of chemically treated alfa, coir and bagasse reinforced polypropylene.* Composites Part B: Engineering, 2013. **47**(0): p. 35-41.

205. Elkhaoulani, A., et al., *Mechanical and thermal properties of polymer composite based on natural fibers: Moroccan hemp fibers/polypropylene.* Materials & Design, 2013. **49**(0): p. 203-208.

206. Yan, Z.L., et al., *Reinforcement of polypropylene with hemp fibres.* Composites Part B: Engineering, 2013. **46**(0): p. 221-226.

207. Essabir, H., et al., *Dynamic mechanical thermal behavior analysis of doum fibers reinforced polypropylene composites.* Materials & Design, 2013. **51**(0): p. 780-788.

208. Ausias, G., et al., *Study of the fibre morphology stability in polypropylene-flax composites.* Polymer Degradation and Stability, 2013. **98**(6): p. 1216-1224.

209. AlMaadeed, M.A., et al., *Date palm wood flour/glass fibre reinforced hybrid composites of recycled polypropylene: Mechanical and thermal properties.* Materials & Design, 2012. **42**(0): p. 289-294.

210. Asumani, O.M.L., R.G. Reid, and R. Paskaramoorthy, *The effects of alkali–silane treatment on the tensile and flexural properties of short fibre non-woven kenaf reinforced polypropylene composites.* Composites Part A: Applied Science and Manufacturing, 2012. **43**(9): p. 1431-1440.

211. Vilaseca, F., et al., *Biocomposites from abaca strands and polypropylene. Part I: Evaluation of the tensile properties.* Bioresource Technology, 2010. **101**(1): p. 387-395.

212. Demir, H., et al., *The effect of fiber surface treatments on the tensile and water sorption properties of polypropylene–luffa fiber composites.* Composites Part A: Applied Science and Manufacturing, 2006. **37**(3): p. 447-456.

213. Arbelaiz, A., et al., *Mechanical properties of flax fibre/polypropylene composites. Influence of fibre/matrix modification and glass fibre hybridization.* Composites Part A: Applied Science and Manufacturing, 2005. **36**(12): p. 1637-1644.

214. Faruk, O., et al., *Biocomposites reinforced with natural fibers: 2000–2010.* Progress in Polymer Science, 2012. **37**(11): p. 1552-1596.

215. Bharath, K.N. and S. Basavarajappa, *Applications of biocomposite materials based on natural fibers from renewable resources: a review.* Science and Engineering of Composite Materials, 2016. **23**(2): p. 123-133.

216. Majeed, K., et al., *Potential materials for food packaging from nanoclay/natural fibres filled hybrid composites.* Materials & Design, 2013. **46**(0): p. 391-410.

217. Tang, C.-S., et al., *Tensile strength of fiber-reinforced soil.* Journal of Materials in Civil Engineering, 2016: p. 04016031.

218. Shao, X., L. He, and L. Ma, *Study on Tensile Behavior of Natural Fiber Reinforced PP Composites.* 2016.

219. Vilaseca, F., et al., *Hemp Strands as Reinforcement of Polystyrene Composites.* Chemical Engineering Research and Design, 2004. **82**(11): p. 1425-1431.

220. Jain, S., R. Kumar, and U.C. Jindal, *Mechanical behaviour of bamboo and bamboo composite.* Journal of Materials Science, 1992. **27**(17): p. 4598-4604.

221. Nurul Fazita, M., et al., *Green Composites Made of Bamboo Fabric and Poly (Lactic) Acid for Packaging Applications—A Review.* Materials, 2016. **9**(6): p. 435.

222. Abdul Khalil, H.P.S., et al., *Bamboo fibre reinforced biocomposites: A review.* Materials & Design, 2012. **42**(0): p. 353-368.

223. Arif, M.F., P.S.M. Megat-Yusoff, and F. Ahmad, *Effects of Chemical Treatment on oil Palm Empty Fruit Bunch Reinforced High Density Polyethylene Composites.* Journal of Reinforced Plastics and Composites, 2009.

224. Buggy, M., *Natural fibers, biopolymers, and biocomposites. Edited by Amar K Mohanty, Manjusri Misra and Lawrence T Drzal.* Polymer International, 2006. **55**(12): p. 1462-1462.

225. Ibrahim, H., et al., *Characteristics of starch-based biodegradable composites reinforced with date palm and flax fibers.* Carbohydrate Polymers, 2014. **101**(0): p. 11-19.

226. Jasmi, N.F., et al. *The Role of Oil Palm (Elaeis guineensis) Frond as Filler in Polypropylene Matrix with Relation of Filler Loading and Particle Size Effects*. in *Regional Conference on Science, Technology and Social Sciences (RCSTSS 2014)*. 2016. Springer.

227. Nayak, S.K. and S. Mohanty, *Sisal Glass Fiber Reinforced PP Hybrid Composites: Effect of MAPP on the Dynamic Mechanical and Thermal Properties.* Journal of Reinforced Plastics and Composites, 2010. **29**(10): p. 1551-1568.

228. Oksman, K., M. Skrifvars, and J.F. Selin, *Natural fibres as reinforcement in polylactic acid (PLA) composites.* Composites Science and Technology, 2003. **63**(9): p. 1317-1324.

229. Hariharan, A.B.A. and H.P.S.A. Khalil, *Lignocellulose-based Hybrid Bilayer Laminate Composite: Part I - Studies on Tensile and Impact Behavior of Oil Palm Fiber-Glass Fiber-reinforced Epoxy Resin.* Journal of Composite Materials, 2005. **39**(8): p. 663-684.

230. Ray, D., et al., *The mechanical properties of vinylester resin matrix composites reinforced with alkali-treated jute fibres.* Composites Part A: applied science and manufacturing, 2001. **32**(1): p. 119-127.

231. Ray, D., et al., *Effect of alkali treated jute fibres on composite properties.* Bulletin of materials science, 2001. **24**(2): p. 129-135.

232. Sreekala, M.S., S. Thomas, and G. Groeninckx, *Dynamic mechanical properties of oil palm fiber/phenol formaldehyde and oil palm fiber/glass hybrid phenol formaldehyde composites.* Polymer Composites, 2005. **26**(3): p. 388-400.

233. Triki, A., et al., *Spectroscopy analyses of hybrid unsaturated polyester composite reinforced by Alfa, wool, and thermo-binder fibres.* Polymer Science Series A, 2016. **58**(2): p. 255-264.

234. Sanchez-Garcia, M.D., A. Lopez-Rubio, and J.M. Lagaron, *Natural micro and nanobiocomposites with enhanced barrier properties and novel functionalities for food biopackaging applications.* Trends in Food Science & Technology, 2010. **21**(11): p. 528-536.

235. La Mantia, F., et al., *Thermomechanical degradation of PLA-based nanobiocomposite.* Polymers for Advanced Technologies, 2015.

236. Shamsabadi, M.A., T. Behzad, and R. Bagheri, *Optimization of acid hydrolysis conditions to improve cellulose nanofibers extraction from wheat straw.* Fibers and Polymers, 2015. **16**(3): p. 579-584.

237. Trifol, J., et al., *A comparison of partially acetylated nanocellulose, nanocrystalline cellulose, and nanoclay as fillers for high-performance polylactide nanocomposites.* Journal of Applied Polymer Science, 2016. **133**(14).

238. Shen, D., S. Gu, and A. Bridgwater, *The thermal performance of the polysaccharides extracted from hardwood: cellulose and hemicellulose.* Carbohydrate Polymers, 2010. **82**(1): p. 39-45.

239. Li, X., L.G. Tabil, and S. Panigrahi, *Chemical treatments of natural fiber for use in natural fiber-reinforced composites: a review.* Journal of Polymers and the Environment, 2007. **15**(1): p. 25-33.

240. Grunert, M. and W.T. Winter, *Nanocomposites of cellulose acetate butyrate reinforced with cellulose nanocrystals.* Journal of Polymers and the Environment, 2002. **10**(1-2): p. 27-30.

241. Baheti, V., et al., *Influence of noncellulosic contents on nano scale refinement of waste jute fibers for reinforcement in polylactic acid films.* Fibers and Polymers, 2014. **15**(7): p. 1500-1506.

242. Jonoobi, M., et al., *Mechanical properties of cellulose nanofiber (CNF) reinforced polylactic acid (PLA) prepared by twin screw extrusion.* Composites Science and Technology, 2010. **70**(12): p. 1742-1747.

243. Fortunati, E., et al., *Lignocellulosic nanostructures as reinforcement in extruded and solvent casted polymeric nanocomposites: an overview.* European Polymer Journal, 2016. **80**: p. 295-316.

244. Bondeson, D., A. Mathew, and K. Oksman, *Optimization of the isolation of nanocrystals from microcrystalline cellulose by acid hydrolysis.* Cellulose, 2006. **13**(2): p. 171-180.

245. Huang, J., Y. Chen, and P.R. Chang, *Surface ModIfIcatIon of celluloSe nanocryStalS for nanocoMpoSIteS.* Surface Modification of Biopolymers, 2015: p. 258.

246. Lin, N. and A. Dufresne, *Surface Modification of Polysaccharide Nanocrystals.* Polysaccharide-Based Nanocrystals: Chemistry and Applications, 2014: p. 63-108.

247. Marra, A., et al., *Polylactic acid/zinc oxide biocomposite films for food packaging application.* International journal of biological macromolecules, 2016. **88**: p. 254-262.

248. Bitinis, N., et al., *Structure and properties of polylactide/natural rubber blends.* Materials Chemistry and Physics, 2011. **129**(3): p. 823-831.

249. Hashima, K., S. Nishitsuji, and T. Inoue, *Structure-properties of super-tough PLA alloy with excellent heat resistance.* Polymer, 2010. **51**(17): p. 3934-3939.

250. Bitinis, N., et al., *Physicochemical properties of organoclay filled polylactic acid/natural rubber blend bionanocomposites.* Composites Science and Technology, 2012. **72**(2): p. 305-313.

251. Jaratrotkamjorn, R., C. Khaokong, and V. Tanrattanakul, *Toughness enhancement of poly (lactic acid) by melt blending with natural rubber.* Journal of Applied Polymer Science, 2012. **124**(6): p. 5027-5036.

252. Suksut, B. and C. Deeprasertkul, *Effect of nucleating agents on physical properties of poly (lactic acid) and its blend with natural rubber.* Journal of Polymers and the Environment, 2011. **19**(1): p. 288-296.

253. Hua, Y., T. Huang, and H. Huang, *Micropropagation of self-rooting juvenile clones by secondary somatic embryogenesis in Hevea brasiliensis.* Plant breeding, 2010. **129**(2): p. 202-207.

254. González, L., et al., *Effect of the network topology on the tensile strength of natural rubber vulcanizate at elevated temperature.* Journal of applied polymer science, 2005. **98**(3): p. 1219-1223.

255. Trabelsi, S., P.-A. Albouy, and J. Rault, *Stress-induced crystallization properties of natural and synthetic cis-polyisoprene.* Rubber chemistry and technology, 2004. **77**(2): p. 303-316.

256. Huang, M., et al., *Strain-Dependent Dielectric Behavior of Carbon Black Reinforced Natural Rubber.* Macromolecules, 2016. **49**(6): p. 2339-2347.

257. Le, H., et al., *Effect of rubber polarity on selective wetting of carbon nanotubes in ternary blends.* Express Polymer Letters, 2015. **9**(11).

258. Lu, F., et al., *Polylactic acid nanocomposite films with spherical nanocelluloses as efficient nucleation agents: effects on crystallization, mechanical and thermal properties.* RSC Advances, 2016. **6**(51): p. 46008-46018.

259. Zhao, H., et al., *Enhancing Nanofiller Dispersion Through Prefoaming and Its Effect on the Microstructure of Microcellular Injection Molded Polylactic Acid/Clay Nanocomposites.* Industrial & Engineering Chemistry Research, 2015. **54**(28): p. 7122-7130.

260. Ahn, E.-B., et al., *Beating Properties with Swelling agent and Concentration for Preparation of MicroFibrillated Cellulose (MFC).* Journal of Korea Technical Association of The Pulp and Paper Industry, 2015. **47**(3): p. 3-10.

261. Lu, Q., et al., *A mechanochemical approach to manufacturing bamboo cellulose nanocrystals.* Journal of Materials Science, 2015. **50**(2): p. 611-619.

262. Waser, H., *Elastomer blends and tire sidewalls prepared therefrom*. 1974, Google Patents.

263. Dinsmore, R.P., *Synthetic rubber and method of making it*. 1929, Google Patents.

264. Suttivutnarubet, C., et al., *Synthesis of polyethylene/coir dust hybrid filler via in situ polymerization with zirconocene/MAO catalyst for use in natural rubber biocomposites.* Iranian Polymer Journal, 2016. **25**(10): p. 841-848.

265. Shimizu, A., M. Kusano, and T. Takami, *Rubber compositions and methods for production thereof stabilized*. 1977, Google Patents.

266. Mochizuki, I. and K. Egawa, *Contacting part made of thermoplastic resin composition with reduced squeaking noises*. 2016, Google Patents.

267. Bledzki, A.K., V.E. Sperber, and O. Faruk, *Natural and Wood Fibre Reinforcement in Polymers*. 2002: Rapra Technology Limited.

268. *DaimlerChrysler Annual Report*. 2014 01.09.2014 [cited 2014 01.09]; Available from: http://www.daimler.com/Projects/c2c/channel/documents/1364373_2006_DaimlerChrysler_Annual_Report.pdf%20(accessed%20September%201,%202014).

269. *DaimlerChrysler uses a natural-fiber component in the exterior of the Mercedes-Benz A-Class*. 2014 [cited 2014 06.09]; Available from: http://www.baby-benz.com/portal/a-class-w169/246-daimlerchrysler-uses-a-natural-fiber-component-in-the-exterior-of-the-mercedes-benz-a-class.

270. Nilsson, S. and S.o.A. Engineers, *Prototype and Low-volume Fabrication of Automotive Sheet Metal Parts Applying Flexforming*. 1989: Society of Automotive Engineers.

271. Mohanty, A.K., M. Misra, and L.T. Drzal, *Natural fibers, biopolymers, and biocomposites*. 2005: CRC Press.

272. Baillie, C., *Green Composites: Polymer Composites and the Environment*. 2005: Taylor & Francis.

273. Bishopp, J.A., *The history of Redux® and the Redux bonding process.* International Journal of Adhesion and Adhesives, 1997. **17**(4): p. 287-301.

274. Piggott, M.R., *Short Fibre Polymer Composites: a Fracture-Based Theory of Fibre Reinforcement.* Journal of Composite Materials, 1994. **28**(7): p. 588-606.

275. GangaRao, H.V.S., N. Taly, and P.V. Vijay, *Reinforced Concrete Design with FRP Composites*. 2006: Taylor & Francis.

276. Haupt, P. and P. Kamalluddien, *Acumen in advanced aerospace materials expertise.* CSIR Science Scope, 2006. **1**(5): p. 12-13.

277. Rychlý, J. and L. Rychlá, *Polyolefins: From Thermal and Oxidative Degradation to Ignition and Burning*, in *Polyolefin Compounds and Materials*. 2016, Springer. p. 285-314.

278. Dubey, P., et al., *Photodegradation Effect on LLDPE/LDPE/PLA Blend Films.* European Journal of Advances in Engineering and Technology, 2016. **3**(4): p. 54-59.

279. Zheng, T., et al., *Study on preparation of microwave absorbing MnOx/Al 2 O 3 adsorbent and degradation of adsorbed glyphosate in MW–UV system.* Chemical Engineering Journal, 2016. **298**: p. 68-74.

280. Sayadi, A.A., T.R. Neitzert, and G.C. Clifton, *Feasibility of a Biopolymer as Lightweight Aggregate in Perlite Concrete.* World Academy of Science, Engineering and Technology, International Journal of Civil, Environmental, Structural, Construction and Architectural Engineering, 2016. **10**(6): p. 690-700.

281. Monreal, C.M., et al., *Nanotechnologies for increasing the crop use efficiency of fertilizer-micronutrients.* Biology and Fertility of Soils, 2016. **52**(3): p. 423-437.

282. Soroudi, A. and I. Jakubowicz, *Recycling of bioplastics, their blends and biocomposites: A review.* European Polymer Journal, 2013. **49**(10): p. 2839-2858.

283. Bastioli, C., *Global status of the production of biobased packaging materials.* Starch-Stärke, 2001. **53**(8): p. 351-355.

284. Auras, R.A., et al., *Poly (lactic acid): synthesis, structures, properties, processing, and applications*. Vol. 10. 2011: John Wiley & Sons.

285. Carrasco, F., et al., *Processing of poly (lactic acid): characterization of chemical structure, thermal stability and mechanical properties.* Polymer Degradation and stability, 2010. **95**(2): p. 116-125.

286. Fukushima, K., et al., *Biodegradation of poly (lactic acid) and its nanocomposites.* Polymer Degradation and Stability, 2009. **94**(10): p. 1646-1655.

287. Ferri, J., et al., *The effect of beta-tricalcium phosphate on mechanical and thermal performances of poly (lactic acid).* Journal of Composite Materials, 2016: p. 0021998316636205.

288. Shogren, R., et al., *Biodegradation of starch/polylactic acid/poly (hydroxyester-ether) composite bars in soil.* Polymer Degradation and Stability, 2003. **79**(3): p. 405-411.

289. Ho, K.-L.G., et al., *Degradation of polylactic acid (PLA) plastic in Costa Rican soil and Iowa state university compost rows.* Journal of environmental polymer degradation, 1999. **7**(4): p. 173-177.

290. Avinc, O., et al., *Investigation of the influence of different commercial softeners on the stability of poly (lactic acid) fabrics during storage.* Polymer Degradation and Stability, 2010. **95**(2): p. 214-224.

291. Sun, B.X., et al. *Biodegradability of Poly (butylene succinate) under Enzymatic Degradation*. in *Advanced Materials Research*. 2013. Trans Tech Publ.

292. Wu, C.S., *Improving polylactide/starch biocomposites by grafting polylactide with acrylic acid–characterization and biodegradability assessment.* Macromolecular bioscience, 2005. **5**(4): p. 352-361.

293. Urayama, H., T. Kanamori, and Y. Kimura, *Properties and Biodegradability of Polymer Blends of Poly(L-lactide)s with Different Optical Purity of the Lactate Units.* Macromolecular Materials and Engineering, 2002. **287**(2): p. 116-121.

294. Avinc, O., et al., *Investigation of the influence of different commercial softeners on the stability of poly(lactic acid) fabrics during storage.* Polymer Degradation and Stability, 2010. **95**(2): p. 214-224.

295. Steinbuchel, A. and J. Lunt, *Biodegradable Polymers and MacromoleculesLarge-scale production, properties and commercial applications of polylactic acid polymers.* Polymer Degradation and Stability, 1998. **59**(1): p. 145-152.

296. Ho, K.-L.G. and A.L. Pometto III, *Temperature Effects on Soil Mineralization of Polylactic Acid Plastic in Laboratory Respirometers.* Journal of environmental polymer degradation, 1999. **7**(2): p. 101-108.

297. Harmaen, A.S., et al., *Thermal and biodegradation properties of poly (lactic acid)/fertilizer/oil palm fibers blends biocomposites.* Polymer Composites, 2015. **36**(3): p. 576-583.

298. Devi, R.S., et al., *The Role of Microbes in Plastic Degradation.* Environmental Waste Management, 2016: p. 341.

299. Seshikala, D. and M.S. Charya, *Collection and screening of Basidiomycetes for better lignin degraders.* International Journal of Life Sciences Biotechnology and Pharma Reseach, 2012. **1**(4): p. 203-211.

300. Chen, W., et al., *Optimization of ultrasonic-assisted extraction of water-soluble polysaccharides from Boletus edulis mycelia using response surface methodology.* Carbohydrate Polymers, 2012. **87**(1): p. 614-619.

301. Harmaen, A.S., et al., *Characterisation and Biodegradation of Poly (Lactic Acid) Blended with Oil Palm Biomass and Fertiliser for Bioplastic Fertiliser Composites.* BioResources, 2016. **11**(1): p. 2055-2070.

302. Hosseinihashemi, S.K., et al., *Long-term water absorption behavior of thermoplastic composites produced with thermally treated wood.* Measurement, 2016. **86**: p. 202-208.

303. Öztürk, İ., et al., *Hydrolysis of kenaf (Hibiscus cannabinus L.) stems by catalytical thermal treatment in subcritical water.* Biomass and Bioenergy, 2010. **34**(11): p. 1578-1585.

304. Ali, M.E., et al., *Effect of single and double stage chemically treated kenaf fibers on mechanical properties of polyvinyl alcohol film.* BioResources, 2014. **10**(1): p. 822-838.

305. Zhou, L.M., et al., *Characterization of ramie yarn treated with sodium hydroxide and crosslinked by 1,2,3,4-butanetetracarboxylic acid.* Journal of Applied Polymer Science, 2004. **91**(3): p. 1857-1864.

306. Edeerozey, A.M.M., et al., *Chemical modification of kenaf fibers.* Materials Letters, 2007. **61**(10): p. 2023-2025.

307. Kargarzadeh, H., et al., *Effects of hydrolysis conditions on the morphology, crystallinity, and thermal stability of cellulose nanocrystals extracted from kenaf bast fibers.* Cellulose, 2012. **19**(3): p. 855-866.

308. Zaini, L.H., et al., *Isolation and characterization of cellulose whiskers from kenaf (Hibiscus cannabinus L.) bast fibers.* 2013.

309. Karimi, S., et al., *Kenaf bast cellulosic fibers hierarchy: A comprehensive approach from micro to nano.* Carbohydrate Polymers, 2014. **101**: p. 878-885.

310. Fierro, V., et al., *Influence of the demineralisation on the chemical activation of Kraft lignin with orthophosphoric acid.* Journal of hazardous materials, 2007. **149**(1): p. 126-133.

311. Parshetti, G.K., S.K. Hoekman, and R. Balasubramanian, *Chemical, structural and combustion characteristics of carbonaceous products obtained by hydrothermal*

carbonization of palm empty fruit bunches. Bioresource Technology, 2013. **135**: p. 683-689.

312. Oh, S.Y., et al., *Crystalline structure analysis of cellulose treated with sodium hydroxide and carbon dioxide by means of X-ray diffraction and FTIR spectroscopy.* Carbohydrate Research, 2005. **340**(15): p. 2376-2391.

313. Zuluaga, R., et al., *Cellulose microfibrils from banana rachis: Effect of alkaline treatments on structural and morphological features.* Carbohydrate Polymers, 2009. **76**(1): p. 51-59.

314. Sun, Y., et al., *Structural changes of bamboo cellulose in formic acid.* BioResources, 2008. **3**(2): p. 297-315.

315. Kargarzadeh, H., et al., *Effects of hydrolysis conditions on the morphology, crystallinity, and thermal stability of cellulose nanocrystals extracted from kenaf bast fibers.* Cellulose, 2012. **19**(3): p. 855-866.

316. Zaini, L.H., et al., *Isolation and characterization of cellulose whiskers from kenaf (Hibiscus cannabinus L.) bast fibers.* Journal of Biomaterials and Nanobiotechnology, 2013. **4**(1): p. 37.

317. Mayer, Z.A., A. Apfelbacher, and A. Hornung, *Effect of sample preparation on the thermal degradation of metal-added biomass.* Journal of analytical and applied pyrolysis, 2012. **94**: p. 170-176.

318. Yang, H., et al., *Characteristics of hemicellulose, cellulose and lignin pyrolysis.* Fuel, 2007. **86**(12): p. 1781-1788.

319. Lim, L.T., R. Auras, and M. Rubino, *Processing technologies for poly(lactic acid).* Progress in Polymer Science, 2008. **33**(8): p. 820-852.

320. Tsukegi, T., et al., *Racemization behavior of l, l-lactide during heating.* Polymer degradation and stability, 2007. **92**(4): p. 552-559.

321. Grijpma, D.W. and A.J. Pennings, *(Co) polymers of L-lactide, 2. Mechanical properties.* Macromolecular Chemistry and Physics, 1994. **195**(5): p. 1649-1663.

322. Salmieri, S., et al., *Antimicrobial nanocomposite films made of poly (lactic acid)-cellulose nanocrystals (PLA-CNC) in food applications: part A—effect of nisin release on the inactivation of Listeria monocytogenes in ham.* Cellulose, 2014. **21**(3): p. 1837-1850.

323. Yang, X., et al., *Two step extrusion process: From thermal recycling of PHB to plasticized PLA by reactive extrusion grafting of PHB degradation products onto PLA chains.* Macromolecules, 2015. **48**(8): p. 2509-2518.

324. Spinella, S., et al., *Polylactide/cellulose nanocrystal nanocomposites: Efficient routes for nanofiber modification and effects of nanofiber chemistry on PLA reinforcement.* Polymer, 2015. **65**: p. 9-17.

325. Oksman, K., et al., *Manufacturing process of cellulose whiskers/polylactic acid nanocomposites.* Composites Science and Technology, 2006. **66**(15): p. 2776-2784.

326. Pradhan, S., I. Chakraborty, and B. Kar, *CHEMICALLY MODIFIED LIGNIN–A POTENTIAL RESOURCE MATERIAL FOR COMPOSITES WITH BETTER STABILITY*.

327. Murphy, C.A. and M.N. Collins, *Microcrystalline cellulose reinforced polylactic acid biocomposite filaments for 3D printing.* Polymer Composites, 2016.

328. Kim, K.-J., et al., *Enzyme activity and beating properties for preparation of microfibrillated cellulose (MFC).* Journal of Korea Technical Association of The Pulp and Paper Industry, 2015. **47**(1): p. 59-65.

329. Pan, Y., et al., *Cellulose fibers modified with nano-sized antimicrobial polymer latex for pathogen deactivation.* Carbohydrate polymers, 2016. **135**: p. 94-100.

330. Almasi, H., et al., *Heterogeneous modification of softwoods cellulose nanofibers with oleic acid: Effect of reaction time and oleic acid concentration.* Fibers and Polymers, 2015. **16**(8): p. 1715-1722.

331. Azeredo, H., et al., *Nanocellulose reinforced chitosan composite films as affected by nanofiller loading and plasticizer content.* Journal of Food Science, 2010. **75**(1): p. N1-N7.

332. Hossain, K.M.Z., et al., *Physico-chemical and mechanical properties of nanocomposites prepared using cellulose nanowhiskers and poly (lactic acid).* Journal of Materials Science, 2012. **47**(6): p. 2675-2686.

333. Mader, A., et al., *Surface properties and fibre-matrix adhesion of man-made cellulose epoxy composites–Influence on impact properties.* Composites Science and Technology, 2016. **123**: p. 163-170.

334. Rana, A., B. Mitra, and A. Banerjee, *Short jute fiber-reinforced polypropylene composites: Dynamic mechanical study.* Journal of Applied Polymer Science, 1999. **71**(4): p. 531-539.

335. Gong, X., et al., *Surfactant-assisted processing of carbon nanotube/polymer composites.* Chemistry of materials, 2000. **12**(4): p. 1049-1052.

336. Martin-Gallego, M., et al., *Comparison of filler percolation and mechanical properties in graphene and carbon nanotubes filled epoxy nanocomposites.* European Polymer Journal, 2013. **49**(6): p. 1347-1353.

337. Menard, K.P., *Dynamic mechanical analysis: a practical introduction*. 2008: CRC press.

338. Ranganathan, N., et al., *Regenerated cellulose fibers as impact modifier in long jute fiber reinforced polypropylene composites: Effect on mechanical properties, morphology, and fiber breakage.* Journal of Applied Polymer Science, 2015. **132**(3).

339. Suksut, B. and C. Deeprasertkul, *Effect of Nucleating Agents on Physical Properties of Poly(lactic acid) and Its Blend with Natural Rubber.* Journal of Polymers and the Environment, 2011. **19**(1): p. 288-296.

340. Esmizadeh, E., G. Naderi, and S.M.R. Paran, *Preparation and characterization of hybrid nanocomposites based on NBR/Nanoclay/Carbon black.* Polymer Composites, 2016.

341. Khalid, M., et al., *Mechanical and physical performance of cowdung-based polypropylene biocomposites.* Polymer Composites, 2016.

342. Zaaba, N.F., H. Ismail, and M. Jaafar, *A study of the degradation of compatibilized and uncompatibilized peanut shell powder/recycled polypropylene composites due to natural weathering.* Journal of Vinyl and Additive Technology, 2015.

343. Grigoriadi, K., et al., *Interplay between processing and performance in chitosan-based clay nanocomposite films.* Polymer Bulletin, 2015. **72**(5): p. 1145-1161.

344. Nair, K.G. and A. Dufresne, *Crab shell chitin whisker reinforced natural rubber nanocomposites. 2. Mechanical behavior.* BIOMACROMOLECULES-WASHINGTON-, 2003. **4**(3): p. 666-674.

345. Gregorova, A., et al., *Effect of Compatibilizing Agent on the Properties of Highly Crystalline Composites Based on Poly(lactic acid) and Wood Flour and/or Mica.* Journal of Polymers and the Environment, 2011. **19**(2): p. 372-381.

346. Kang, H., et al., *Employing a novel bioelastomer to toughen polylactide.* Polymer, 2013. **54**(9): p. 2450-2458.

347. Quaresimin, M., et al., *Toughening mechanisms in polymer nanocomposites: From experiments to modelling.* Composites Science and Technology, 2016. **123**: p. 187-204.

348. Sun, Q., et al., *Novel Biodegradable Cast Film from Carbon Dioxide Based Copolymer and Poly(Lactic Acid).* Journal of Polymers and the Environment, 2016. **24**(1): p. 23-36.

349. Ropers, S., M. Kardos, and T.A. Osswald, *A thermo-viscoelastic approach for the characterization and modeling of the bending behavior of thermoplastic composites.* Composites Part A: Applied Science and Manufacturing, 2016.

350. Aranguren, M.I., et al., *Effect of the nano-cellulose content on the properties of reinforced polyurethanes. A study using mechanical tests and positron anihilation spectroscopy.* Polymer Testing, 2013. **32**(1): p. 115-122.

351. Guerriero, G., et al., *Lignocellulosic biomass: biosynthesis, degradation, and industrial utilization.* Engineering in Life Sciences, 2016. **16**(1): p. 1-16.

352. Ismail, H., A. Norjulia, and Z. Ahmad, *Curing characteristics, mechanical and morphological properties of kenaf fibre/halloysite nanotubes hybrid-filled natural rubber compounds.* Polymer-Plastics Technology and Engineering, 2010. **49**(9): p. 938-943.

353. Gnanavel, G., V. MohanaJeyaValli, and M. Thirumarimurugan, *A review of biodegradation of plastics waste.* Int. J. Pharm. Chem. Sci, 2012. **1**(3): p. 670-673.

354. Kovács, J. and T. Tabi, *Examination of starch preprocess drying and water absorption of injection-molded starch-filled poly (lactic acid) products.* Polymer Engineering & Science, 2011. **51**(5): p. 843-850.

355. Dogu, B. and C. Kaynak, *Behavior of polylactide/microcrystalline cellulose biocomposites: effects of filler content and interfacial compatibilization.* Cellulose, 2016. **23**(1): p. 611-622.

APPENDIX

A1. RSM solutions for extraction of MCF from kenaf fibre

Number	NaOH	$NaClO_2$	Ultrasound	Size	D-TGA	Desirability
1	0.109866	5.003105	10.80412	8.991407	328.2941	1
2	0.138217	4.823955	10.63821	9.811921	332.3372	1
3	0.1093	4.527065	10.92964	8.286361	327.0063	1
4	0.201396	5.00273	10.04128	9.774894	325.4835	1
5	0.150963	4.603704	10.42593	10.05858	332.3264	1
6	0.133426	4.409908	10.6319	9.773041	330.9836	1
7	0.098623	5.143759	10.16232	8.277364	327.2084	1
8	0.125657	4.340695	10.91782	9.707189	329.487	1
9	0.165575	4.733608	10.1454	10.04272	332.2932	1
10	0.145722	4.671451	10.37843	9.780106	332.718	1
11	0.119473	4.486548	11.1344	9.218805	328.4574	1
12	0.10704	5.23228	10.54453	9.64911	328.7269	1
13	0.126055	4.590089	11.45356	9.828271	328.8906	1
14	0.148913	4.833763	10.51425	10.06621	332.8672	1
15	0.149781	4.625959	10.0003	9.576565	333.3901	1
16	0.161735	4.694008	10.19656	10.04706	332.4496	1
17	0.108978	4.288165	10.08318	7.850966	328.2419	1
18	0.108773	4.489594	11.20204	8.493238	326.2374	1
19	0.149789	4.725284	10.3681	9.898118	332.8657	1
20	0.160771	4.843961	10.08557	9.912927	333.3298	1
21	0.115091	4.118819	10.61184	9.389036	328.0464	1
22	0.141258	4.811273	10.0479	9.331475	333.8435	1
23	0.147415	4.498948	10.38052	10.03827	332.1854	1
24	0.146181	4.592854	10.33945	9.813784	332.5691	1

25	0.17445	4.709635	10.05136	10.06802	331.1105	1
26	0.135854	4.948119	10.54109	9.849879	332.7589	1
27	0.108906	3.842569	10.1351	9.85887	327.1111	1
28	0.116907	4.1228	10.46933	9.398376	328.6429	1
29	0.109202	4.96139	11.58055	9.481639	326.1435	1
30	0.115951	4.952993	11.23844	9.568703	328.4222	1
31	0.123798	4.169694	10.27713	9.567071	330.1407	1
32	0.130341	4.668692	10.15852	8.892119	332.4498	1
33	0.145911	4.566885	10.19795	9.695474	332.8051	1
34	0.198357	4.794655	10.18811	10.02175	325.1979	1
35	0.107128	4.293194	10.29115	7.874576	327.4064	1
36	0.12075	3.108018	29.99998	10.07565	313.5017	0.914186
37	0.125088	3.15805	29.99986	10.07572	313.4525	0.913801

A2. RSM solutions for extraction of CNP from kenaf fibre

Number	NaOH	$NaClO_2$	Ultrasound	Size quality	D-TGA	Desirability
1	0.2	5	20	2.986813	335.1818	0.802157
2	0.2	4.999995	20.03578	2.98657	335.1638	0.800712
3	0.199872	4.999996	20.00024	2.979048	335.182	0.800605
4	0.2	4.987829	20.00003	2.976297	335.1801	0.799902
5	0.199696	4.999998	20.00002	2.968433	335.1826	0.798499
6	0.2	4.999998	20.11907	2.986046	335.1219	0.797348
7	0.2	4.999998	20.16289	2.985782	335.0998	0.795576
8	0.19944	4.999996	20.0103	2.952934	335.1781	0.795007
9	0.2	4.950549	20.00001	2.944421	335.1751	0.793037
10	0.198993	5	20.00038	2.926177	335.1843	0.79001
11	0.199192	4.984416	20.00001	2.924653	335.182	0.789526

12	0.2	4.999999	20.37635	2.98458	334.9923	0.786907
13	0.198172	4.999999	20.00008	2.877302	335.1866	0.780097
14	0.2	4.873032	20	2.879691	335.1645	0.778928
15	0.197648	4.999999	20.00003	2.846441	335.188	0.773763
16	0.2	4.811075	20.00002	2.829491	335.156	0.767827
17	0.2	4.63411	20.00002	2.693514	335.1319	0.737011
18	0.1	4	30	1.967033	339.4545	0.695353
19	0.1	4.004904	29.99973	1.964783	339.4431	0.694544
20	0.100316	4.000004	29.99999	1.956802	339.427	0.691665
21	0.100264	4.039852	29.99999	1.940749	339.3393	0.685838
22	0.101271	4.002155	30	1.92539	339.3388	0.680217
23	0.101329	4.000004	29.99999	1.924547	339.3387	0.679907
24	0.2	4.271574	20.00002	2.44933	335.0825	0.678518
25	0.2	4.261732	20.00001	2.443353	335.0811	0.677028
26	0.1	4.177735	29.99999	1.892116	339.0425	0.667876
27	0.2	4.189431	20.00001	2.400433	335.0713	0.666239
28	0.1	4.000001	29.25479	1.874652	339.2743	0.661306
29	0.2	4.074676	20.00001	2.336087	335.0556	0.649749
30	0.104012	4.000001	29.99989	1.843228	339.1047	0.649318
31	0.2	4.051059	20.0014	2.323475	335.0518	0.64643
32	0.2	4.00465	20	2.299076	335.0461	0.640081
33	0.2	4.229018	21.83855	2.486063	334.2538	0.628562
34	0.1	4.515301	29.99999	1.780418	338.26	0.624667
35	0.108917	4.000006	29.99999	1.71019	338.6771	0.595898
36	0.2	4.000005	26.27812	2.628163	332.3402	0.487991
37	0.179707	4	29.73085	2.004143	332.5848	0.402762
38	0.179614	4.000004	29.84184	2.010501	332.5601	0.402105
39	0.112293	4.999999	29.98587	1.411784	336.2757	0.40189

A3. RSM solutions for processing parameters of PLA

No.	Mixing speed	Mixing temp	Mixing duration	Max stress	Young Modulus	Impact	Desirability
1	99.99996	180	9.694923	56.84423	651.1368	32.23309	0.922203
2	99.81966	180	9.72391	56.83349	651.1384	32.23686	0.922115
3	99.91666	180.0035	9.709723	56.83686	651.1367	32.23462	0.922106
4	99.93184	180	9.732103	56.80788	651.6119	32.24389	0.921838
5	99.19823	180.0001	9.822989	56.79417	651.1373	32.24883	0.921729
6	99.28765	180.0148	9.814693	56.78953	651.1366	32.24623	0.921545
7	99.99968	180.0093	9.771076	56.74791	652.4526	32.25842	0.921118
8	98.44147	180.0001	9.942833	56.74042	651.1374	32.26157	0.921073
9	97.99371	180	9.999989	56.7234	650.889	32.26345	0.920178
10	98.67702	180.0861	9.939576	56.69559	651.1381	32.25192	0.919834
11	98.64	180.2158	9.99527	56.59929	651.1384	32.24298	0.917567
12	99.99987	180	9.400061	57.18706	646.0453	32.12986	0.912658
13	99.99991	180.6819	9.958588	56.35592	651.1371	32.18157	0.910489
14	99.99983	180.847	9.999996	56.26175	650.7986	32.16025	0.906996
15	99.99994	180	8.809066	57.7659	637.1652	31.93492	0.893603
16	99.99991	180	7.131156	58.62213	621.5804	31.46821	0.848245
17	99.99881	180	7.11357	58.62506	621.4903	31.46398	0.847878
18	99.99997	180	6.986203	58.64145	620.902	31.43391	0.845351
19	99.99994	180	6.864291	58.65099	620.4141	31.40581	0.843073
20	99.99991	180	6.825372	58.65274	620.2742	31.39699	0.842376

21	99.99964	180	5.898711	58.50938	619.2033	31.20717	0.830227
22	99.99992	180	5.155861	58.13797	621.482	31.08329	0.826507
23	99.99949	180	5.14117	58.12836	621.5547	31.08109	0.826481
24	99.99939	180	5.003933	58.03395	622.2912	31.06105	0.826336
25	99.36677	180	5.071652	58.13784	621.3629	31.07118	0.825731
26	50	210	5	52.52502	650.72	30.0543	0.751341
27	50.00008	209.9617	5.000009	52.53812	650.4001	30.05534	0.751031
28	50.00891	209.9999	5.007725	52.52964	650.5683	30.047	0.750871
29	50.00007	210	5.073197	52.56388	649.5108	29.98861	0.747352
30	50.00002	209.51	5.000001	52.69046	646.6932	30.06731	0.747305
31	50.11831	209.3717	5.000001	52.74197	645.2879	30.06638	0.745484
32	51.04799	209.9968	5.000018	52.56856	648.1136	30.01168	0.745451
33	50.00007	210	5.286331	52.66441	646.1449	29.79873	0.735657
34	50.00071	209.7565	5.330981	52.76771	643.4218	29.76749	0.731106
35	53.75699	209.9999	5.000002	52.64627	641.6818	29.8933	0.729422
36	50.00002	209.9997	5.41614	52.71653	644.205	29.68412	0.728489
37	61.23601	210	5.00002	52.63307	625.4191	29.50747	0.679174